



universität
wien

DISSERTATION

Titel der Dissertation

„The Threat of NEA's and the Origin of Terrestrial Planets
Impactors“

Verfasser

M.Sc. Mattia Galiazzo

angestrebter akademischer Grad

Doktor der Naturwissenschaften (Dr.rer.nat.)

Wien, 2013

Studienkennzahl lt. Studienblatt:

A 096 9367 Dr.-Studium der Naturwissenschaften

Astronomie UnitStG

Dissertationsgebiet lt. Studienblatt:

413 Astronomie

Betreuerin / Betreuer:

Univ.-Prof. Dr. Rudolf Dvorak, Univ.-Prof. Dr. Christian Koeberl

To my love, Ketii

To my dearest in Italy, my father, my mother and my brother, my friends and friends around the world and my "second" "italo-albanian family and nephews"

To Juan Lu, my dearest friend, my "Nonni di Bassano" and "Nonni di Black" and my "Zio Ennio", who are in the skies

Contents

Glossary	VI
Astronomical System of Units	VII
1 Introduction	1
1.1 Scope of this work	3
1.2 Asteroids	5
1.3 Orbital distribution of the asteroids	7
1.4 Physical properties of the Asteroids	10
1.4.1 Internal composition, Size and Surface of the asteroids: spectroscopy and photometry	10
1.4.2 Meteorites and asteroids	12
1.4.3 Asteroids spectral type	13
1.4.4 Period distribution	15
1.5 Orbital integrations	16
1.5.1 Used Numerical integrations codes	17
1.6 An overview on the resonances	18
1.6.1 Mean Motion Resonance	20
1.6.2 Three-body mean motion resonances	20
1.6.3 Secular evolution of asteroids orbits	21
1.7 NEAs and their origins	23
1.8 Sources of PCAs for Terrestrial planets	31
1.8.1 Close encounters	31
1.8.2 Impacts	33
1.8.3 Impacts rate on the Earth (and Moon)	36
2 Fugitives from the Hungaria region	38
3 Hungarias: close encounters and impacts with terrestrial planets	49
4 Lunar effects on close encounters of Hungarias	62

5	Water delivery in the early Solar System	68
6	Other sources of PCAs	80
6.1	V-types asteroids and close encounters	80
6.1.1	Results	82
6.2	Centaurs (Inner Centaurs) close encounters with terrestrial planets	87
7	The origin of the Bosumtwi impactor	91
8	Photometry of Comet <i>C/2012 S1 (ISON)</i>	97
9	Conclusions	102
9.1	<i>NEAs</i> ' origin	102
9.2	Close encounters with the terrestrial planets	103
9.3	Impacts	106
9.3.1	Impacts with terrestrial planets and the Sun	106
A	Secular resonances for the asteroids	110
B	Meteorites, Parent Bodies and connections	112
B.1	Meteorites	112
B.2	Spectral Type classification of asteroids	115
	Acknowledgements	120
	Bibliography	128
	Abstract	129
	Zusammenfassung	131
	Curriculum Vitae: Mattia Galiazzo	133



And asteroids fall down

*As drops from the leaves, when vapour condenses
shining in front of a yellowish star
the leaves are crying
autumn has come
but the drops of water are smiling
the spring will come...*

Mattia

Glossary

2BP	Two-Body Problem
3BMMR	Three-Body Mean Motion Resonance
CE	Close Encounter
ECA	Earth-Crossing Asteroid
ECOM	Ecliptic Comet Population
HCM	Hierarchical Clustering Method
HED	Howardite Eucrite Diogenite
HTC	Halley Type Comet
IEO	Inner Earth Orbit
IMB	Inner Main Belt
JFC	Jupiter Family Comet
KBO	Kuiper Belt Object
LHB	Late-Heavy Bombardment
LINEAR	Lincoln Near-Earth Asteroid Survey
LONEOS	Lowell Near-Earth Objects Search
LPC	Long Period Comet
MOC	Moving Objects Catalogue
MMB	Mean motion resonance
MPEC	Minor Planet Electronic Circular
NEA	Near-Earth Asteroid
NEO	Near-Earth Object
NIC	Nearly Isotropic Population
OMB	Outer Main Belt
PCA	Planet-Crossing Asteroid
PPN	Parameterized Post-Newtonian
S³SO²	Small Solar System Objects Spectroscopic Survey
SFD	Size Frequency Distribution
SINEO	Spectroscopic Investigatio of Near-Earth Objects
SMASS	Small Main-Belt Asteroid Spectroscopic Survey
SDSS	Sloan Digital Sky Survey
TNO	Trans-Neptunian Objecy
WAV	Wavelet Analysis Method
WISE	Wide-field Infrared Survey Explorer

Astronomical System of Units

au (AU)	astronomical unit	149597870700 m
k	gaussian gravitational constant	$0.01720209895 \text{ au}^{3/2} m_{\odot}^{-1/2} D^{1/2}$
m_{sun}	solar mass	$1.9891 \cdot 10^{30}$ kg
D	mean solar day	86400 SI seconds
Ly	Light-year	63241.077 au

Chapter 1

Introduction

This work is in the frame of the Doctoral School at the University of Vienna, Austria: “ Planetology: From asteroids to Impact Craters (*NEO* asteroids and Impact Crater Studies)”.

The topic of this doctoral program deals with aspects of planetary geology and planetary astronomy. The astronomical part is the one which is considered in this thesis: minor bodies of the solar system are studied from their origins to the evolution of their orbits into the terrestrial planets orbits with a special emphasis on close encounters and impacts with the Earth, Mars and Venus, focusing more at the Planet-Crossing Asteroids, called also *PCAs*.

The history of the Solar System is full of catastrophic events during the evolution of its planets. This was pointed out after the first exploratory space missions which have discovered craters on several planets and satellites: Mars, Mercury and some Moons of Jupiter and Saturn (by the survey of Mariner 4, Mariner 10 and the two Voyagers). The causes of these impacts for the inner Solar System are the Near-Earth Objects, *NEOs*, asteroids (*NEAs*) and comets, which were formed out of the formation of the protoplanetary disk.

NEOs are comets and asteroids that have been nudged by the gravitational attraction of nearby planets into orbits that allow them to enter the Earth’s neighborhood. In terms of orbital elements, they are asteroids and comets with perihelion distance $q < 1.3$ au.

The presence of the asteroids in the Solar System was relevant to the planets during different important collisional times, like the Late Heavy Bombardment, *LHB*, a period which is thought to have lasted until 3 Gyr ago (Bottke et al. , 2012), starting from some ten million years after the birth of the Solar System. Terrestrial Planets are dotted with impact craters. This is very visible on planets like Mars and Mercury (or a natural satellite like the Moon), as it can be seen in fig 1.1, because they are not as geologically active, as the Earth. In fact it is very difficult to see clearly crater’s sites on the Earth.

For this reason the study of the asteroids is very important, both for a major

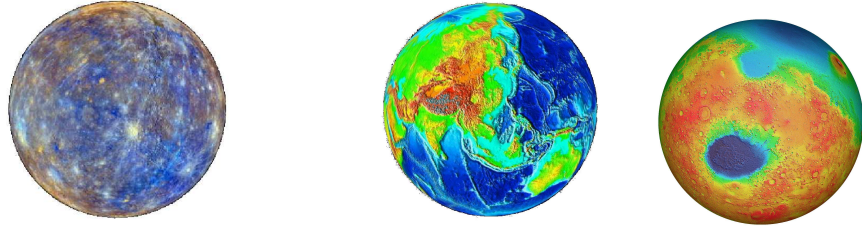


Figure 1.1: From left to right: First picture: This colorful view of Mercury was produced by using images from the color base map imaging campaign during *MESSENGER*'s primary mission. These colors are not what Mercury would look like to the human eye, but rather the colors enhance the chemical, mineralogical, and physical differences between the rocks that make up Mercury's surface. Credit: *NASA/Johns Hopkins University Applied Physics Laboratory/Carnegie Institution of Washington*. Second picture: Earth Topography. Height, above and below sea level, is coded by color. The topography map comes from the National Geophysical Data Center at the National Oceanic and Atmospheric Administration. Third picture: Global false-color topographic views of Mars at one orientation from the Mars Orbiter Laser Altimeter (*MOLA*). The map is orthographic projections that contain over 200,000,000 points and about 5,000,000 altimetric crossovers. The spatial resolution is about 15 kilometers at the equator and less at higher latitudes. The vertical accuracy is less than 5 meters. Credit: *MOLA Science Team*.

knowledge of the evolution of the Solar System and for a prevention of the terrestrial life, protecting planet Earth and its inhabitant by a potential killing-impactor. In fact many funds were settled for researches and missions on these bodies, ones of the most important is *SPACEGUARD* (*LINEAR*, *LONESS* and *NEAT*¹), with the goal of discovering as many *NEAs* (particularly an important subgroup of them, the Planetary Hazard Objects, *PHOs*) as possible. The most recent mission is *WISE* (Wide-fields Infrared Survey Explorer). One of the most important aims of this mission is to complete the knowledge of the *NEAs*, especially their size distribution (see Fig. 1.2).

¹Lincoln Near-Earth Asteroids, Lowell Observatory Near-Earth Objects Search and Near-Earth Asteroid Tracking.

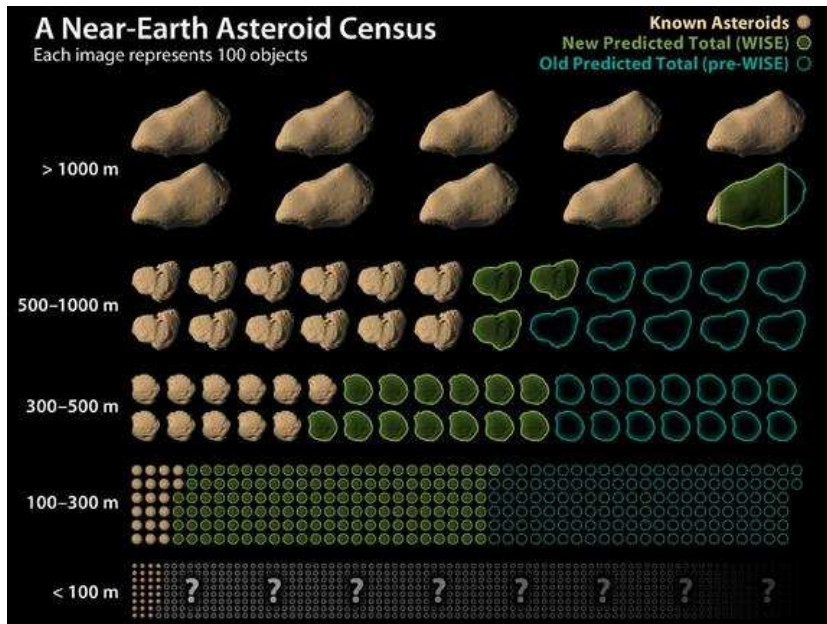


Figure 1.2: This chart illustrates how infrared is used to more accurately determine an asteroid’s size and presents the known size distribution with the predicted total one. CREDIT: NASA/JPL-Caltech.

1.1 Scope of this work

The scope of this work is searching for possible asteroid families and groups, which might be the source of bodies that can have close encounters with Earth, Mars and Venus and eventually lead to impact events with them. The contribution of the *NEAs* is computed statistically for close encounters and impacts with terrestrial planets and in addition some studies about their origins: the families of the Main Belt, the Centaurs, and the trans-Neptunian objects (*TNOs*). Then, also, the dynamical effects that can cause close encounters with the Terrestrial Planets will be studied.

Investigation on asteroids is performed studying their orbital behavior and the relevance of the resonances and other possible effects which might change significantly their orbits, i.e., close encounters and their possible impacts on the relative planet. The impact angle and velocity, the diameter of a possible crater after an impact are computed. In addition, a study on the origin of a paleo-impact event, specifically the Bosumtwi case (see Chapter 7), will be presented in details with a suggested methodology for this problem. The region of asteroids which will be studied more in details is the Hungaria one (see Chapter 2, 3, 4 and 5), a region in the Inner Main Belt (*IMB*) and the closest one to Mars. Then, in similar way, V-types asteroids (see section 6.1) will be briefly studied, especially the *NEAs*’

ones. Finally a study on the Centaurs (see Section 6.2) is shown with also some brief considerations on the *TNOs*, and the Orion Belt, where some comets start their path toward the Inner Solar System (Duncan, Levison & Budd , 1995; Levison & Duncan , 1997). Also a short photometric study of a sun-grazing comet with some details about its orbit in the inner Solar system is presented (see Section 8): Comet *C/2012 S1 ISON* (forecasted to be one of the brightest comet of the century and whose dust will affect the Earth, “isonids”, http://science.nasa.gov/science-news/science-at-nasa/2013/19apr_isonids, prediction of Prof. P. Wiegert, 2013).

1.2 Asteroids

Asteroids were initially named after Greek and Roman goddesses. As their numbers have increased, asteroids have been named after the family members of the discoverers, after observatories, universities, cities, provinces, historical figures, scientists, writers, artists, literary figures, and, in at least one case, the astronomer's cat. Initial discoveries of asteroids are designated by the year of their discovery and a letter/number code (McFadden, Weissmann & Johnson, 2007). Once the orbits of the asteroids are firmly established, they are given official numbers in the asteroid catalog: over about 615,155 asteroids have been numbered (as of May, 18 2013, JPL Small-Body Database Search Engine). The discoverer(s) of an asteroid are given the privilege of suggesting its name, if done so within 10 years from when it was officially numbered. Asteroids are minor planets (small Solar System bodies and dwarf planets, i.e. 1 Ceres and 4 Vesta) that are not comet (an icy rock body, which perform some activity, i.e. ejection of material, like dust, gas or liquid in a tail upon its main body/nucleus. It is believed that planetesimals in the asteroid belt evolved similarly to the rest of the solar nebula until Jupiter neared its current mass and from that point excitation from orbital resonances with Jupiter ejected the majority of the planetesimals in the belt. These rocky bodies are now present all over the Solar System, especially in the Main Belt region, where they have higher density compared to other regions, after they evolved from the Solar nebula as it is shown in Fig. 1.3, 1.4.

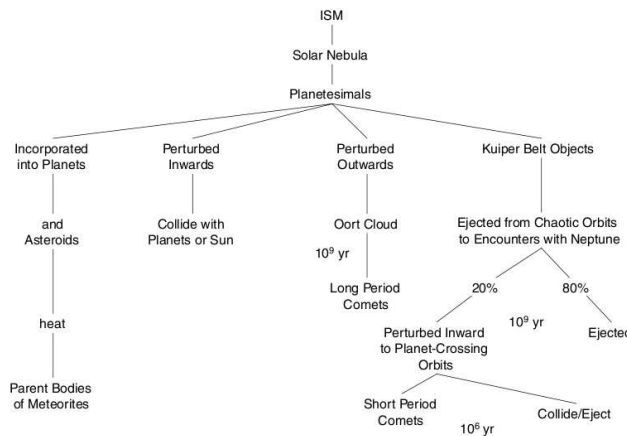


Figure 1.3: A scenario for the evolution of the planetesimals in the solar nebula. The approximate dynamical lifetimes in years for some stages in the development are shown. Adapted from Barucci et al., 2002.

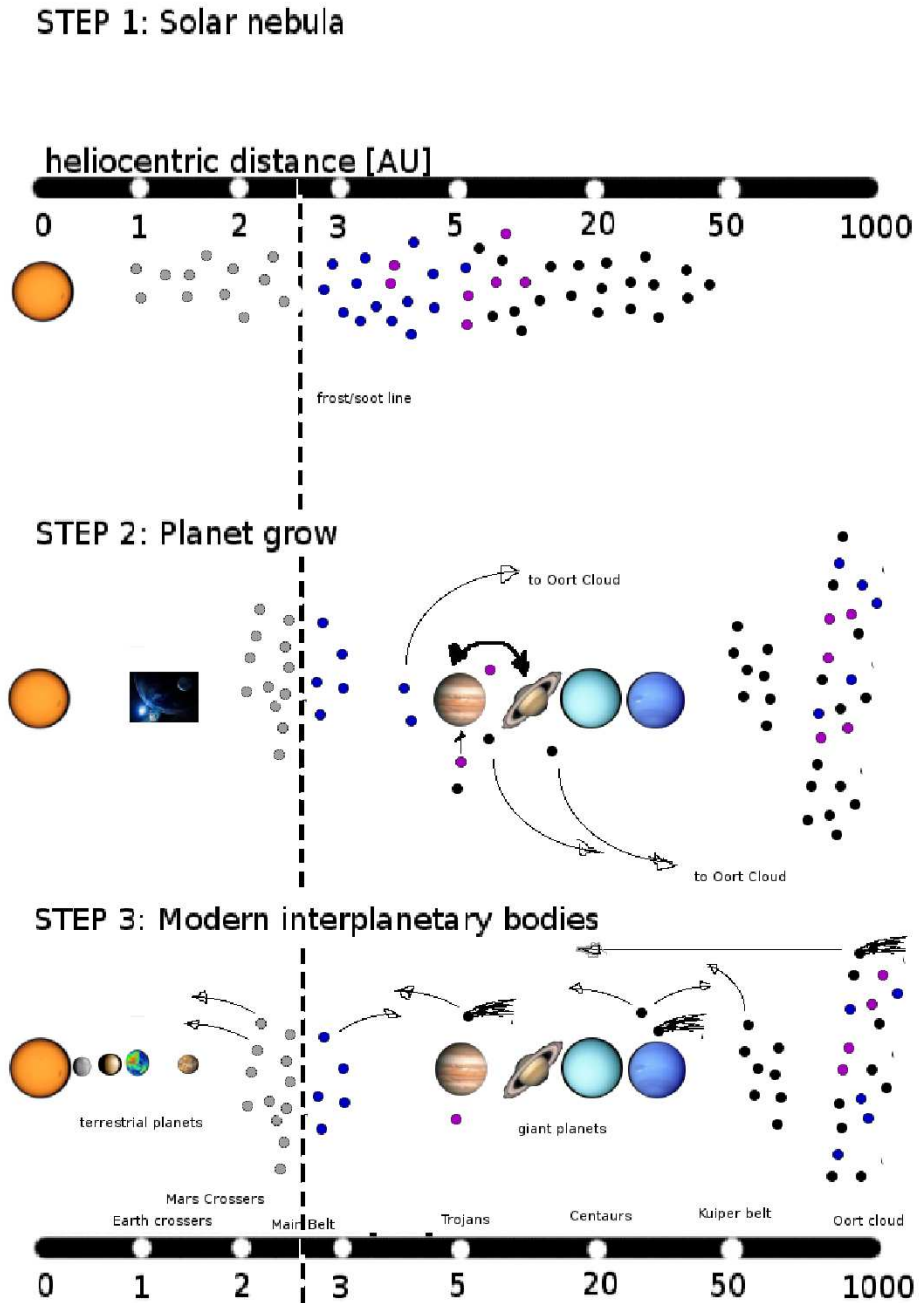


Figure 1.4: Formation of asteroids. Green, violet, blue and black bodies represent respectively silicate/metal, C-, P- and D- carbonaceous/icy bodies (see Appendix B). Credit: <http://lasp.colorado.edu/~bagenal>, with some modifications from the author of these thesis.

1.3 Orbital distribution of the asteroids

Asteroid groups and subgroups in the Solar System:

The **Near-Earth Asteroids** are mainly subdivided in 4 principal types (see Fig.1.5 and Bottke et al. (2002); Galiazzo, Bazso & Dvorak (2013a)):

Inner Earth Orbits (IEOs) NEAs² whose orbits are contained entirely with the orbit of the Earth with $a < 1.0$ au, $Q < 0.983$ au;

Atens Earth-crossing *NEAs* with semi-major axes smaller than Earth's, named after (2062) Aten – with $a < 1.0$ au, $Q > 0.983$ au;

Apollos Earth-crossing *NEAs* with semi-major axes larger than Earth's, named after (1862) Apollo, with $a > 1.0$ au, $q < 1.017$ au;

Amors Earth-approaching *NEAs* with orbits exterior to Earth's but interior to Mars', named after (1221) Amor, with $a > 1.0$ au, 1.017 au $< q < 1.3$ au.

The **Main Belt** can be subdivided in 3 regions in the following semi-major axis borders (see Galiazzo et al. (2013b)):

Inner Main Belt (IMB) 1.78^{*3} au $\leq a \leq 2.06$ au

Middle Main Belt (MMB) 2.06 au $< a < 3.28$ au

Outer Main Belt (OMB) 3.28 au $< a < 5.05$ au

Regions are defined by the semi-major axis that corresponds to strong Mean Motion Resonance⁴, see Section 1.5.

Comets can be subdivided in 2 main populations:

The ecliptic Comet Population (ECOM) Comets having $T_j > 2$ (Levison , 1996). The Tisserand parameter⁵ in respect to Jupiter (Kresak , 1979) is:

$$T_j = \frac{a_j}{a} + 2\sqrt{(1 - e^2)\frac{a}{a_j}} \cos i \quad (1.1)$$

²For the definition of the different types of *NEAs*, the perihelion, $q = a(1 - e)$, and the aphelion, $Q = a(1 + e)$, of the asteroid is used. e and a are respectively the eccentricity and the semi-major axis of the orbit of the bodies (comets/asteroids).

³The asterisk means that it is the minimum semi-major axis (and not a specific *MMR*) for the innermost group of asteroids (the Hungaria Group, see Galiazzo et al. (2013b)).

⁴2.06 au for $J4 : 1$ and 3.28 au for $J2 : 1$ (resonances with Jupiter).

⁵The pseudo-energy of the Jacobi integral that must be conserved in the restricted three-body problem. Basically, the Tisserand parameter is used to distinguish between the orbit of a comet, $T_j > 3$, and the orbit of an asteroid, $T_j < 3$.

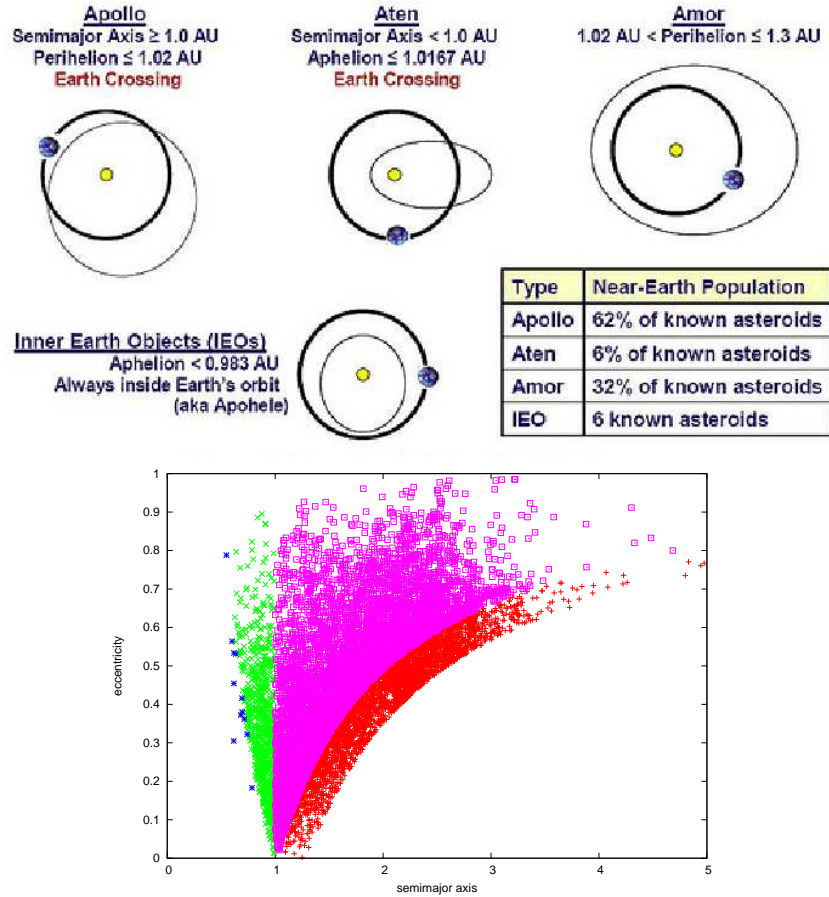


Figure 1.5: Upper panel: orbit of the *NEAs* compared to the one of the Earth (from <http://neo.jpl.nasa.gov/neo/groups.html>). Bottom panel: eccentricity versus semimajor axis (in au) of the *NEAs* and their types. Each color represents different *NEA*-types: *IEOs* in blue (very few ones are known, now), *Atens* in green, *Apollos* in pink and *Amors* in red. Asteroids with $a > 5$ au are not considered in this plot.

where a_j is the semi-major axis of Jupiter and a , e and i are the actions of the osculating elements of the considered comet or asteroid. The *ECOM* contains the Encke-type comets, the Jupiter-family comets, the Centaurs, and part of the scattered comet disk beyond Neptune;

The Nearly Isotropic Population Comets (*NICs*) located at a distance of $a > 3000 \text{ AU}$ (Weissman, 1996). They have 2 main types: the long-period comets (*LPCs*), with periods longer than 200 years and $T < 2$, and the Halley-type comets (*HTCs*), with period less than 200 years and $T < 2$

1.3. ORBITAL DISTRIBUTION OF THE ASTEROIDS

(Levison , 1996).

Centaurs Centaurs are asteroids (whose average size is bigger than the mean one of the Main Belt) having a semi-major axis between those of Jupiter and Neptune ($5.5 \text{ au} < a < 30.1 \text{ au}$).

Trans-Neptunian Objects *TNOs* are any object whose semi-major axis is greater than the Neptune's one and they are subdivided (Beatty & Beatty , 2007) like this:

Classical Kuiper Belt Objects (*KBOs*) Asteroids with $30 \text{ au} < a < 55 \text{ au}$, which are subdivided again in 2 subgroups:

Resonant objects locked in an orbital resonance with Neptune: *Twotinos* in N2:1 mean motion resonance (with Neptune) and *Plutinos* in P2:3 (*P* stands for Pluto)

Classical Kuiper belt objects (*Cubewanos*) Objects on almost circular orbits, unperturbed by Neptune, with $40 \text{ au} < a < 55 \text{ au}$;

Scattered disk Bodies with high eccentricities and inclinations orbits, with $p > 30 \text{ au}$. Assumed as objects scattered away from Neptune after a close encounter.

Detached objects Extended scattered disk, generally with very high elliptical orbits and with $a > 100 \text{ au}$. No interactions with Neptune.

Oort Cloud Bodies with semimajor axis in this range: $50000 \text{ au} \lesssim a \lesssim 100000 \text{ au}$.

1.4 Physical properties of the Asteroids

1.4.1 Internal composition, Size and Surface of the asteroids: spectroscopy and photometry

The internal structure of the asteroids can be determined by macroporosity⁶ (Britt et al. , 2002). 3 groups (in internal composition, see fig. 1.6) can be distinguished like this:

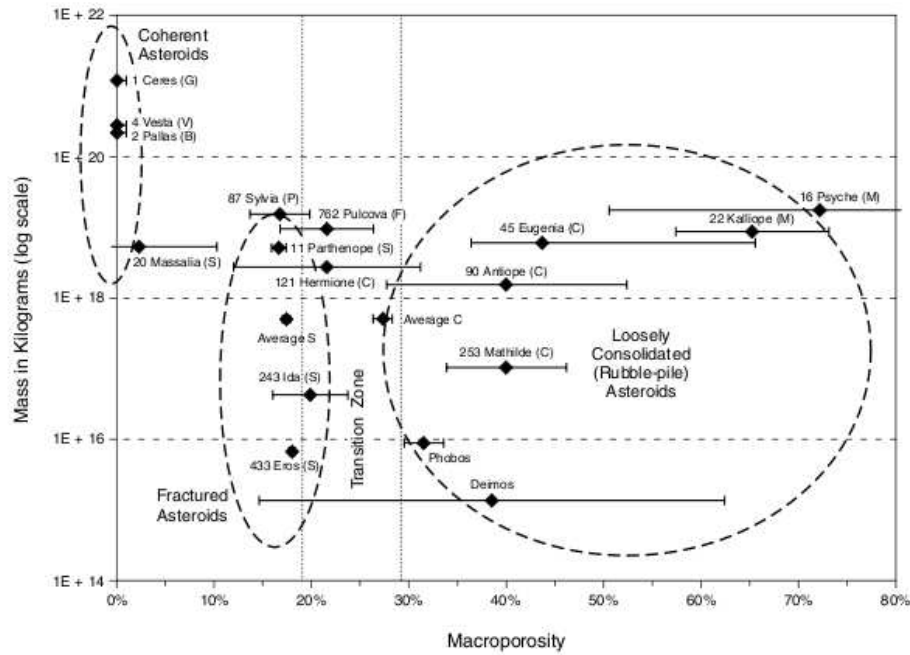


Figure 1.6: Asteroid macroporosity estimated by subtracting the average porosity of asteroid’s meteorite analogue from the bulk porosity. Since microporosity (the type of porosity measured in meteorites: meteorites’ fractures, voids and pores on the scales of tens of micrometers) probably does not seriously effect the structure integrity of asteroids, this is a direct estimate of the large-scale fractures and voids that determine the asteroid’s internal structure (Britt et al. , 2002).

Coherent bodies Essentially solids objects, e.g. 1 Ceres, 2 Pallas and 4 Vesta (see fig. 1.7 for its formation and internal structure) and also 20 Massalia. Their bulk density is similar to the grain one (meteorite analog), meaning a zero macroporosity.

⁶Large scale voids and fractures on the asteroids, probably produced by impacts.

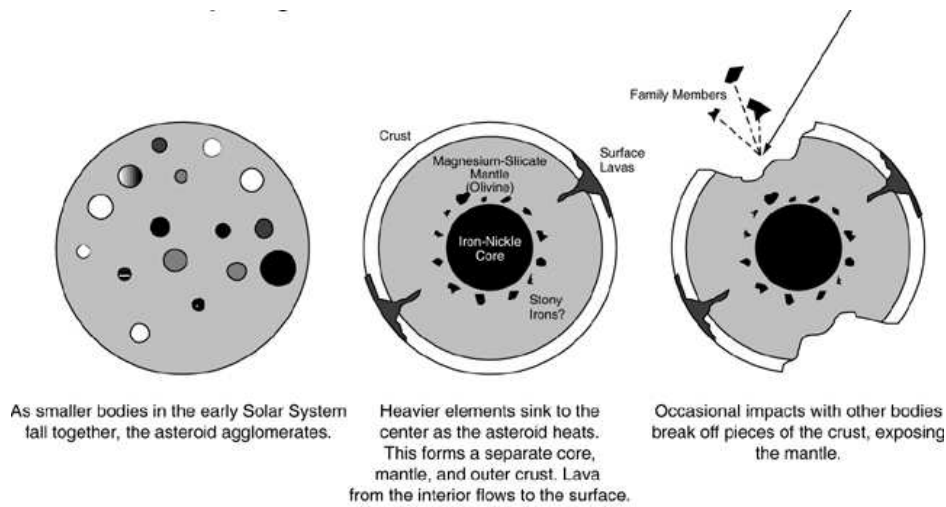


Figure 1.7: Key stages in the evolution of the asteroid 4 Vesta. PB95-20 ST Scl OPO - April 19 1985 Zellner (GA Southern Univ.), USA.

Fractured asteroids Macroporosity between 10-25 %, e.g. S-type asteroids (see Table B.2), like 433 Eros or 243 Ida, which have numerous morphological indications of pervasive fracturing (Belton et al. , 1995; Veverka et al. , 2001). This indicates that primitive asteroids are fundamentally weaker and more likely to be loosely consolidated, while the metamorphic and igneous asteroids tend to be stronger and more likely to be coherent.

Loosely consolidated (rubble pile asteroids) A rubble pile⁷ includes any shattered body whose pieces are furthermore translated and rotated into loose packing (Chapman & Davis, 1975). Macroporosity between 25% and 80%. Asteroids with more empty space than solid material probably pervasively fractured and may have been disrupted by mutual gravity. 16 Psyche is the most porous observed asteroid.

Gravity of small asteroids can barely hold on to its rocks. Yet the best spacecraft images of ~ 10 km bodies (Phobos, Thomas & Veverka 1977) show fields of boulders, lunar like craters with dramatic rim deposits landscapes mantled in nature regolith and shapes broadly conforming to gravity potential. Instead asteroids between about 100 m and 100 km are probably gravitational aggregates of loosely consolidated material (Richardson et al., 2002).

Here some pictures how the asteroids present themselves due to its interior part and size: Fig. 1.8 and 1.9.

⁷a variety of configurations that range from theoretical constructs like piles of marbles to more realistic speculations on planetesimal interiors (Richardson et al., 2002).

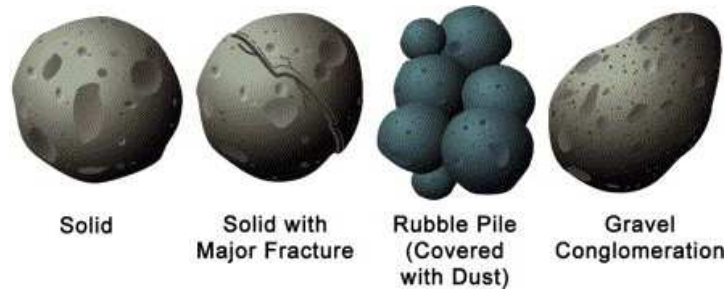


Figure 1.8: Main different types of asteroids' constitution (from www.swri/3pubs/ttoday/spring04/Cosmic.htm).

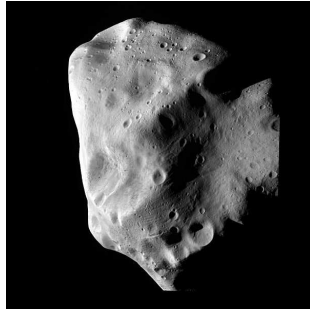


Figure 1.9: Asteroid Lutetia (Rosetta Mission, NASA).

1.4.2 Meteorites and asteroids

The asteroidal origin of meteorites is inferred from their ancient age, and deduced by observations (Grady & Wright 2006). Two features link meteorites to asteroids: (1) spectral reflectance measurements of asteroidal and meteorite surfaces give a close match for asteroids and meteorites of variety of classes, e.g. basaltic achondrites match closely to Vesta (Burbine et al. , 2002a), carbonaceous chondrites match C-class asteroids (Burbine & Binzel , 2002b), see Table B.1 and B.3, summary of the table of Cellino et al. (2002); (2) observations of incoming fireballs and the ability to track trajectory and thus calculate the orbit for meteoroid (Halliday, Griffin & Blackwell , 1996), especially for the most recent meteorites, which can now be classified with their parent body by direct observations and orbital computations (Sitarsky, 1999, Rudawska, Vaubaillon & Atreya (2012), Spurný et al., 2012): very clear is the origin of the Almahata Sitta meteorite, that it was originated by the break-up in the atmosphere of the asteroid 2008 TC_3 (Gayon-Markt et al. , 2012). Also the spectral type and color indices can be useful concerning the origin of the falling extraterrestrial material. Instead the work of Galiazzo et al. 2013b (see Chapter 7) is an example for older impacts, in fact it infers the origin of a paleolithic impact, i.e. the origin of the impactor of the Bosumtwi crater. It is important to note that there are some paradoxes in method (1); in fact the

largest group of stony meteorites, the ordinary achondrites, has no good spectral match with any common asteroidal class (Binzel, Bus & Burbine, 1998). Additionally, the asteroid for which we have the best surface composition, the S-class 433 Eros, might be an altered ordinary chondrite, or, less plausibly, a primitive achondrite (Nittler et al., 2001). Space weathering has been proposed as an explanation for dichotomy and in fact evidence of it was found by Nesvorný et al. (2005), finding that the colors of aging surfaces of S-type asteroids (see Section 1.4.3) become increasingly “redder” and so the spectra of them change; Nesvorný et al. (2005) suggest also that surfaces of C-type asteroids exhibit color alterations opposite to those of the S-type asteroids.

1.4.3 Asteroids spectral type

Main surveys for spectroscopy for asteroids are the *SMASS*⁸ survey (Xu et al. (1995), Bus & Binzel (2002a) and Bus & Binzel (2002b)) and the *S³OS²* (Small Solar System Objects Spectroscopic Survey, Lazzaro et al., 2004), they both focus on the visible region, from 0.45 to 0.92 μm approximately, and basically observed main belt asteroids. *SMASS* has a near-infrared extension, the *SMASSIR*⁹ (Binzel et al. (2001), Burbine & Binzel (2002b)), but covering only the spectra up to 1.6 μm . Then de León et al. (2010) present a list of data in visible and infrared covering the wavelength region from 0.5 to 2.5 μm , studying only *NEAs* (see <http://www.iac.esproyectopcossolar/pagesendata.php>); then the *SINEO* survey¹⁰, visible and infrared (Lazzaro et al., 2004 and Lazzarin et al., 2005, see <http://www.astro.unipd.it/planetssineo.html> and the *MIT – UH – IRTFNEO* reconnaissance program, exclusively infrared, see <http://smass.mit.eduminus.html>). Different spectroscopic surveys in the visible region have been used to develop a taxonomic classification of the asteroids, according to the differences in their reflectance spectra. Although the taxonomic types cannot be used to infer the mineralogy composition of the objects, they help constrain mineral species that may be present on the surface of the asteroid (de León et al., 2010). The most used classifications are the Tholen & Barucci (1989) and Bus (1999), described in Table B.2 (Appendix B).

E-type asteroids, Hungarias and their “duality”

The surface composition¹¹ of the Hungarias¹² (see *SDSS*¹³) is rather peculiar among the asteroids of the Main Belt, see Appendix B. Hungarias’ surfaces were

⁸Small Main-Belt Asteroid Spectroscopic Survey

⁹*SMASS* in infrared (*IR*)

¹⁰Spectroscopic Investigation of Near Earth Objects.

¹¹The surface composition can be studied spectroscopically and in part photometrically.

¹²A group of asteroids in the Inner Main Belt at high inclined orbits, see Chapter 2 for details.

¹³Sloan Digital Sky Survey.

analyzed spectroscopically by Assandri & Gil-Hutton (2008), who found that these asteroids are 59 % X-types, 26% C-types, 9% S-types and Other-types \ll 1 %. The importance thing is that the C-types are not formed originally in this part of the Main Belt, where Hungarias are present, so this could be a sign-factor of a transportation in the Main Belt. Bus & Binzel (2002b) were the first ones to introduce the X-class; the location of Hungaria in this class would seem to favor a mineralogy associated with E- or M-type (Tholen, 1989). There are diverse characteristics of the X-class spectra, that gives rise to their subgroups (*E*, *M* and *P*, see Table B.2, too):

- 3 μm band in M- and E- types spectra.
- absorption bands in the visible spectra of E-type
- absorption bands in the spectra of M-type
- small absorption bands in the *NIR*¹⁴
- mineralogical differences between E-type

E-types are uncommon in the solar system, and they were found only in the Hungarias' region, so they are a characterization of the Hungaria Group, S-types instead are common (perhaps S-types are interlopers). Carvano (2001), too, claims that Hungarias are spectroscopically dominated by 3 different types E-, X, Xe-types. The most representative asteroids with E- and Xe-types taxonomic classification are: 434 Hungaria, 44 Nysa and 64 Angelina. E-type is described in Clark et al. (2004), here a schematic summary of his conclusions:

- Nysa like: silicate mineralogy higher in iron than the mineral enstatite
- Angelina like: silicate mineralogy
- Hungaria like: inconsistent with aubrites (but not all members of Hungaria have similar mineralogy).

Looking at some E-types, the compositional distribution in the group is not as peculiar as it has been assumed. Important source of data about Hungaria asteroids and asteroids in general are large photometric surveys, such *Sloan Digital Sky Survey* into the *Moving Objects Catalogue* (five band photometry for 43424 asteroids!!!). Concerning the chemical connection asteroids-meteorites: it has been observed that there is a probable connection between the asteroid 3103 Eger and aubrites of the meteorite which collapsed near Nyons in 1836. 4483 Petofi is composed by 80% of olivine and pyroxene. The albedo of the Hungaria (0.22 ± 0.06) is very near to the value of the Nysa-group (0.19 ± 0.06) both larger than the *MBA*s, and Nysa-group has found to have spectra of the aubrite. It would be

¹⁴Near Infrared

nice to have a term of comparison also with dynamical integration and see which types can have a different behaviour both in the past and in the future. This would help to have some discrimination that could justify this “extra-hungaria” presence, i.e. C-types and S-types, (looking at the past); perhaps this differentiation could be a hint to confirm which bodies (which types) could become Mars-crossers or even all together could be united to be one new population which crosses Mars.

1.4.4 Period distribution

The synodic orbital periods of asteroids vary from about 2 hours to 1 day (Fig. 1.10). Smaller asteroids ($< 200m$) can rotate very fast, instead larger ones never rotate faster than about 10 times per day (2.4 hours). This periods are found via photometry, studying the light-curve of these bodies better. Some asteroids are not rotating, but tumbling, and so it is difficult to find their rotational period, if any, i.e. (4179) Toutatis. There is an observational suggestion that *NEAs* are indeed similar in rotation and shape to their comparably sized Main Belt counterparts.

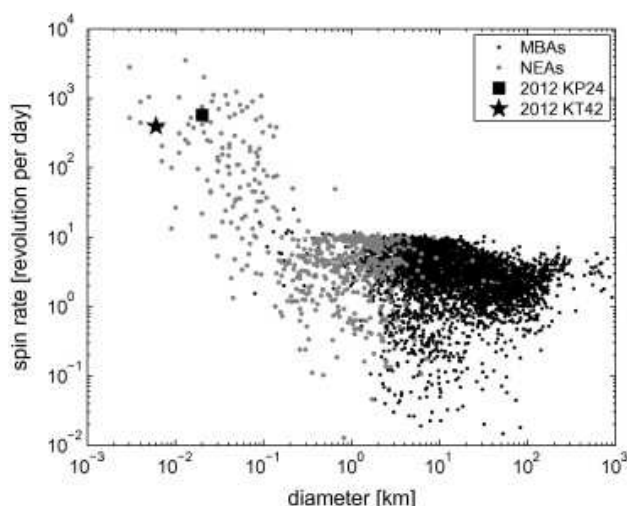


Figure 1.10: The diameter spin rate diagram of asteroids with 2012 KP₂₄ (diameter: 20 ± 6 m, squared one) and 2012 KT₄₂ (diameter: 6 ± 1 m, the one indicated by a star) marked. The background population of asteroids (*NEAs*, gray dots) and *MBAs* (black dots). Only secure rotation are plotted (quality code $U \geq 2$). The data for the background population were taken from the Light Curve Data Base (*LCDB*), version of June 2012 (Warner & Harris, 2007). Credit: Polishook et al., 2012.

1.5 Orbital integrations

The orbit of a body in the Solar System can be studied analytically or numerically. In order to do this, the n-body problem is basilar. The equation of motion in the inertial system for the $N=n+1$ point masses is:

$$\frac{d(m_i)\ddot{\vec{x}}_i}{dt} = -k^2 m_i \sum_{j=0, j \neq i}^n m_j \frac{\vec{x}_i - \vec{x}_j}{|\vec{x}_i - \vec{x}_j|^3}, \quad i = 0, 1, 2, \dots, n \quad (1.2)$$

$k = 0.01720209895 \sqrt{(AU)^3 m_{sun}^{-1} d^{-2}}$ is the Gaussian constant. Apart for comets, usually m_i is constant, so it can be cancelled out, and so the left hand side of the equation become only $\ddot{\vec{x}}_i$. Eqn. 1.2 represents a system of ordinary, nonlinear differential equation of second order in time. Unique trajectories exist (under certain conditions) for all times $t \in (-\infty, +\infty)$, provided the initial state of the system is known: $\vec{x}_i(t_o) \stackrel{def}{=} \vec{x}_{i0}$ and $\dot{\vec{x}}_i(t_o) \stackrel{def}{=} \dot{\vec{x}}_{i0}$.

The equation used to generate ephemerides of the Sun, Moon, planets and the 5 major asteroids, i.e. in the Astronomical Almanac (Beutler, 2005) is the relativistic version of the equations of motion of the planetary system also called *PPN* (Parameterized Post-Newtonian) equation of motion of the planetary N-body problem:

$$\begin{aligned} \ddot{\vec{x}}_i = & -k^2 \sum_{j=0, j \neq i}^n m_j \frac{\vec{x}_i - \vec{x}_j}{|\vec{x}_i - \vec{x}_j|^3} \left\{ 1 - \frac{2k^2(\beta + \gamma)}{c^2} \sum_{k=0, k \neq i}^n \frac{m_k}{|\vec{x}_i - \vec{x}_k|} \right. \\ & - \frac{k^2(2\beta - 1)}{c^2} \sum_{k=0, k \neq j}^n \frac{m_k}{|\vec{x}_j - \vec{x}_k|} + \gamma \frac{\dot{\vec{x}}_i^2}{c^2} + (1 + \gamma) \frac{\dot{\vec{x}}_j^2}{c^2} - \frac{2(1 + \gamma)}{c^2} \dot{\vec{x}}_i \dot{\vec{x}}_j \\ & - \frac{3}{2c^2} \left[\frac{(\vec{x}_i - \vec{x}_j) \dot{\vec{x}}_j}{|\vec{x}_i - \vec{x}_j|^3} \right]^2 - \frac{(\vec{x}_i - \vec{x}_j) \dot{\vec{x}}_j}{2c^2} \left. \right\} + \frac{k^2}{c^2} \sum_{j=0, j \neq i}^n \frac{m_k}{|\vec{x}_i - \vec{x}_j|^3} \\ & + \left\{ (\vec{x}_i - \vec{x}_j) [(2 + 2\gamma)\dot{\vec{x}}_i - (1 + 2\gamma)\dot{\vec{x}}_j] \right\} (\vec{x}_i - \vec{x}_j) + \frac{k^2(3 + 4\gamma)}{2c^2} \\ & \sum_{j=0, j \neq i}^n m_j \frac{\dot{\vec{x}}_j}{|\vec{x}_i - \vec{x}_j|^3} \quad i = 0, 1, 2, \dots, n \end{aligned} \quad (1.3)$$

β and γ come from the Lorentz factor: $\gamma = \frac{1}{\sqrt{1-v^2/c^2}} = \frac{1}{\sqrt{1-\beta^2}} = \frac{dt}{d\tau}$ and $c = 173.14463$ au/d is the light speed. The bodies are considered to be point masses in an isotropic *PPN* N-body metric. The accelerations showing up on the right-hand side may be approximated by the non-relativistic equation (Equation 1.2): the difference between relativistic and non-relativistic equations are of the order of (at maximum) a few parts in 10^{-8} ($\frac{k^2}{c^2} \approx 0.98710^{-8}$).

In case Mercury is inserted in the Solar System model, the integrations¹⁵ of the or-

¹⁵The Radau integrator (Everhart (1974) and Eggl & Dvorak (2010)) was implemented with *PPN_{red}*

bits that will be used in the works of Chapter 6, use a reduced equation (PPN_{red}) of the relativistic version of the equation of motion and not the “full” PPN, for computational reasons.

This “light version” is achieved by retaining only those correction terms proportional to m_0 , the point mass which dominates all the other masses (justified by the assumption that $m_i \ll m_0$ for $i = 1, 2, \dots, n$). With these assumptions \vec{x}_0 is infinitesimal and then calculating the correction terms, it is therefore allowed to replace \vec{x}_i by the corresponding heliocentric velocity vector \vec{r}_i . With these approximations the PPN for bodies like planets and moons may be reduced to the following equation PPN_{red} :

$$\vec{\ddot{x}} = -k^2 \sum_{j=0, j \neq i}^n m_j \frac{\vec{x}_i - \vec{x}_j}{|\vec{x}_i - \vec{x}_j|^3} + \frac{k^2 m_0}{c^2 r_i^3} \left\{ \left[4 \frac{k^2 m_0}{r_i} - \vec{r}_i^2 \right] \vec{r}_i + 4(\vec{r}_i \vec{r}_i) \vec{r}_i \right\} \quad (1.4)$$

1.5.1 Used Numerical integrations codes

Numerical integrations are performed mainly via the Lie-integrator (apart the works in Chapter 6, that are performed via Radau-integrator). The Lie-integrator is based on the Lie-series

$$L(z, t) = e^{tD} f(z) \quad (1.5)$$

where D is the Lie-operator, $D = \theta_1(z) \frac{\partial f}{\partial z_1} + \theta_2(z) \frac{\partial f}{\partial z_2} + \dots + \theta_n(z) \frac{\partial f}{\partial z_n}$. The point $z = (z_1, z_2, \dots, z_n)$ lies in the n -dimensional z -space, the function $f(z)$ is holomorphic in the same region as the function $\theta_i(z)$, which are so within a certain domain G , i.e., they can be expanded in a converging power series and they are used to represent the equation of motions of the asteroids (their orbits) (Hanslmeier & Dvorak , 1984; Delva , 1984; Eggl & Dvorak , 2010).

Close encounters and impacts are also implemented in the integrators used in this thesis. An asteroid close encounter is considered when the asteroid passes closer than a fixed distance from the planet in consideration, see Table 1.1 and Chapter 2. Instead, an impact is assumed when the body surmounts the limit of the atmospheric entry (see fig. 1 of Westman, Wannberg & Pellinen-Wannberg (2004)), for this cutoff, it has been chosen in this work a value¹⁶ for the Earth equal to 65.4 km. For the other planets an empirical equation is derived, using a constant k which depends on the scale height h_{atm} of the atmosphere, measured in astronomical units and the (surface) density of each planet (for parameters, see Table 1.2):

$$k = \rho^{(E)} h_{tot}^{(E)} / h_{atm}^{(E)}$$

¹⁶see <http://neo.jpl.nasa.gov/news/2008tc3.html>

where

$$h_{tot}^{(E)} = r^{(E)} + h_{atm}^{(E)}.$$

Here $h_{atm}^{(E)}$ is the scale height of the Earth atmosphere, $\rho^{(E)}$ the density, and $r^{(E)}$ is the radius of the Earth (also in astronomical units). The atmospheric entry (r_{imp}) for Venus and Mars is given by the equation:

$$r_{imp} = r^{(P)} + h_{tot}^{(P)} \rho^{(P)} / k$$

P stands for impact planet.

Planet/M.B.	r_{clo} [AU]	r_{imp} [AU]
Mercury	$0.30 \cdot 10^{-3}$	$1.66713 \cdot 10^{-5}$
Venus	$1.70 \cdot 10^{-3}$	$4.13258 \cdot 10^{-5}$
Earth	$2.50 \cdot 10^{-3}$	$4.30247 \cdot 10^{-5}$
Moon	$0.57 \cdot 10^{-3}$	$1.17779 \cdot 10^{-4}$
Mars	$1.66 \cdot 10^{-3}$	$2.30240 \cdot 10^{-5}$
Jupiter	$85.74 \cdot 10^{-3}$	$48.04940 \cdot 10^{-5}$
Saturn	$104.29 \cdot 10^{-3}$	$40.40027 \cdot 10^{-5}$

Table 1.1: All the data relative to the close encounters with the terrestrial planets are stored, during the orbital numerical integrations, for later examination. The close encounter limiting distance (r_{clo}) for the Earth is the average lunar distance; for other planets or minor bodies (M.B.), it is used the (planetocentric) distance scaled in proportion to the ratio of their relative Hill spheres with respect to the r_{clo} of the Earth

The integrators were also implemented with new subroutines, provided by the author of this work, in order to compute important physical parameters of impacts and close encounters, e.g. impact angle, deflection angle, impact velocity etc. (see Sections 1.8.2 and Chapter 2).

1.6 An overview on the resonances

A resonance arises when two periods or frequencies are in a simple numerical ratio. In the cases of studying the orbit of the asteroids in motion toward the Inner Main Belt, three kinds of resonances are important: (1) the mean motion resonances (*MMRs*), (2) the three body mean motion resonances (*3BMMRs*) and (3) the secular resonances (*SRs*). Resonances are very important perturbation that let asteroids from Main Belt crossing Mars' orbits increasing their eccentricity, and then entering in the *NEA*'s region as it is shown in the Subsection 1.6.3 and in Chapter 2.

Planet	radius R [km] pressure P [bar]	density ρ_1 [kg/m^3] h_{atm} [km]	density ρ_2 [kg/m^3] g [m/s]
Mercury	2439.7 ~ 0	2734 10^{-4}	- 3.7
Venus	6051.8 92	2800 15.9	3000 8.9
Earth	6371.0 1.01325	2500 8.5	2750 9.8
Moon	1738.1 ~ 0	2550 10^{-4}	- 1.62
Mars	3396.2 0.00636	2500 11.11	2800 3.71

Table 1.2: ρ_1^{Earth} and ρ_2^{Earth} are the densities of sedimentary and crystalline rock, respectively (Collins, Melosh & Marcus, 2005); ρ_1^{Venus} is the (surface) density given by the fact sheet of NASA, <http://nssdc.gsfc.nasa.gov/planetary/fact-sheet/venusfact.html>) and ρ_2^{Venus} is the upper limit of basalt given in http://geology.about.com/cs/rock_types/a/aarockspecgrav.htm. ρ_1^{Mars} is the density for Mars: we have considered the lower value for andesite (see the link mentioned just before, for Venus). $\rho_1^{Mercury}$ is the density for Mercury, from Martellato et al. (2007). ρ_1^{Moon} is the density for the Moon, from Wiczorek & Neumann (2013). For the scale heights of the atmospheres (h_{atm}), it is chosen for the Earth the value mentioned at <http://neo.jpl.nasa.gov/news/948tc3.html>. All the other parameters come from the NASA fact-sheets for each planet.

1.6.1 Mean Motion Resonance

A mean motion for an asteroid is present when there are terms, which dominate the perturbed motion of the asteroid, such as $jn_k + kn_j \approx 0$, where j and k are integers and n_j and n_k are the two bodies in resonance (or if it is considered the semimajor axis $a \approx (|j|/|k|)^{2/3}a'$), because these will contribute to the creation of a small divisor in the equation derived from the Lagrange equations, i.e. $(\Delta a)_{res} \propto \left| \frac{Ce}{2j-k-\tilde{\omega}} \right| + \left| \frac{C'-2\alpha}{2j-k} \right|$. This is visible also via the Delaunay elements: $\Gamma = \Gamma_0 + \Gamma_1 t + \sum_{j \neq k \neq 0} \frac{E_{jk}}{jn_k + kn_j} \cos(jn_k + kn_j)t + D_{jk}$, where the respective perturbations for such asteroid are large, because the amplitudes E_{jk} are divided by a quantity close to zero. D_{jk} is the phase coefficient and it is a function of $\omega_1, \Omega_1, \omega_2, \Omega_2$. E_{jk} depends on C_{jk} , a function of the osculating elements.

Therefore, e.g. when an asteroid is inside the 2:1 resonance with Jupiter¹⁷ (J2:1), the dominant terms are likely to be these with $j = \pm 1$ and $k = \pm 1$, since it will be then $2j - k \approx 0$.

It was shown that bodies in the main *MMRs* with Jupiter (J3:1, J4:1 and J5:2), can reach very high orbital eccentricities (Ferraz-Mello & Klafke , 1991; Klafke, Ferraz-Mello & Michtchenko , 1992; Saha , 1992) and so getting the asteroid close to the terrestrial planets starting from the Main Belt in a few million of years. In fact the strongest *MMRs* are where the number of asteroids are quite small in semimajor axis position, the so called Kirkwood gaps, the most prominent resonances are: J4:1 at 2.06 au, J3:1 at 2.5 au, J3:2 at 2.82 au, J7:3 at 2.95 au and J2:1 at 3.27 au. If one tries to approximate the perturbing function (a function coming out from the Lagrange's planetary equations, which are best derived using an Hamiltonian formulation. To quantify the resulting orbital variations, of the perturbed asteroid, it is needed to expand these equations using the Legendre Polynomials) for a resonance, e.g. J2:1, by an analytical approach using series of terms of different orders in the small parameters e (eccentricity) and i (inclination), the lowest order terms depend on the critical angles $\sigma = 2\lambda - \lambda_j - \varpi$ and $\sigma_1 = 2\lambda - \lambda_j - \varpi_j$ ($\varpi = \Omega + \omega$ is the longitude of the periapsis). These terms are the ones that usually librate in the case of asteroids located in the resonance. Higher order terms, and, consequently dynamically less important ones, depend on other combinations of $\lambda, \varpi, \Omega, \lambda_j, \varpi_j$ and Ω_j , which define other critical angles. In very particular cases, these critical angles librate too (Murray & Dermott , 1999; Morbidelli et al. , 2002; Dvorak & Freistetter , 2007; Gallardo et al. , 2011).

1.6.2 Three-body mean motion resonances

The three-body mean motion resonances (*3BMMRs*), or Laplace resonances, are resonances among the mean motions of a particle (a "massless" asteroid or a comet), Jupiter and Saturn (Nesvorny & Morbidelli, 1998). The typical width is at most just a few 10^{-5} au. Nesvorny & Morbidelli (1998) have identified 255

¹⁷this happens when the asteroid has its semi-major axis in the vicinity of 3.27 au.

asteroids presently locked on *3BMMRs* and extrapolating their method many more should be found in this kind of resonances. In fact also some Hungarias too, were found locked in these resonances looking in the data of Galiazzo, Bazso & Dvorak (2013a) (see Fig. 1.14). Theoretically the *3BMMR* correspond to the relation $m_j \dot{\lambda}_j + m_s \dot{\lambda}_s + m \dot{\lambda} \sim 0$ ($m_j m_s m$ three body resonances) where $\dot{\lambda}_j, \dot{\lambda}_s, \dot{\lambda}$ denote the mean motions of Jupiter, Saturn and asteroid, respectively m_j, m_s, m are integers.

The resonant angles associated to such resonances turn out to be any combination $\sigma_{p_j, p_s, p} = m_j \lambda_j + m_s \lambda_s + m \lambda + p_j \varpi_j + p_s \varpi_s + p \varpi$, where λ_j, λ_s and λ are the mean longitudes and ϖ_j, ϖ_s and ϖ are the perihelion longitudes of Jupiter, Saturn and asteroid, respectively, and p_j, p_s and p are integers which fulfill the d’Alembert rule $m_j + m_s + m + p_j + p_s + p = 0$. Since the perihelion longitudes have a small, but non zero frequency, angles $\sigma_{p_j, p_s, p}$ with different p_j, p_s and p have zero derivative at different locations. Therefore a mixed mean motion resonance of type $m_j \dot{\lambda}_j + m_s \dot{\lambda}_s + m \dot{\lambda} \sim 0$ splits in a natural way into a “multiplet” of resonances. The exact location of each component of the multiplet is given by the relation $\bar{\sigma}_{p_j, p_s, p} = m_j \dot{\lambda}_j + m_s \dot{\lambda}_s + m \dot{\lambda} + p_j \dot{\varpi}_j + p_s \dot{\varpi}_s + p \dot{\varpi}$, the dot represents the time derivative (Nesvorný & Morbidelli, 1998).

1.6.3 Secular evolution of asteroids orbits

According to secular perturbation theories, the orbital elements of the planet change with periods ranging from thousands to million of years. The changes are quasi-periodic with three basic frequencies, restricting the Solar System to the Sun-Jupiter-Saturn system. These frequencies are g_5 (or ν_5), g_6 (or ν_6) and s_6 (or ν_{16}), respectively $\langle \dot{\varpi}_{jup} \rangle$, $\langle \dot{\varpi}_{sat} \rangle$ and $\langle \dot{\Omega}_{sat} \rangle$. The planets exert also secular perturbation on asteroids and force the precession of their orbits (Froeschlé & Morbidelli, 1994).

The most important secular resonance for the distribution of the asteroids in the Main Belt is the ν_6 secular resonance, this resonance happens when the rate g_0 , of pericenter precession of a massless particle (or asteroid) is equal to the g_6 eigenfrequency of the solar system. In the current solar system, the g_6 frequency is associated with the secular mode with the most power in Saturn’s eccentricity-pericenter variations (Minton & Malhotra, 2011), then also g_5 and s_6 play an important role. These kind of resonances are called *linear secular resonances* (when they involve one asteroid and one planet frequency), otherwise they are called *non-linear secular resonances*. Milani and Knezevic (1990, 1992) developed an analytical theory based on an explicit expansion of the Hamiltonian in powers of the eccentricity and inclination of both the asteroid and the planets, truncated at degree 4 concerning the quadratic part, improved later (Milani and Knezevic, 1994), by implementing the degree 4 terms in the quadratic part. This step allowed to point out the effect of the mean motion resonances on the locations of the linear and non-linear *SRs*.

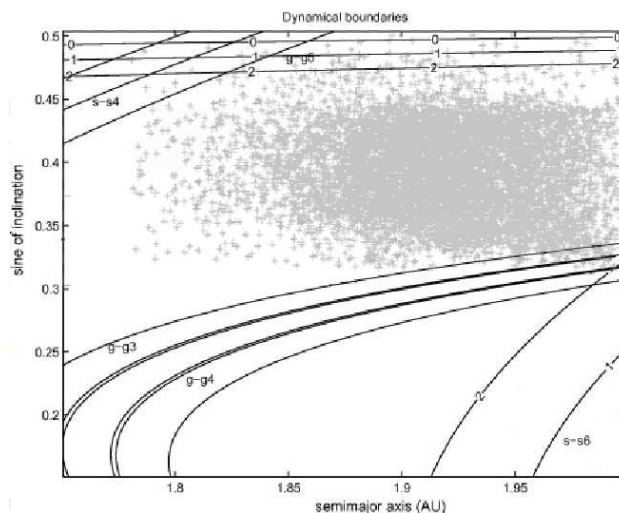


Figure 1.11: Location of the Hungaria group of asteroids in a plot with inclination (y-axis) versus the semimajor axis (x-axis). The different secular resonances are explained in the text. (Picture taken from Milani, Knežević & Cellino (2010) and modified substituting the former Hungaria family with the Hungaria group. Courtesy permission from Prof. A. Milani and Prof. Z. Knežević).

Also Morbidelli and Henrard (1991a, b) revisited the semi-numerical method by Williams, 1969, avoiding the expansion in powers of the asteroid's eccentricity and inclination. See also Appendix A.

Another form of SR exists for small objects on highly inclined orbits, although it does not involve any of the eigenfrequencies of the system, this is the *Kozai resonance*, which occurs when $\omega = 0$.

Resonances in the Hungaria region

One interesting location for resonances in the Main Belt is the Hungaria region (see also Chapter 2), which is surrounded by four main linear secular resonances (Gladman et al., 1997): $g - g_5$, $g - g_4$, $s - s_6$ and $s - s_4$ (Fig.1.11) which control the outer boundary.

They pump up the inclination, especially in the region between Mars and Earth up to 30° . In addition the M2:3 and the J4:1 are acting there, but also some higher order SR s involving Jupiter and Saturn. Two of these resonances that turn out to be of great importance in the Martian region are the $2g - g_5 - g_6$ and the $g - s - g_5 + s_6$. They act in the Martian region at low-orbital inclination (Morbidelli & Henrard, 1991a), producing eccentricities that increase on time scales of a few hundred thousand years; in fact in the sample of this thesis, the fugitives (see

Chapter 2) show in some cases this dynamical behavior.

As one can see, during the dynamical evolution the asteroids cross many *MMRs* which perturb significantly the orbits. As it was shown in McEachern, Čuk & Stewart (2010), the most destabilizing *MMRs* are M3:4, M2:3, M7:9, M5:7, M10:13 and J5:1. Then, also higher loss rates correlate well with lower order resonances, with a few exceptions.

Effects on the inclinations are clear when Hungarias pass from Mars-crossing asteroids to *NEAs*, from data in Galiazzo, Bazso & Dvorak (2013a), indicating that asteroids increase their inclinations, and then after becoming *NEAs* they immediately decrease it. These resonances act on the inclination of an hungaria's asteroid, (211279) 2002 RN₁₃₇ (whose orbit was integrated for 100 Myrs in Galiazzo, Bazso & Dvorak (2013a), see Chapter 2), around 50 Myrs (Fig. 1.13). Furthermore 2002 RN₁₃₇ is a good example for a (Hungaria-)NEA which changes from one NEA-family to another, starting to be an Amor at 64.015 Myr and then an Apollo for the first time at 72.669 Myr. The most important resonances, acting on this asteroid, are the J5:1 (that is very important just before the object becomes a *NEA*), M7:9 and E5:12. Then the asteroid pass through *MMRs* of higher order like E12:29, E8:19, V7:17 etc. and some *3BMMRs*, that play a role when no *MMRs* are present (see Fig. 1.14). This asteroid stay in particular on 2 resonances for longer time, about 0.8 Myr: V9:35 and M7:9. Just before it becomes a *NEA* and after having 2 close encounters with Mars (see fig. 1.13), it stays inside the V23:6 for about 1 Myr (at ~ 1.795 AU), probably influenced by a non-linear secular resonance, too. Fig. 1.12 shows the proof for previous resonances, in particular J5:1 and M5:7.

1.7 NEAs and their origins

The knowledge of the *NEAs*¹⁸ has grown a lot in the last years due to the activity of large surveys such as Spacewatch, the Lincoln Near-Earth Asteroid Survey (*LINEAR*), the Lowell Near-Earth Objects Search (*LONEOS*), *PannSTARSS* and finally *WISE* (observing in ultraviolet band, UV). Currently there are over ~ 9000 known *NEAs*, defined as having perihelia $q < 1.3$ au (Minor Planet Center, <http://cfa-www.harvard.edu/iau/mpc.html> and horizon.neo). The average life-time of a *NEA* is about 10 Myrs (Gladman et al. , 1997).

Abundant literature concerning the orbit and dynamical evolution of Near-Earth asteroids and Mars-crossers exists. Here a schematic discussion on their origins and interrelations with *NEA* region and other (outer) regions of the Solar System:

Near-Earth Asteroids (and *NEOs*) *NEAs* (but also some comets), originated especially in the main belt, are transported to their present position via the

¹⁸The first *NEA* was discovered in 1898, 433 Eros.

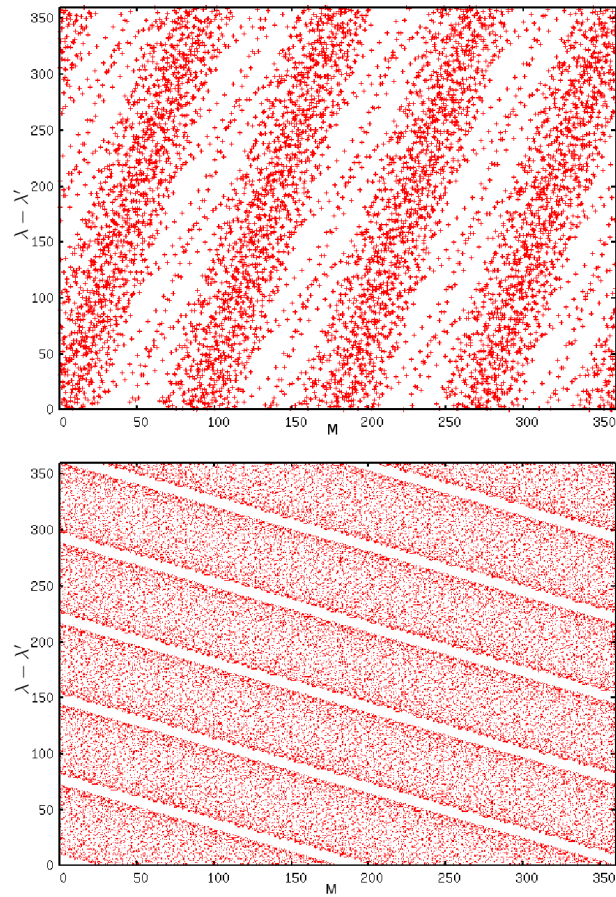


Figure 1.12: The horizontal axis displays the mean anomaly, M of the asteroid, while the vertical axis corresponds to the differences between the mean orbital longitudes $\lambda - \lambda'$ of the asteroid and the planet (Jupiter, upper panel, or Mars, lower panel). These plots confirm the existence of the resonances J5:1 (upper panel) and M5:7 (lower panel) for the Hungaria asteroid (see Erdi et al., 2012).

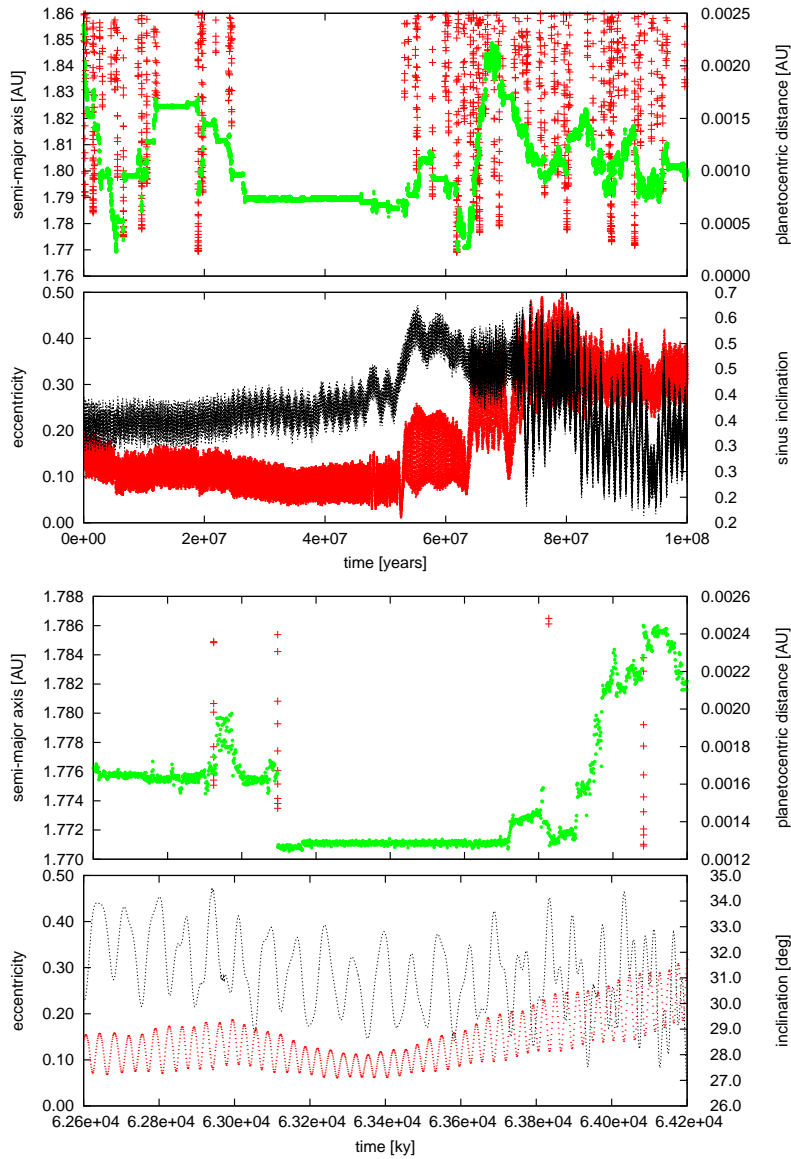


Figure 1.13: Dynamical evolution of a clone of (211279) 2002 RN₁₃₇ over 100 Myrs. From top to bottom: Semimajor axes (left, green) and planetocentric distances in astronomical units of approaches to Mars (right, red crosses); eccentricity (left, black) and inclination ($\sin(i)$, right, black) Clearly in the upper graph for a certain period of time the object has no close encounters with Mars. Lower: magnification of upper picture inside the interval of time just before the asteroid becomes an Amor. There is a very well defined periodicity of the eccentricity, with a feeble average increase due to the the resonance V23:6. A periodicity is visible also in the inclination, which is decreasing slowly.

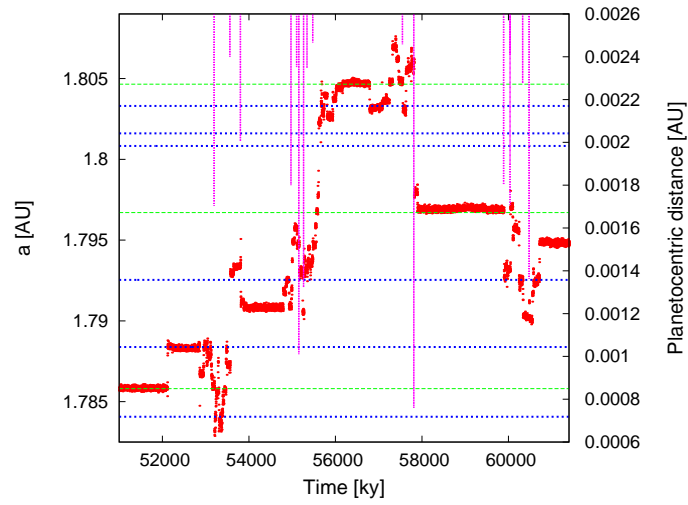


Figure 1.14: Dynamical evolution for a clone of 2000 RN₁₃₇ (member of the Hungaria family) around 5 Myrs which becomes an Amor and then an Apollo: semimajor axes (left, red) and minimum distance to Mars (right violet vertical lines). *NEA*. Resonances are indicated with straight horizontal lines (for more see text) also indicated are the resonant values in semi-major axis. Vertical lines shows when close encounters with Mars happen. The resonances act at (*MMRs* in dots and *3BMMRs* in dashes): 1.8033 au for M16:63, 1.8030 au for E19:46, 1.8016 au for M7:9, 1.8008 au for E12:29, 1.7946 au for V11:43, 1.7926 au for E5:12, 1.7884 au for V9:35, 1.7841 au for V8:31; 1.7858 au for J7:S-5:-1, 1.7967 au for J20:S-13:-3 1.8047 au for J13:S-8:-2. Red color is for the evolution of the semi-major axis for the clone (of 2000 RN₁₃₇).

action of many different resonances and close encounters with important massive bodies, like Mars. The 3:1 mean motion resonance with Jupiter and the ν_6 secular resonance with Saturn (Morbidelli & Gladman, 1998; Michel et al., 2000) are the most relevant in the inner Solar System (see also Section 1.6). *NEAs* have a probability of collision with the Earth every 500 y (Morbidelli et al., 2002). They can collide with the terrestrial planets making a crater on their surfaces. It is possible to compute the diameter of the crater considering the impact velocity (from a numerical-integration of the impactor's orbit), the impact angle, the diameter, and the density of the asteroid (Minton & Malhotra, 2010).

If they are originated by Near-Earth asteroids, the crater dimension should be smaller than the average (see also Section 6.1); in fact *NEAs* have on average smaller size compared to typical *MBAs* or other external asteroids of the Solar System. The reason is that energy equipartition among the fragments in a collisional break-up would lead to a larger spread in trajectories for smaller bodies and thus higher probability of reaching any nearby chaotic zone of phase space with subsequent increase of eccentricity (Yeomans, 1998).

Then *NEAs* of cometary origin are not so observed, there is a lack of observed *NEA*'s in Jupiter-crossing orbits and this led Rickman & Froeschlé (1980) to conclude that only a small percentage of comets can develop into *NEAs*, but this must still be evaluated better, especially after the discovering of many new sun-grazing comets like comet C/2012 S1 Ison (Chapter 8) which can give rise to some "cometal" *NEAs* of smaller sizes than its original body after crossing its perihelion.

Main Belt Asteroids The asteroids between Mars and Jupiter are a sufficient source of *NEAs* (Rabinowitz, 1996) with a chaotic diffusion towards the inner ($a < 2.5$ au) and outer parts of the Main Belt ($a > 2.8$ au) (Morbidelli & Nesvorný, 1999).

Asteroids in the main belt can be subdivided in different clusters where they share similar characteristics. One of the most accepted subdivision is based on dynamics. The personal opinion of the author of this thesis is that, together with the osculating elements, a metric that involve also observational data, both spectroscopical and photometrical should be considered. A similar approach has been followed by Nesvorný et al. (2005) and Paker et al. (2008). In fact, members of a real asteroid family share not only the orbit, but also the physical properties, as they originate from the same parent body.

Dynamically an *asteroid family* is defined as a population of asteroids that shares similar proper elements, such as proper semi-major axis, proper eccentricity and proper inclination, these elements are found via the *HCM* (Hierarchical Clustering Method), Zappalá et al. (1990, 1995) and then also via the *WAM* (Wavelet Analysis Method, Bendjoya and Zappalá, 2002).

Instead an *asteroid group* is a population of asteroids which share similar osculating elements.

All the major important properties of the families are shown in Table B.3 and B.4. Fig. 1.15 shows the distributions of the asteroids' families, represented by the osculating elements of their biggest asteroid. It is clearly visible that the majority of them stay close the osculating elements of the biggest ones, apart 2 Pallas' case, for which no family is detected at the moment.

The existence of asteroid families is a clear consequence of the collisional activity in the Main Belt.

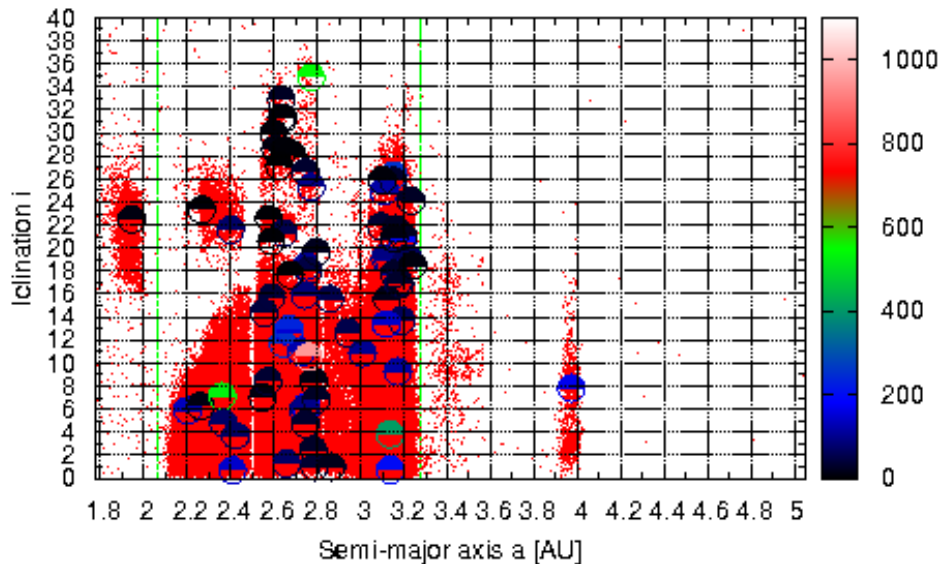


Figure 1.15: *MBAs* represented in the 3D-diagram: inclination versus semi-major axis and the diameter of the biggest asteroids (represented in colors, vertical bar: darker colors are the smallest ones and lighter ones are the largest ones, from 0 to 1100 km. Balls represent the biggest about 1000 km of diameter) of the known family in the asteroid Belt. The Main Belt is divided in 3 main regions: *IMB*, *MMB* and *OMB*, in fact the green dashed lines represents the position of the main resonances which are the borders of the regions, see Section 1.2.

From a spectroscopical point of view, it is visible from Figure 1.16, that E-type asteroids dominate the *IMB*, C-type in the *MMB* and secondarily

the S-type. Then the *OMB* is dominated by the D-type asteroids.

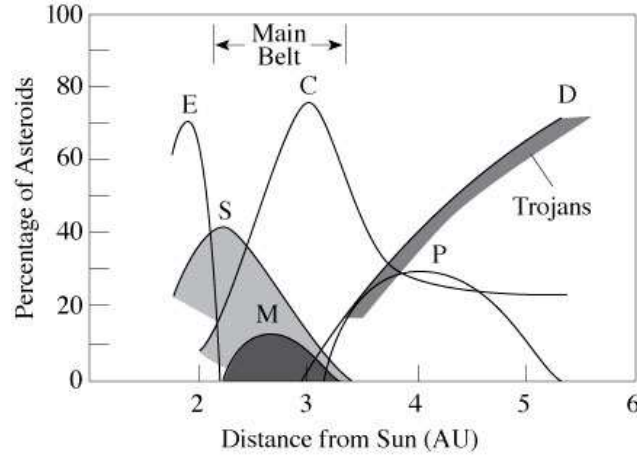


Figure 1.16: The color, or surface composition, of the asteroids is correlated with distance from the Sun. In order of increasing distance, there are white *E* asteroids, the reddish *S* silicate ones, the black *C* carbonaceous ones, and the unusually red *D* asteroids. This systematic change has been attributed to a progressive decrease in temperature with distance from the Sun at the time the asteroids formed. Simple temperature differences within the primeval solare nebula cannot, however, explain the rare metallic *M* asteroids found in the middle of the asteroid belt; they are probably the cores of former, larger parent bodies. Copyright 2010, Professor Kenneth R. Lang, Tufts University.

Concerning the density (Fig. 1.17) no clear correlation is found between the known densities and their semi-major axis, but it is clear that the smallest asteroids tend to have higher densities than the bigger ones.

The Hungaria Group is considered one relevant source of asteroids for the *NEAs* (Michel et al. , 2000; Warner et al. , 2009; McEachern, Čuk & Stewart , 2010; Milani, Knežević & Cellino , 2010; Galiazzo, Bazso & Dvorak , 2013a). Morbidelli et al. (2012) confirm that the Hungarias are the most convincing candidates that provide a considerable proportion of *NEAs* with Phocaeas (2.1-2.5 au) than the present population model estimates. They are in the *IMB* and in fact Bottke et al. (2002) assert that 85% of the *NEAs* come from there. A recent study states that Hungarias could be the cause of some lunar basins during the Late Heavy Bombardment era (Bottke et al. , 2012).

Also Nysa family seems a source region of *NEAs*, in fact some meteorites, in particular the aubritic ones, are found to fit their spectra type (Gaffey & Kelley, 2004).

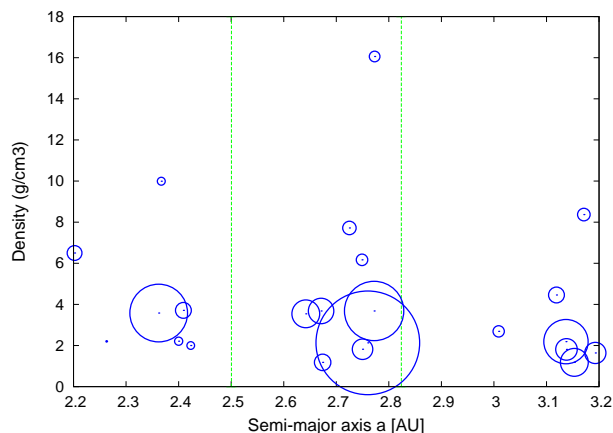


Figure 1.17: *MBAs* represented in the 3D-diagram Semi-major axis versus Inclination and diameter of asteroids proportional to the surface covered by the circle. The asteroid with the biggest density is in the *MMB* at high inclinations (Gallia Family). Green lines represent the highest Jupiter's resonances in the zone. Data from JPL-horizon database.

A large number of basaltic meteorites (e.g., the eucrites) are derived from the asteroid 4 Vesta, or from the Vesta family (so called V-types) of which 4 Vesta is considered its parent body; even if a recent basaltic meteorite (the Bunburra Rockhole Meteorite, South West Australia), which has a different oxygen isotope composition, suggests a distinct parent body for basaltic meteorites. Although its orbit was almost entirely contained within Earth's orbit, modeling indicates that it originated from the innermost Main Belt (Bland et al., 2009). This is probably because the Vesta family is supposed to be very diffusive (Delisle & Laskar , 2012).

Centaurs and *TNOs*: Trans-Jupiter Objects (*TJOs*) Objects beyond Jupiter are also sources of *NEOs* (so *NEAs*, too), but also of Main Belt Asteroids. Comets, sources of *NEAs*, are the Ecliptic comets defined by Levison (1996) as having $T_j > 2$, contains the Centaurs (objects of which orbits lie between those of Jupiter and Neptune) and part of the scattered comet disk beyond Neptune. Inside the *ECOMs*, there are the Jupiter-family comets (*JFCs*) with $2 < T_j < 3$ and some of them are just *NEAs*, now. Centaurs are likely to evolve into *JFCs*, *TNOs* (Duncan, Levison & Budd , 1995; Levison & Duncan , 1997; Tiscareno & Malhotra , 2003, 2009) and some of the Trojan populations (Rabe , 1971; Levison, Shoemaker & Shoemaker , 1997).

From the Oort Cloud, located at $a > 3000$ au (Weissman , 1996), the nearly isotropic population comets (*NICs*) pass in the *NEO's* region. This population of comets is subdivided in two main types: (i) long-period comets (*LPCs*), with periods longer than 200 years and $T_j < 2$, and (ii) Halley-

type comets (*HTCs*), with periods less than 200 years and $T_j < 2$ (Levison, 1996).

This thesis will compare in particular the acquired results from Hungarias, V-types asteroids and Centaurs orbital integrations with other past works dealing with sources of *NEAs*, i.e. Bottke et al. (2002) and Greenstreet, Ngo & Gladman (2012), see Chapter 2 and 6. Also a comparison with past literature, regarding *NEAs*' impacts with terrestrial planets, i.e. Ivanov's works (Ivanov et al., 2002), see Chapter 3.

1.8 Sources of PCAs for Terrestrial planets

Planet-Crossing Asteroids are asteroids which cross the terrestrial planets. Main Belt asteroids, Centaurs and even *TNOs* are sources of *PCAs* (Migliorini et al., 1997; Bottke et al., 2002). Inside the Main Belt, the the Hungaria family is suggested to be an important source of Earth-Crossing Asteroids (*ECAs*). This was firstly suggested at the *International Workshop On Paolo Farinella: The scientist and the Man* by Milani et al., who continued their work in Milani, Knežević & Cellino (2010) and Knežević, Novaković & Milani (2010). The last work about the Hungaria asteroids as source of *PCAs* is presented in this thesis and it is the core of it (Chapter 2, 3, 4 and 5).

1.8.1 Close encounters

For planetary close encounters Öpyk method (see Öpyk, 1976) is fundamental. A formalism based on a two-body approximation, to predict encounter outcomes, given the precounter orbit. The basic idea underlying Öpyk's computational method is that heliocentric orbits can be considered constant and Keplerian between encounters, but that during an encounter of a particle (or an asteroid) with a planet, the particle experiences a velocity change identical to that given by two-body scattering as if the Sun had no effect during the encounter. In practice, one can thus use the initial heliocentric orbit of planet and particle to determine their relative velocity U and their relative geometry as they approach one another; then use that result to compute the outcome of planet-particle Rutherford (two-body gravitational) scattering (Carusi, Valsecchi & Greenberg, 1990).

The rotation angle¹⁹ due to a close encounter is defined as so:

$$\Theta = 2\arcsin \left(1 + \frac{\Delta_{min}^2 v^4}{G^2 (M + m_o)^2} \right)^{-1/2} = 2\operatorname{arccot} \left(\frac{Gb}{Mv^2} \right) \quad (1.6)$$

v = encounter velocity, G = gravitational constant, Δ_{min} = perigee, M = mass of the planet and m_o = mass of asteroid, that it can be considered negligible in front

¹⁹called also deflection angle, see chapter 2

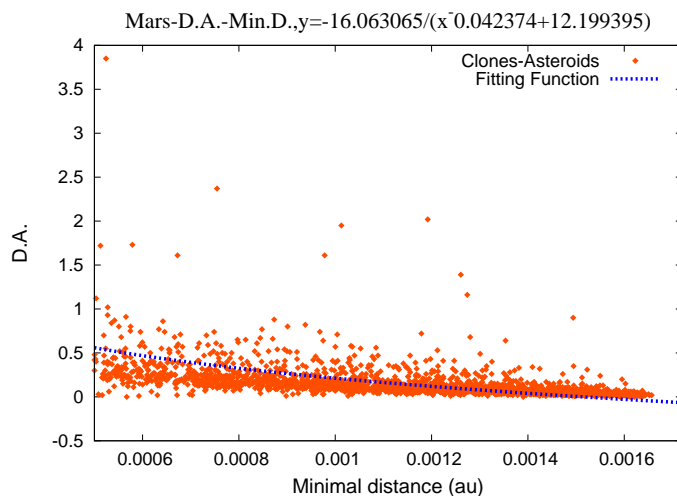


Figure 1.18: Correlation in a close encounter with Mars by all the clones of (30935) Davasobel (see Chapter 2) between angle of dispersion and minimum distance to Mars with the fitting function given by Eqn. 1.8.

of the mass of a planet, see Greenberg (1981). b is the impact parameter, that satisfy this equation:

$$1 - \left(\frac{b}{\Delta_{min}} \right) - 2 \frac{G}{Mv^2 \Delta_{min}} = 0 \quad (1.7)$$

The author of this work has found that the computation of the deflection angle can also be approximated by this equation:

$$y = a/x^b + c \quad (1.8)$$

where $y = \Theta$ and $x = \Delta_{min}$ (perigee in astronomical units). This equation is very similar to the approximation of the system to a $2BP$ (two body problem, planet plus asteroid). See Fig. 1.18, where these deflections are plotted for multiple close encounters with Mars for a hungaria asteroid during its orbital evolution of 100 Myr (see Chapter 2).

Close encounters with a planet can be modelled in a easy way, also with a restricted three body problem, i.e. the Sun-Earth-asteroid model. If close approaches are treated as causing fast (quasi-impulsive changes of the osculating Keplerian elements) these changes can be expressed as a function of the impulsion velocity increment δV . So the variation for the semimajor axis (δa) and the eccentricity (δe) can be correlated, considering the Gauss' perturbation formulae (see e.g. Bertotti & Farinella (1990)):

$$\delta a = \frac{2}{n\sqrt{1-e^2}} [\delta V_1 \cos f + e(\delta V_2 \sin f)] \quad (1.9)$$

$$\delta e = \frac{\sqrt{1-e^2}}{na} [\delta V_2 \sin f + \delta V_1 (\cos f + \frac{e + \cos f}{1 + e \cos f})] \quad (1.10)$$

where f is the asteroid's true anomaly at the time of the encounter and n is its mean motion. δV_1 and δV_2 are the transverse and radial components of the impulsive velocity increment. Assuming that the geometry of the asteroid's orbit is such that the approaches to the Earth always occur near perihelion (a good approximation, as the perihelion distance keeps close to 1 au), one can approximate those equations by taking $f \approx 0$. Then from Eqn. 1.9, it is:

$$\delta V_1 \approx \frac{n\delta a \sqrt{1-e^2}}{2(1+e)} \quad (1.11)$$

and substituting this expression in Eqn. 1.10, it is finally obtained:

$$\delta e \approx \frac{\delta a}{a} (1-e) \quad (1.12)$$

Thus δe is proportional to δa and the evolutions of e and a are well correlated. Note that Eqn. 1.12 implies that the perihelion distance q of the orbit of the asteroid is almost constant. This is consistent with the (approximate) conservation of the Tisserand invariant of this problem. Indeed, if the Earth's orbital eccentricity is neglected, the model provides just a restricted three-body problem, for which the Jacobi constant is conserved and the Tisserand parameter, defined like: $T = 1/a + 2[a(1-e^2)]^{1/2} \cos i$ (i is the inclination, a is expressed in units of the perturbing planet's semimajor axis, namely, in this case, au) is not modified by the encounters. Thus the orbit must remain close to a surface $T = \text{constant}$ in the orbital element space. For $i \sim 0$, $e \sim 0$ and $q = 1$, then $T = 3 + O(e^2)$; therefore, the orbit of a body with small inclination and $T \approx 3$ will evolve near $q = 1$, thus causing frequent Earth approaches (Michel et al., 1996)! In case of Mars $T \approx 3.514$ and Venus $T \approx 2.723$.

1.8.2 Impacts

For different reasons, it is important to date the impacts, in particular to understand the origin of the impactor. In case of the Earth, this can be done studying certain isotopes, i.e. via the $^{40}\text{Ar}/^{39}\text{Ar}$ method, used by Koeberl et al. (1997a)²⁰, to estimate the date of the impact of the Bosumtwi crater (in Ghana). In some cases also the material of the impactor can be found (Shaw & Wasserburg, 1982; Koeberl, Shukolyukov & Lugmair, 2007), again it is important to know where the impactor might come from (Galiazzo et al., 2013b). On the Moon and on Mars, the age can be estimated by the density of the impact inside a certain region and by their sizes, like the so called size frequency distribution (*SFD*) (Ivanov et al., 2002) or other methods (McEwen & Bierhaus, 2006; Werner & Neukum, 2003;

²⁰ $^{40}\text{Ar}/^{39}\text{Ar}$ step-heating age of five-Ivory Coast tektites and four mikrotektites.

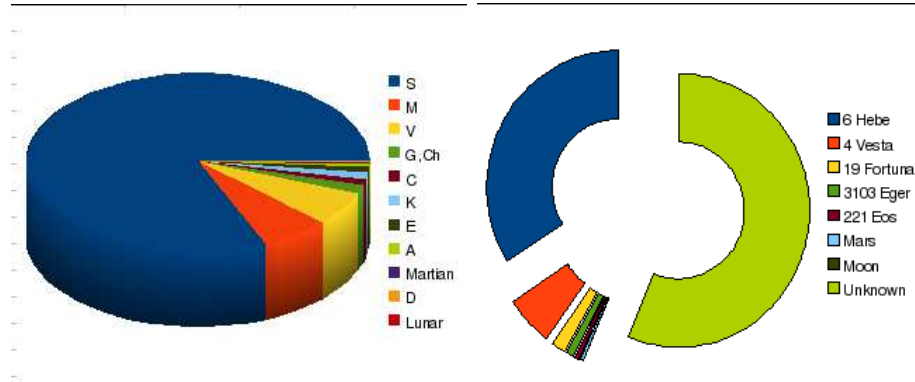


Figure 1.19: Left panel: source bodies for the Terrestrial meteorites and their relative percentage. Letters indicate the spectral type of the source, see Section 1.4.3 for details. Data source: Burbine et al. (2002a). Right panel: postulated parent bodies for the Terrestrial meteorites. Data source: Burbine et al. (2002a).

Hartmann et al. , 2012). These clashes generate craters that are now investigated in order to find their diameter, their original shape, the energy released in the impact, the velocity of the impactor, the direction and its angle of impact, all important factors to estimate the past orbit of the impactor (Galiazzo et al., 2013b). In fact impacts are classified by their size and their material and sometimes they can be associated with their impactor (Gaffey & Gilbert , 1998; Gayon-Markt et al. , 2012; Galiazzo et al. , 2013b). In case of the Earth Burbine et al. (2002a) claims that S-type asteroids seem the most probable source of meteorites, about 81.1 % of the total number of the fallen ones on the Earth, then M-type, 6.6 % and V-type 4 %; the remnants type are negligible sources in front of the previous ones (see Fig. 1.19 and the appendix B). The most prominent parent bodies for Earth’s meteorite are from the asteroids 6 Hebe and 4 Vesta (so from the Vesta family); some meteorites comes from Mars and Moon too (Figure 1.19, recently also one of Mercury’s origin was found (Malavergne et al. , 2012).

One of the most important events associate to impacts was thought to be the so called Late Heavy Bombardment, see Fig. 1.20 and Gomes et al. (2005). It is also suggested that the basin-forming portion of the *LHB* lasted from approximately 4.1-4.2 to 3.7-3.8 billion years ago on the Moon (Garrison, Rao & Bogard , 1995; Bogard , 2011; Swindle et al. , 2009; Bottke et al. , 2012), relative similarly to the other terrestrial planets. Recent studies, e.g. Nemchin et al. (2013), suggest that the *LHB* was prolonged, justifying the secondary high peaks in the rate of impacts, as it was found by Muller (2001), see Fig. 1.21. Brož et al. (2013) confirm the theory of the Nice model, studying the cometary flux through the

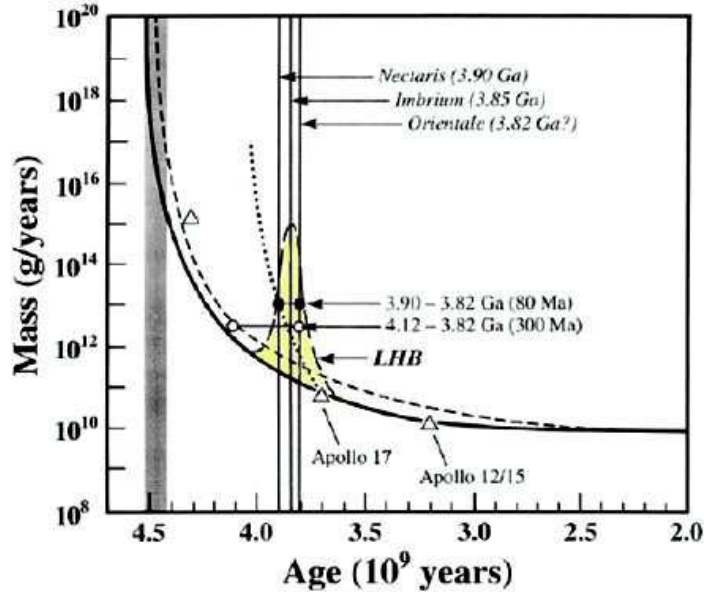


Figure 1.20: Impact flux to the Earth. Solid curve represents the flux with exponential decay, and dotted curve represents the *LHB* (i.e. the cataclysm). Ages of the major impact basin on the Moon are indicated (modified from Koeberl (2006)).

asteroid belt. On the other hand Brassler & Morbidelli (2011) suggest a passage of an escaped Giant Planet (called Planet V), which perturbed the orbits of the asteroids creating general chaos in their orbits and consequently increasing the rate of impacts on the planets.

Since this so called Late-Heavy Bombardment, the impact rate has decreased almost constantly, to within factors of a few (at least averaged over intervals of 10^8 yrs, Morrison 2002). The types of bodies responsible for impacts in the last ~ 3.5 Gyr have probably not changed appreciably (Bottke et al., 2002) and they are mostly asteroids (90%), rather than *JFCs* or Trojans. Analyses of lunar samples suggest variations in flux by up to a factor 4 (Culler et al., 2000): basically a decrease followed by an increase in the last few hundred Myrs. No evidence of shorter, sharper spikes in the flux due to hypothesized comet showers break-ups, except that they can have made at most a modest contribution to the cumulative impacts. Over a time scale of $\sim 10^7$, $\sim 10^8$ yrs, a defunct comet would either collide with a terrestrial planet (an impact by a *NEA* of cometary origin) or experience a close encounter with such an orbit with aphelion distance $\lesssim 4$ au, decoupled from Jupiter's gravitational influence (Rickman, 1991). This thesis will deal with the impact rate of 3 different regions, spreading from the *NEAs* region to the Centaurs one (Chapter 2, 3, 5 and 6).

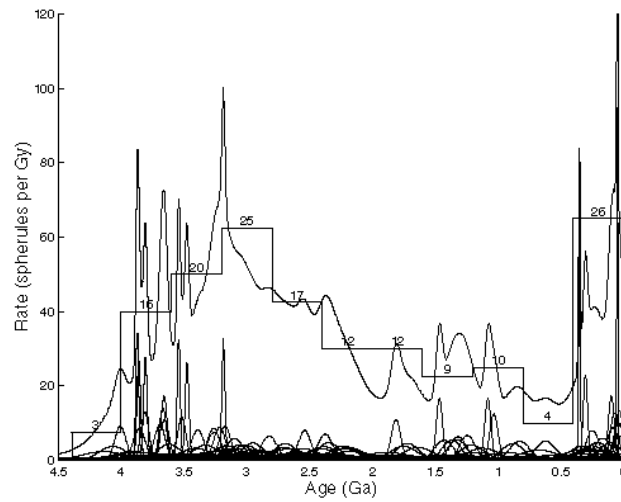


Figure 1.21: Age distribution of 155 lunar spherules for the Apollo-14 soil sample #14164, which gives an estimation on the relative cratering rate on the Moon over the time evolution of the Solar System (Muller , 2001).

1.8.3 Impacts rate on the Earth (and Moon)

The confirmed impact craters²¹ on the Earth are 185, their distribution on the planet is shown on Fig. 1.22. It is possible to get data only till 2.5 Ga, not more (see the Earth Impact Data Base²²), because the Earth is geologically active and it can erase many traces of craters, especially into the Oceans. It is currently provided that most of the terrestrial planet impact craters come from $a < 7.4$ au orbits (i.e. over 90 %), Bottke et al. 2002.

²¹as of April 7, 2013

²²<http://www.passc.net/EarthImpactDatabase>



Figure 1.22: Crater World map, updated to the 7th of April 2013. Credit: Earth Impact database. <http://www.passc.net/EarthImpactDatabase/Worldmap.htmlPhase-space>.

Chapter 2

Fugitives from the Hungaria region: Close encounters and impacts with terrestrial planets

The following article study with a numerical and statistical investigation the possibility that asteroids from the inner Main Belt, namely the Hungaria region, can be a source for Near-Earth Asteroids and Planet Crossing Asteroids too. This work is in part a continuation of a section of Bottke et al. (2002) and Greenstreet et al. (2012). Orbital evolution of these asteroids and a statistical study on their close encounters and impacts with Mars, Venus and Earth, are performed.

Authors: Mattia Alvise Galiazzo, Akos Bazso and Rudolf Dvorak²⁴

Publication state: Published August , 2013 (Online: July 15th, 2013)

Publication details: Planetary and Space Science, 84:5 (8pp), 2013

Contribution of the first author: The first author was responsible for the idea to investigate a region of the inner Main Belt, combining numerical orbital evolution of the asteroids with physical evaluations of the close encounters and impacts with the terrestrial planets. He also made the averaging methods on the orbit of Near-Earth asteroids. The development, implementation and evaluation of the proposed methodology as well as the composition of the following article were performed by the first author, too.

Contribution of the co-authors: The idea to investigate in particular the Hungaria group as well as the resources necessary for the project' success were mostly supplied by the coauthors.

²⁴Author affiliations are presented in the header of the following article.

Furthermore, the coauthors' contributions encompassed a part of the “physical” numerical integration. Finally, the co-authors played a vital role in scientific discussions and in providing proposals for some improvements of the article.



Contents lists available at SciVerse ScienceDirect

Planetary and Space Science

journal homepage: www.elsevier.com/locate/pss

Fugitives from the Hungaria region: Close encounters and impacts with terrestrial planets



M.A. Galiazzo*, Á. Bazsó, R. Dvorak

Institute of Astronomy, University of Vienna, Türkenschanzstrasse 17, A-1180 Wien, Austria

ARTICLE INFO

Article history:

Received 13 August 2012

Received in revised form

28 March 2013

Accepted 29 March 2013

Available online 25 May 2013

Keywords:

Hungaria

NEAs

Close encounters

Impacts

ABSTRACT

Hungaria asteroids, whose orbits occupy the region in element space between $1.78 < a < 2.03$ AU, $e < 0.19$, $12^\circ < i < 31^\circ$, are a possible source of Near-Earth Asteroids (NEAs). Named after (434) Hungaria these asteroids are relatively small, since the largest member of the group has a diameter of just about 11 km. They are mainly perturbed by Jupiter and Mars, possibly becoming Mars-crossers and, later, they may even cross the orbits of Earth and Venus. In this paper we analyze the close encounters and possible impacts of escaped Hungarias with the terrestrial planets. Out of about 8000 known Hungarias we selected 200 objects which are on the edge of the group. We integrated their orbits over 100 million years in a simplified model of the planetary system (Mars to Saturn) subject only to gravitational forces. We picked out a sample of 11 objects (each with 50 clones) with large variations in semi-major axis and restarted the numerical integration in a gravitational model including the planets from Venus to Saturn. Due to close encounters, some of them achieve high inclinations and eccentricities which, in turn, lead to relatively high velocity impacts on Venus, Earth, and Mars. We statistically analyze all close encounters and impacts with the terrestrial planets and determine the encounter and impact velocities of these fictitious Hungarias.

© 2013 Elsevier Ltd. All rights reserved.

1. Introduction

For the purposes of this paper we consider as belonging to the Hungaria group the asteroids whose orbital elements are in the range $1.78(\text{AU}) < a < 2.03(\text{AU})$, $12^\circ < i < 31^\circ$ and $e < 0.19$, so that our sample finally consists of 8258 asteroids; the orbital data were taken from the ASTORB database (<http://www2.lowell.edu/elgb>, updated August 2010). This orbital region is confined by the ν_6 secular resonance and by the mean motion resonances 4:1 with Jupiter and 3:4 with Mars.

There is evidence that some meteorites may originate from the Hungarias. This is deduced in the first place from the spectra of the majority of the Hungarias; about 77% of them are of the E-type, 17% belong to the S-type and 6% to the C-type (Warner et al., 2009). The E-type asteroids are consistent with the composition of some meteorites (aubrites, Zellner et al., 1977) found on the Earth.

Because of their typical composition, the Hungarias have an average albedo of $p_v \sim 0.4$ (Warner et al., 2009, hereafter abbreviated as WH), which distinguishes them from other asteroids in the main belt having $p_v \sim 0.18$ or lower.

The largest member of the group, (434) Hungaria, has a diameter of just about 11 km (Morrison, 1977).

The majority of Hungarias have a retrograde rotation and similar spin rates (Pravec et al., 2008; Rossi et al., 2009). Warner and Harris (2007) found a consistent group of binaries (more than 10%) with fast rotating primaries, this presence being a sign of a collisional origin (Durda et al., 2004; Zappalá et al., 2002). Based on the study of Lemaître and Morbidelli (1994) on proper elements WH assumed that the Hungarias formed after a catastrophic collision of (434) Hungaria, presumably the largest fragment of the Hungaria collisional family. Starting from this collisionary assumption they computed an age for the family of about 0.5 Gy that comes from the degree of spreading versus size of family members. WH, considering 2859 family members, found a value of 26 km for the diameter of the putative parent body.

Milani et al. (2010) confirmed this collisional origin, underlining the possibility of the presence of a subfamily, especially for the uniform number distribution in semi-major axis for values above 1.92 AU. They suggested a half life of 960 My and a diameter of 30 km for the parent body, this latter value in good agreement with WH. Bottke et al. (2011), in contrast to the previous suggestions about the origin, assumed that the Hungarias evolved from the depletion of a part of the primordial main belt with semi-major axes between 1.7 AU and 2.1 AU.

In the rest of this paper we present the results of our statistical investigation of the close encounters of the escaped Hungarias

* Corresponding author. Tel.: +43 1427751840.

E-mail addresses: mattia.galiazzo@gmail.com, mattia.galiazzo@univie.ac.at (M.A. Galiazzo).

with the terrestrial planets, in a model including only gravitational interactions. The methods used are described in Section 2; the results are shown in Section 3 and in Section 4 we discuss the production of NEAs from the Hungaria population. The conclusions are in Section 5.

2. Methods

Out of our 8258 Hungarias, we selected 200 according to a criterion based on the action variables (semi-major axis, a , eccentricity, e and inclination, i of the asteroid); we chose the following variable:

$$d = \sqrt{\left(\frac{e}{\langle e \rangle}\right)^2 + \left(\frac{a}{\langle a \rangle}\right)^2 + \left(\frac{\sin i}{\langle \sin i \rangle}\right)^2}$$

and picked up the 200 Hungarias with the highest values of d .

Our study of the dynamical transport to the terrestrial planets and the possible impacts was performed in two steps:

1. We integrated the orbits of the 200 asteroids in a simplified dynamical model for the solar system (Sun, Mars, Jupiter, Saturn and the massless asteroids) for 100 million years (My) to identify possible escapers (that from now on we call “fugitives”), based on the variation in of the semi-major-axis; in this way we identify 11 fugitives.
2. The 11 fugitives found (see Table 1) were then cloned, adding to each of them 49 additional sets of initial conditions (see later). We integrated the 550 objects in a model solar system including the planets from Venus to Saturn, again for 100 My; all the results presented in the paper referred to the outputs of these integrations.

All the integrations have been done using the Lie-series integrator (Eggl and Dvorak, 2010; Hanslmeier and Dvorak, 1984).

The criterion of selection for the fugitives was to check whether the excursion in semi-major axis $\Delta a = a_{max} - a_{min}$ for an individual object was $\Delta a > \Delta a_{group}/16 = 0.0156$ AU, where Δa_{group} corresponds to $\sim 7\%$ of the total range of semi-major axis spanned by the Hungarias.

For the generation of clones, we generated random values for (a, e, i), starting with the initial conditions of the escapers in the following ranges: $a \pm 0.005$ AU, $e \pm 0.003$ and $i \pm 0.005^\circ$.

It turns out that the 11 fugitives belong to the Hungaria family (see the AstDys website, <http://hamilton.dm.unipi.astro.it/>, for comparisons with the elements), so we can speak about fugitives from the Hungaria family. Two of them (30935) Davasobel and (211279) 2002 RN₁₃₇ are also present in the list of Milani et al. (2010) for the Hungaria asteroids in strongly chaotic orbits.

Table 1
Osculating elements for the escaping Hungarias: semi-major axis (a), eccentricity (e), and inclination (i) in degrees.

Asteroid	a (AU)	e	i (deg)
(211279) 2002 RN ₁₃₇	1.8538	0.1189	22.82
(41898) 2000 WN ₁₂₄	1.9073	0.1062	17.11
(39561) 1992 QA	1.8697	0.1116	26.23
(30935) Davasobel	1.9034	0.1178	27.81
(171621) 2000 CR ₅₈	1.9328	0.1051	17.19
(152648) 1997 UL ₂₀	1.9894	0.1841	28.88
(141096) 2001 XB ₄₈	1.9975	0.1055	12.32
(24883) 1996 VC ₉	1.8765	0.1556	22.71
(41577) 2000 SV ₂	1.8534	0.1843	24.97
(129450) 1991 JM	1.8512	0.1263	24.50
(175851) 1999 UF ₅	1.9065	0.1874	19.24

All the data relative to the close encounters with the terrestrial planets were stored for later examination; for the Earth we took as close encounter limiting distance the average lunar distance, 2.50×10^{-2} AU, for Mars and Venus, we used a distance scaled in proportion to the ratio of their Hill spheres with respect to the one of the Earth, namely 1.70×10^{-2} AU for Venus and 1.66×10^{-2} AU for Mars.

3. Results

Once our fugitives have left the Hungaria region, their orbital evolution becomes strongly chaotic and is strongly affected by close encounters with one or more of the terrestrial planets.

(211279) 2002 RN₁₃₇ is one example for these Hungarias fugitives that becomes NEA: it changes from one NEA-type to another, starting to be an Amor at 64.015 My and then an Apollo for the first time at 72.669 My.

We found that, when the fugitives start to be NEAs, some observed NEAs pass through similar semi-major axis and eccentricities. In fact, more than 70% of the clones are inside these ranges: $1.71(\text{AU}) < a < 2.04(\text{AU})$ and $0.21 < e < 0.38$, with a peak around $1.92(\text{AU}) < a < 2.04(\text{AU})$ and $0.32 < e < 0.38$; inside the first range we have ~ 880 known NEAs, while inside the second one we find 61 known NEAs (from http://ssd.jpl.nasa.gov/sbdb_query.cgi#x, JPL Small-Body Database Search Engine). In particular we mention 143409 (2003 BQ₄₆), 249595 (1997 GH₂₈) and 285625 (2000 RD₃₄), because they are inside the range of the absolute magnitude in visual (H_V) of Hungarias, $14 < H_V < 18$ (for details see Warner et al., 2009, Figure 3).

3.1. Close encounters

The sample of Hungarias which we used has a high probability ($> 77\%$) to have close encounters (CEs) with terrestrial planets, especially with Mars, in the 100 My time interval. We show the detailed results in Table 2 counting the CEs for every planet separately (first three columns) and the CEs (last three columns) exclusively to only one of the terrestrial planets.

Not surprisingly, most of the fictitious asteroids have CEs with Mars. The CEs to Earth and Venus tend to take place in the expected order, because the dynamical transport the inner system needs more time for Venus than for the Earth and Mars. Almost half of our bodies just meet Mars and then undergo either an ejection or a collision with the Sun (see later). None of them have only CEs with the Earth and only one of them has CEs exclusively with Venus and the Earth; three of them have CEs exclusively with Mars and Venus.

In the first three columns of Table 3 the encounter probabilities for two of the planets are not so different for any pair and also not for CEs with all the three planets. The possibility that an object meets only a specific pair is very low especially for Mars-Venus and Earth-Venus, but it is more probable for Mars-Earth.

In Table 4 one can see that the average time for a first close encounter with Venus is quite long (~ 63 My), but it is somewhat

Table 2
Close encounters for the sample of 550 Hungarias during 100 My with the terrestrial planets. Columns 2–4 for every planet separately, Columns 5–7 for a planet alone. “N.” stands for number and “%” for percentage.

	Close encounters to ...			Close encounters only to ...		
	Mars	Earth	Venus	Mars	Earth	Venus
N.	427	158	132	243	0	0
%	77.6	28.7	24.0	44.2	0.0	0.0

Table 3

Close encounters for the sample of 550 Hungarias during 100 My with the terrestrial planets. Columns 2–4 for at least two planets and columns 5–7 ONLY for two planets. M stands for Mars, E for the Earth and V for Venus. “N.” stands for number and “%” for percentage.

	Close encounters to pair ...				Close encounters only to pair ...		
	M & E	M & V	E & V	M & E & V	M & E	M & V	E & V
N.	143	122	119	138	24	3	1
%	26.0	22.2	21.6	25.1	4.4	0.6	0.2

Table 4

Average value of the time of the first CE with the planets for all objects (2nd column) and for the shortest time of a first CE with the planets for a single object 3rd column.

Planet	$\langle T_{pl} \rangle$ (My)	$T_{pl,min}$ (My)
Venus	63.34	(41577) 2000 SV ₂ 10.9
Earth	62.45	(152648) 1997 UL ₂₀ 10.5
Mars	13.51	(24883) 1996 VG ₉ 0.07

Table 5

T is the average time (of the real asteroid and the clones) when the object becomes member of the NEA family, T_{min} is the minimum time for the indicated object.

Family	$\langle T \rangle$ (My)	T_{min} (My)
Amor	46.67	(41577) 2000 SV ₂ 0.09
Apollo	60.82	(152648) 1997 UL ₂₀ 1.68
Aten	61.44	(152648) 1997 UL ₂₀ 8.40
Atira	69.37	(152648) 1997 UL ₂₀ 8.92

surprising that this time is not much smaller for the Earth (~62 My). For the first CE with Mars the average time is very low (~14 My); we already explained it with the relative closeness of the semi-major axes of Mars with the perihelion distances of the Hungarias.

In Table 5 the average time $\langle T_{pl} \rangle$ for an object to become member of a NEA type (i.e. Amor, Apollo, Aten and IEO) is listed. These four groups are defined as follows:

- *IEOs (Inner Earth Orbits)*.¹ NEAs whose orbits are contained entirely with the orbit of the Earth with $a < 1.0$ AU, $Q < 0.983$ AU.
- *Atens*. Earth-crossing NEAs with semi-major axes smaller than Earth's, named after (2062) Aten – with $a < 1.0$ AU, $Q > 0.983$ AU.
- *Apollos*. Earth-crossing NEAs with semi-major axes larger than Earth's, named after (1862) Apollo, with $a > 1.0$ AU, $q < 1.017$ AU.
- *Amors*. Earth-approaching NEAs with orbits exterior to Earth's but interior to Mars, named after (1221) Amor, with $a > 1.0$ AU, $1.017(\text{AU}) < q < 1.3(\text{AU})$.

The table shows how $\langle T_{pl} \rangle$ increases going from the outer NEAs (the Amors) to the inner ones (the IEOs).

In Table 6 we show the percentage of the clones which collide with the Sun. In particular the clones of (41577) 2000 SV₂ have the highest probability to hit the Sun, while also (152648) 1997 UL₂₀, (141096) 2001 XB₄₈ and (39561) 1992 QA have high chances to do so (Table 6).

According to our statistics we can say that about 18% from the escaping Hungarias end up as Sun colliders within 100 My.

¹ Sometimes we will call them also Atiras.

Table 6

Number of clones per 100 My per asteroid that end up as sun-impactors (we assume an impact with the Sun at whenever its perihelion is less than 0.0047 AU, approximately the radius of the Sun) with the average and the minimum perihelion of their clones.

Asteroid	Imp. Sun (%/100My)	$\langle P \rangle$ (AU/100My)	q (AU)
(211279) 2002 RN ₁₃₇	4	0.90 ± 0.33	0.00
(41898) 2000 WN ₁₂₄	0	1.55 ± 0.07	1.02
(39561) 1992 QA	22	0.96 ± 0.30	0.00
(30935) Davasobel	14	0.69 ± 0.19	0.00
(171621) 2000 CR ₅₈	2	1.61 ± 0.17	0.00
(152648) 1997 UL ₂₀	36	0.82 ± 0.34	0.00
(141096) 2001 XB ₄₈	50	0.54 ± 0.23	0.00
(24883) 1996 VG ₉	4	1.37 ± 0.07	0.00
(41577) 2000 SV ₂	40	0.68 ± 0.37	0.00
(129450) 1991 JM	4	1.20 ± 0.20	0.00
(175851) 1999 UF ₅	20	1.07 ± 0.28	0.00

Table 7

Dynamical evolution for clones (211279) 2002 RN₁₃₇ and (41577) 2000 SV₂ describing to which asteroid group the objects belong to; in addition the semi-major axes a , the eccentricity e , the inclination i and the Tisserand parameter and its variation are given in columns 3–6.

Family/group	T (My)	a (AU)	e	i (deg)	T. Par.	Var. (%)
(211279) 2002 RN ₁₃₇						
Hungaria	0	1.8552	0.1175	22.82	1.51625	0.0
First enc. Mars	0.050	1.8551	0.1625	25.46	1.48297	2.2
leaves Hungarias	0.063	1.8540	0.1904	23.47	1.49585	1.4
NEA-Amor	64.016	1.7817	0.2719	29.09	1.40315	7.5
NEA-Apollo	72.670	1.8166	0.4478	28.23	1.33699	11.9
(41577) 2000 SV ₂						
Hungaria	0	1.8517	0.1850	24.97	1.48231	0.0
leaves Hungarias	0.004	1.8517	0.1988	24.16	1.48684	0.3
NEA-Amor	0.085	1.8490	0.2991	24.29	1.45306	2.0
First enc. Mars	0.226	1.8501	0.2331	23.25	1.48553	0.2
First enc. Earth	77.926	2.0553	0.5048	3.98	1.47785	0.3
First enc. Venus	78.544	2.1634	0.7259	5.61	1.23792	16.5
NEA-Apollo	77.889	2.0485	0.5036	0.73	1.48050	0.1
Sun-impact	85.545	2.3541	0.9999	20.89	0.23267	84.3

From the first sample (200 fictitious asteroids out of ~8000) we found only 5% of escapers, so our estimate of an upper limit of Sun-impactor Hungarias in the time scale of 100 My is 0.98%, instead for the planet's impacts (0.23%). Only a very minor fraction escape beyond Jupiter's orbit and become Centaurs and afterwards Trans-Neptunian Objects (TNOs), just < 1% of them.

3.2. Analysis of close encounter data

As an example of the dynamical evolution we discuss two examples out of our sample, (211279) 2002 RN₁₃₇, that ends as member of the Apollo group, and (41577) 2000 SV₂, that has an impact on the Sun. Both show the characteristic behavior of changing the group membership inside the NEAs. In Table 7 details on the escape times from the Hungaria region of these two asteroids are given. Here “escapers” mean that the Hungarias' orbital elements (a, e, i) fall outside the range of semi-major axes a , eccentricity e , or inclination i defined in Section 2.

In general, the fugitives leave the group very soon, sometimes in less than 10^5 years, apart from (41898) 2000 WN₁₂₄, that has only five clones which escape after CEs to Mars. If the escapers have CEs with Mars, they also become NEAs (Table 4, note that here the ones that becomes soon NEAs have a higher probability than the others to become sun grazers, e.g. (41577) 2000 SV₂, Table 7), in particular Apollos and Amors, but changing orbital type during the last millions of years of the integration.

Shoemaker et al. (1979) showed that asteroids frequently change the NEA family due to their chaotic orbits (Tables 8 and 9).

When belonging to the Amor group within 11 My (average on the whole) or less, they become Apollos, and in many cases also Atens and Atiras, e.g. (152648) 1997 UL₂₀, whose clones have a huge number of close encounters with all the terrestrial planets. Their eccentricities will raise up after close encounters with Mars, and then impacts on all terrestrial planets are possible, even on the Sun. Observing the average inclination in Table 10, the inclination of the asteroids that have very likely become NEAs, like (211279) 2002 RN₁₃₇, (30935) Davasobel and (39561) 1992 QA, increases.

It is interesting to see that the normalized Tisserand parameter ($T_{ast} = (1/2a) + \sqrt{a(1-e^2)} \cos(i)$, where a is the semi-major axis of

Table 8

Average velocity of the asteroids in respect to Venus, the Earth, and Mars and standard deviation. The first row is the average of the entry velocity of the all Hungaria fugitives clones per planet, the second one is the average of the real asteroids that cross the orbit of the planets.

Sample	$\langle v_{r,Venus} \rangle$	$\langle v_{r,Earth} \rangle$	$\langle v_{r,Mars} \rangle$
Hungaria fugitives	27.80 ± 1.71	21.54 ± 2.30	10.85 ± 1.01
Real asteroids	21.66 ± 8.69	15.18 ± 7.35	10.83 ± 4.99

Table 9

Data of the planetary close encounters for some of the 11 Hungaria fugitives. All the velocities were measured at the distance for an encounter relative to the planet (2.50×10^{-2} AU for the Earth, 1.70×10^{-2} AU for Venus and 1.66×10^{-2} AU for Mars, as defined in Section 2); \bar{v}_{en} is the mean entry velocity, $\bar{v}_{en,max}$ is the mean maximum entry velocity, and $\bar{v}_{en,min}$ is the mean minimum entry velocity. We found that the exit velocity is always equal to the entry velocity inside a range of 0.01 km/s.

Planet	Ast.	\bar{v}_{en}	$\bar{v}_{en,max}$	$\bar{v}_{en,min}$
Venus	(211279) 2002 RN ₁₃₇	27.32 ± 7.42	35.10	19.26
	(30935) Davasobel	29.76 ± 7.38	37.42	24.38
	(39561) 1992 QA	29.28 ± 11.67	42.03	22.66
Earth	(211279) 2002 RN ₁₃₇	20.03 ± 6.64	29.94	12.60
	(30935) Davasobel	20.36 ± 6.07	28.64	16.54
	(39561) 1992 QA	22.32 ± 12.17	31.32	13.05
Mars	(211279) 2002 RN ₁₃₇	10.71 ± 1.71	16.63	5.96
	(30935) Davasobel	13.15 ± 1.72	19.12	7.91
	(39561) 1992 QA	11.05 ± 1.50	16.29	7.14

Table 10

Data of the planetary close encounters for some of the 11 Hungaria fugitives (1=(211279) 2002 RN₁₃₇, 2=(30935) Davasobel and 3=(39517) 1992 QA. All the inclinations was measured at the distance for an encounter relative to the planet (2.50×10^{-2} AU for the Earth, 1.70×10^{-2} AU for Venus and 1.66×10^{-2} AU for Mars, as defined in Section 2); \bar{i}_{en} is the mean entry inclination, $\bar{i}_{en,max}$ is the mean maximum entry inclination and $\bar{i}_{en,min}$ is the mean minimum entry inclination over all clones, \bar{i}_{ex} is the mean exit inclination, $\bar{i}_{ex,max}$ is the mean maximum exit inclination, $\bar{i}_{ex,min}$ is the mean minimum exit inclination.

Planet	Ast.	\bar{i}_{en}	$\bar{i}_{en,max}$	$\bar{i}_{en,min}$	\bar{i}_{ex}	$\bar{i}_{ex,max}$	$\bar{i}_{ex,min}$
Venus	1	25.80 ± 14.42	36.30	15.31	25.82 ± 14.38	36.30	15.35
	2	26.16 ± 14.43	39.43	16.68	26.15 ± 14.41	39.47	16.67
	3	23.94 ± 20.60	33.47	17.88	23.91 ± 20.62	33.28	17.88
Earth	1	22.72 ± 12.55	36.29	11.13	22.66 ± 12.62	36.32	11.05
	2	25.61 ± 11.23	36.85	18.92	25.51 ± 11.26	36.69	18.91
	3	27.34 ± 22.88	39.25	15.72	27.39 ± 22.96	39.20	15.77
Mars	1	23.26 ± 4.14	33.76	12.44	23.26 ± 4.14	37.72	12.43
	2	27.00 ± 4.67	38.59	15.66	27.00 ± 4.68	38.59	15.66
	3	23.85 ± 3.40	32.15	16.01	23.85 ± 3.40	32.15	16.02

the asteroid orbit, e is the eccentricity and i is the inclination) stays almost constant after different close encounters also with the Earth; see Table 7, where in the last column where we have put the variation in percentage of the first value. Till the asteroid is not a NEA, the parameter does not vary more than 2% and stays close to the average value for the Hungaria family, that is 1.546 ± 0.017 which, just for comparison to the value for the Vesta 1.740 ± 0.006 (from data by Galiazzo et al., 2012), is much lower.

From the close encounters we derive information about the duration (time while the body enters and exits from the region defined for a close encounter for each planet, see Section 2) and the relative velocity in front of each terrestrial planets. This last one will be compared with the relative velocity of the observed NEAs.

We study the relation between the duration and the absolute number of close encounters, with one or more terrestrial planets. We underline that the mean duration of close encounters depends on how many planets the Hungaria-fugitive can approach: more often planets are reached, shorter are the duration of the encounters.

In fact for those objects that have the lowest probability to have close encounters we find a bigger duration, i.e. the maximum value with Mars is for (41898) 2000 WN₁₂₄ (0.65 d), which also has only a small probability to have a close approach with the planet, and does not approach the other two planets.

Of course the singular event depends mainly on the entry velocity. The “entry velocity” is the velocity of the asteroid when it arrives for the first time at the maximum distance established for a close encounter from the planet.

On average the mean duration of close encounters with Mars is about half a day, and this is the highest value for the terrestrial planets. In summary: 0.27 ± 0.05 d for Venus, 0.36 ± 0.09 d for Earth and 0.55 ± 0.05 d for Mars.

The Hungaria-fugitives seem to have more close encounters, even if the scattering of encounters' mean is relatively high, with the Earth respect to the other planets. In fact the average number of close encounters for each terrestrial planet in 100 My of orbit-evolution is for Mars 57, for the Earth 77 and for Venus 42, even if almost all of them has a close encounter with Mars, but not with the other two terrestrial planets (see Table 2).

The average deflection angle θ , i.e. the angle between the direction of the entry velocity vector and the one of the exit velocity vector, is usually very small ($< 1^\circ$), though in some cases we get values of more than 60° , and even more than 90° like for (129450) 1991 JM.

The mean entry velocities for the fugitives are compared with the mean velocity of the real known asteroids with respect to each planet.

In order to compute the relative velocity of the known asteroids in front of the planets we considered:

- As Venus-crossers: IEOs (the ones with $Q \geq 0.718$ AU), Atens (the ones with $q \leq 0.728$ AU) and Apollos (the ones with $q \leq 0.728$ AU).
- As Earth-crossers: Atens and Apollos.
- As Mars-crossers: Mars crossing asteroids (the non-NEA ones with $1.300(\text{AU}) < q < 1.666(\text{AU})$ and $a < 3.2$ AU), and all the NEAs with $Q \geq 1.381$ AU (so no IEOs, but a part of the other NEA-types).

The close encounter velocity of the real asteroids (v_r) is computed with the next equations

$$v_r = Uv_{planet}$$

$$v_{planet} = \sqrt{\frac{G(M_{sun} + M_{planet})}{r_{planet}}}$$

$$U = \sqrt{3 - T_{planet}}$$

$$T_{planet} = \frac{a_{planet}}{a_{ast}} + 2 \sqrt{\frac{a_{ast}}{a_{planet}} (1 - e_{ast}^2)} \cos i_{ast}$$

where G , M_{sun} , M_{planet} and r_{planet} are respectively the gravitational constant, the mass of the Sun, the mass of the planet, and the heliocentric distance of the planet from the Sun, assumed as the semi-major axis of the planet, all values in SI, the international system of measures. U is the adimensional encounter velocity at infinity computed via the Tisserand parameter (T_{planet}) in respect to the relative planet. a_{planet} is the semi-major axis of the relative planet, to which we compute the parameter, and the remnants values are the other osculatory elements of each asteroids to compare to the relative planet.

We take in account of the circular orbital velocity of each planet ($v_E = 29.7892$, $v_M = 24.1333$ and $v_V = 34.9084$ respectively for the one of the Earth, Mars and Venus, all in km/s).

By our results the encounter velocity is greater for Hungarias than the mean, especially for Venus and the Earth, Mars is pretty the same, despite the high standard deviation. The values would give a more probable larger impact velocities in case of an impacts than the average one found for all type of impactors, so it seems that possible Hungarias' impactors are faster than the average.

4. Hungarias as a source of NEAs

4.1. Evolution when in NEA orbits

Some fugitives start to be NEAs quite soon with a peak on their rate distribution during their orbital evolution, around 60 My, as it can be seen clearly from Fig. 1. In this histogram the value N is equal to the normalized number of asteroids per each time, found with this equation

$$N = \frac{N_{c-n}}{N_c} \cdot \frac{N_f}{N_s}$$

N_{c-n} , N_c , N_f and N_s are respectively the number of Hungaria-clones (HCs) which has become NEAs, the total number of HCs at the

beginning of the orbital evolution, the number of the fugitives (Hungarias escaped from the initial sample of 200 real Hungarias), and the total number of the initial sample (200), considered as representative of the whole family.

The majority of them are Amors, but there is a consistent number of Apollos that stay constantly growing up till even after all the NEAs reach their maximum value (in fact after the peak of the NEAs, the Amors decrease their quantity). Same behavior, as for the Apollos, is visible for Atens and IEOs; but after 90 My their number go down, because of impacts (with the planets or with the Sun).

The average life and the relative release of NEA-types in comparison with some results of Bottke et al. (2002) are described in Table 11.

Bottke et al. (2002) subdivided the source of NEOs (Near-Earth objects, so not only asteroids, but also comets with $q < 1.3$ AU) in different regions (Bottke et al., 2002 used the so-called extended target region with these constraints: $q < 1.3$ AU, $a < 4.2$ AU, $e < 1.0$, $i < 90^\circ$ and $13 < H < 22$), where we have added the prefix Neas:

- *Neas*(ν_6), where the secular resonance ν_6 (which occurs when the mean precession rates of the longitudes of perihelia of the asteroid and of Saturn are equal to each other) is more active in the Main Belt.
- *Neas*(J3 : 1), where the mean motion resonance with Jupiter J3:1 is more active in the Main Belt.
- *Neas*IMCs, Intermediate source Mars-crossing asteroids, the subset of the Mars-crossing asteroid population that borders the Main Belt.
- *Neas*(OB), the Outer Main Belt.
- *Neas*(ECOMs), the Ecliptic comets.

We find that the average life of the Hungaria-NEAs (Table 11, where last five rows are referred to Bottke et al.'s (2002) regions) is about the double of the asteroid coming from the Outer Main Belt, but much more less then the ones coming from the J3:1 and the ν_6 resonances (see also Bottke et al., 2002, Table 3). Looking at the average life time spent in a region, they are the majorities of their

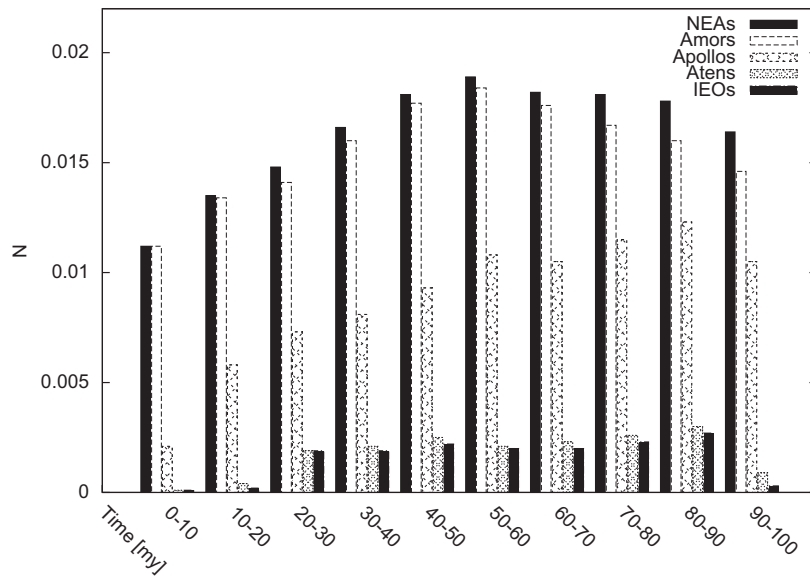


Fig. 1. Evolution of the Hungaria-NEAs: time versus number of NEAs and their types. The number is found like described at the beginning of Section 4.1. Note that during this interval of time, the NEA-type can change. In the interval of time, the first darkest vertical bar on the left is representative of the NEAs and the last, the fourth one, the IEOs.

life Atens during 100 My of integration, but the maximum life is when they are Apollos.

The majority of the fugitives that becomes NEAs are Amors, then IEOs and Atens are moreless in equal number as population of Hungaria-NEAs. The percentage for estimating the population is the normalized number of asteroids per each time (N , described before) in percentage, simply $\% = N \times 100$.

Instead, concerning their relative lost of asteroids in the Main Belt, its supply is quite comparable to the Outer Main Belt Region, but more than two times less the IMCs (see Table 11). If the lost of these family is constant, in case of no external supply, it will finish its own existence in about 3.125 Gy.

Table 11

$\langle L_{TR-100} \rangle$ is the mean life time spent in the target region ($q < 1.3$ AU), and $L_{TR-100,MAX}$ is its maximum value, both during an orbital evolution of 100 My. % is the percentage of Hungarias (the fraction of the total population of the Hungarias, assumed as the first 200 considered as the sample of the whole family, that enter in the target region) which is source of the relative target region in 100 My. Data that are not about Hungarias (H) comes from (Bottke et al., 2002) (see Tables 3 and 1; i. e. for ν_6 , initial number of particles were 3519 and 360 of them became NEO on average, so 10.2%) and are put only as comparisons; here $\langle L_{ETR} \rangle$ (My) and $L_{ETR,MAX}$ as the same meaning as previously said with the only different that the value are taken in the extended target region used by Bottke et al. (2002) and the objects were integrated there for at least 100 My.

Type	$\langle L_{TR-100} \rangle$ (My)	$L_{ETR-100,MAX}$	%
IEOs	0.052 ± 0.001	3.144	0.5
Atens	0.207 ± 0.001	13.981	0.5
Apollos	0.101 ± 0.001	82.38	2.7
Amors	0.016 ± 0.001	12.893	3.2
Neas	0.269 ± 0.001	90.112	3.2
Source region	$\langle L_{TR} \rangle$ (My)	$L_{TR,MAX}$	%
Neas (ν_6)	6.54	–	10.2
Neas (IMCs)	3.75	–	8.1
Neas (J3 : 1)	2.16	–	9.3
Neas (OB)	0.14	–	4.0
Neas (ECOMs)	45	–	–

4.2. Impacts

During the integration we found some tens of impacts with the terrestrial planets, Venus captures the highest number (Fig. 2 and Table 13). The highest rate of impacts is between 20 and 30 My, but this does not affect the behavior of increasing the number of NEAs during this interval of time (see Fig. 1). Then there is a time span of circa 20 My without impacts with planets (but only with the Sun), starting again in the last 30 My. Other objects that finish may have an impact with Jupiter too, but we did not take in account the study of close encounters with this planet in this work and usually we see a not significant value of asteroids that cross the Jupiter's orbit. So the most important bodies in cleaning up the Hungarias-NEAs seems to be in order the Sun and Venus. It is important to notice that there is a certain probability (even if it is very small) that Hungarias may hit the Earth and Mars too, that it is important for nowadays studies: the probability for these fugitives to hit the Earth and Mars in 100 My respectively is 0.7% and 1.1%. Comparing the Hungarias to other sources in respect to the impacts with Venus and Earth, the ratio suggests that Hungarias hit more Venus than the others about three times more (see Table 12), even if the statics is minimal and the quantity of impacts are of low numbers. The impact flux of Mars is less relevant than Venus in comparison to the Earth.

The impact-rate is very lower with the average of the planetary crossers, making a comparison with Ivanov et al. (2002), which take in account the observed planetary crossers with $H < 17$, this is clear in Table 13, the highest contribution by the Hungarias to the impactor populations is $< 3\%$. Between the impactor population the one in which the Hungarias most contribute is the Martian impactor population.

4.3. Averaging the elements and analysis

We averaged all the elements of the 50 clones for each fugitives every 1000 years time step. We subdivided the clones in two groups: (1) asteroids that become NEAs ($HNeas$) and (2) asteroids that do not become NEAs ($HNoNeas$).

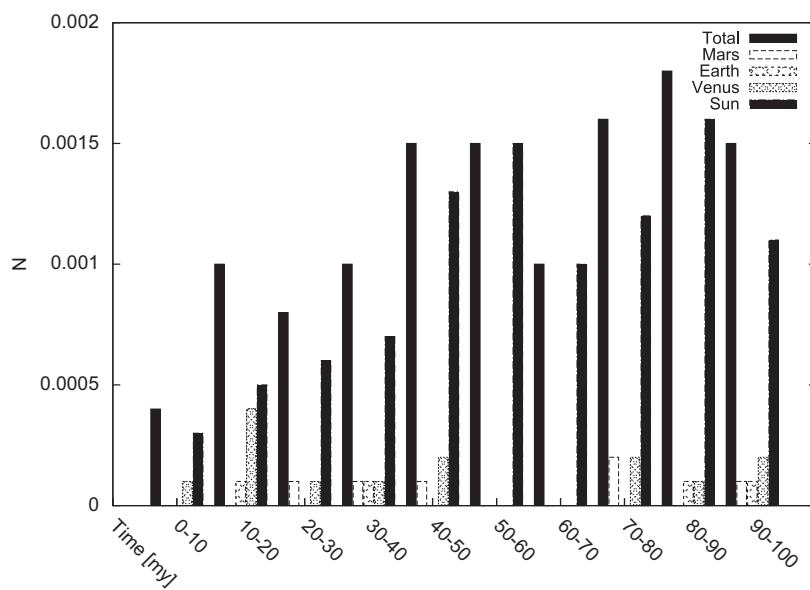


Fig. 2. Evolution of the Hungaria-NEAs: time versus number of impacts and their types. The impacts with the Sun are more determinant for the final life of the asteroids: the number of impact with the Sun is always major than the number of the impacts with all the planets, even if the impacts with Venus are comparable especially in the first 20 My.

Table 12
Impact flux ratios (per unit surface area of target), IFR, for Venus/Earth for the individual asteroidal source integrations compared to values in (Greenstreet et al., 2012, Table 4).

Impact flux ratio	H	ν_6	3:1	IMC	OMB
Venus/Earth	3.16	1.22	1.19	1.10	0.77
Mars/Earth	0.43	–	–	–	–

Table 13
Average collision probability per one body (planetary crosser) per Gy. The value of the asteroids with $H < 17$ is from Ivanov et al. (2002). % ratio is the ratio in percentage between the rate of impacts in 1 Gy between the two tested populations.

Planet	Hungarias	Asteroids ($H < 17$)	% Ratio
Venus	0.014	4.500	0.3
Earth	0.004	3.400	0.12
Mars	0.006	0.210	2.86

Finally we consider the data of the group $HNeas$ from the time instant when they start to be NEAs to 10 My after: putting time 0 at the moment when they become NEAs, we do the averaging for the following 10 My (so we average all the Hungaria-NEAs, the clones of the fugitives which are NEAs) and we call this one $NormHNeas$ from now on. For all these cases we will show in detail the averaging over two fugitives only, representative for the others nine ones.

In the case of $HNeas$ we see (Figs. 3–5) that their semi-major axis oscillates much more than $HNoNeas$, especially after the majorities of them become NEAs and they only decrease this value; instead for the $HNoNeas$, the stability is visible (semi-major axis and eccentricity are almost constant) till arriving in the proximity of the end of the integration. At the end of evolution, in the last ~30 millions year of integration, the scattering increase visibly, due to some impacts and close encounters with Mars, too.

The eccentricity for the $HNeas$ has an average increase of about 0.002 My^{-1} .

The big scattering visible in Figs. 3–5, at ~88 My for (211279) 2002 RN₁₃₇ and at 65 My for (152648) 1997 UL₂₀, is due to some

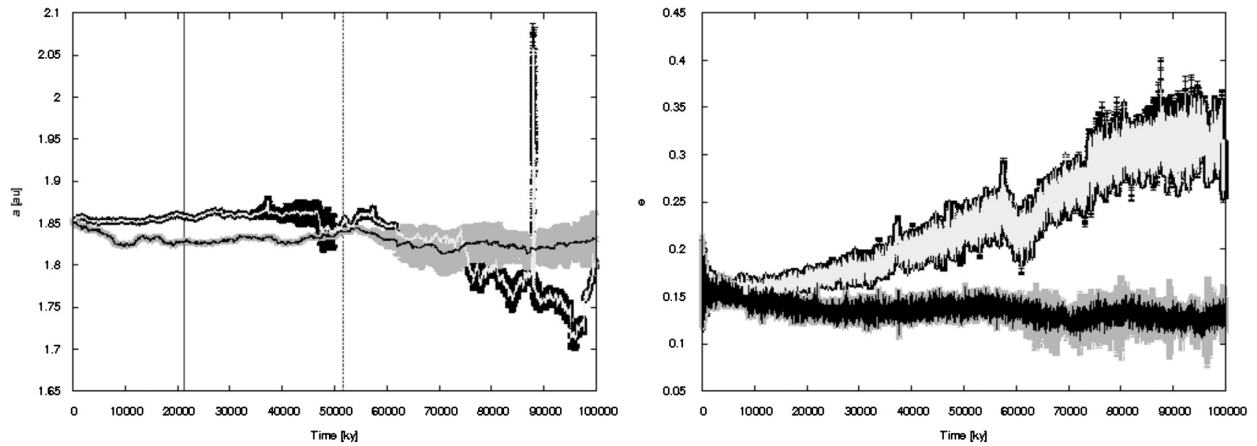


Fig. 3. Averaging of the elements with the standard deviation of the 50 clones of the asteroid (211279) 2002 RN₁₃₇. All points with a standard deviation major than 50% of the measure of the average have been rejected. Left panel: semi-major axis versus time for the averaging. The first vertical line is the time when the first clone become a NEA. The second one is the average time for the clones to become NEAs. Right panel: eccentricity versus time.

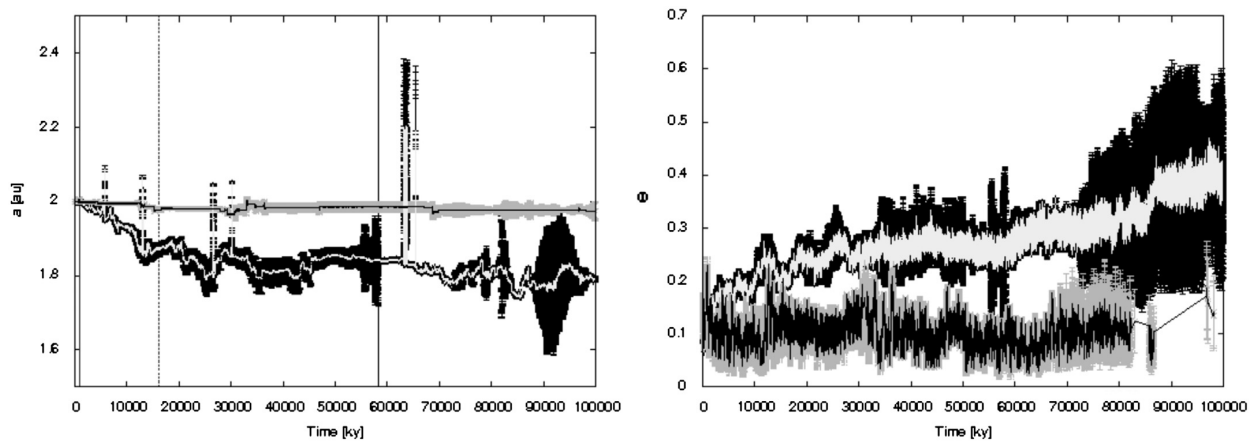


Fig. 4. Averaging of the elements with the standard deviation of the 50 clones of the asteroid (152648) 1997 UL₂₀. All points with a standard deviation major than 50% of the measure of the average have been rejected. Left panel: semi-major axis versus time for the averaging, at ~58 My there is a large scattering. The first vertical line is the time when the first clone become a NEA. The second one is the average time for the clone to become NEAs. Right panel: eccentricity versus time.

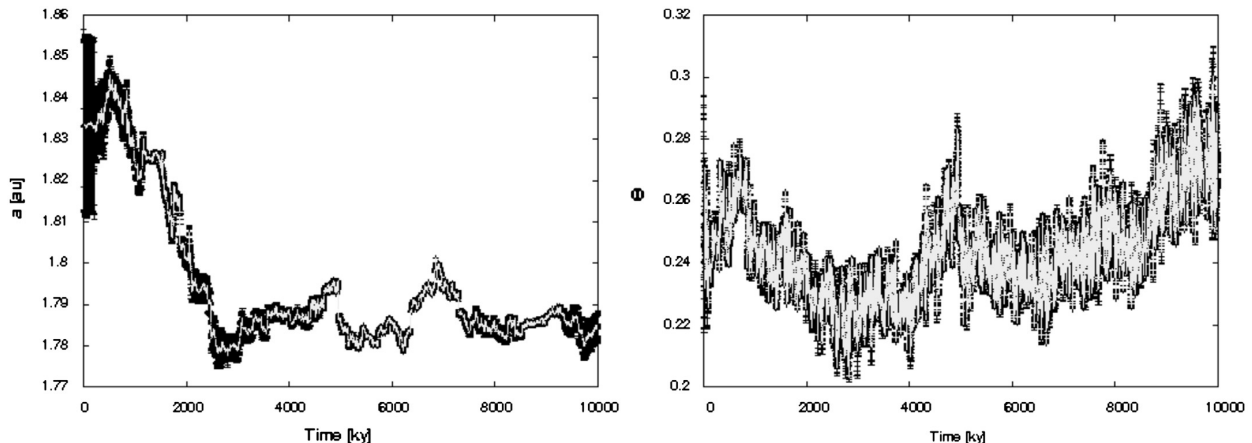


Fig. 5. Averaging of the elements with the standard deviation of the 50 clones of the asteroid (211279) 2002 RN₁₃₇ when they are NEAs. All points with a standard deviation major than 50% of the measure of the average has been rejected. Left panel: semi-major axis versus time for the averaging. Right panel: eccentricity versus time.

fugitives that escaped immediately out as Centaur or TNO; the same is for some bigger oscillations where the scattering is even higher.

The asteroids that do not become NEAs show such a peak in the scattering because they are a small number in comparison to the ones that become fugitives.

The *NormHNeas* initially decreases their semi-major axis more than 0.05 AU (as a whole) in the first million years and then after this negative gradient, the decreasing of the semi-major axis stops.

Instead the eccentricity after a couple of million years, in the cases where the most unstable clones have important close encounters or even impacts, starts to steadily increase, but below the value of the *HNeas*.

It is relevant a certain big scattering just when they start to be NEAs. Then some fugitives escaped immediately out as Centaur or TNO, or have some impact and the behavior become more homogeneous (less scattering).

The analysis on the inclination presents strong scattering giving the studying no possible interpretations.

5. Conclusions

As main result of our integration we found that the preponderance of the Hungaria escapers become NEAs, so also Mars-crossers. About 78% have CE with Mars, 29% with the Earth and 24% with Venus. Also 37% finish their lives as Sun-grazers, if they do not collide with a planet before that.

There is a small number of them (with a very low probability: < 1%) that leave the inner main belt crossing the region of the Centaurs and Trans-Neptunian Objects (TNOs).

Some Hungarias pass a long time in the outer solar system, via comet-like orbits, because we observed very high eccentricities when they are NEAs and even at higher inclinations than the initial conditions.

The average time for a first close encounter with Venus is ~63 My after the initial conditions, but it is somewhat surprising that this time is not much smaller for the Earth ~62 My; the first CE with Mars the average time is lower ~14 My. They become NEAs on average after ~47 My.

In the case of Hungaria-derived Apollos or Amors, the Earth is flattening the orbits of the asteroids (decreasing the inclination) close to the ecliptic, which is a well known phenomenon.

These asteroids tend to reducing their heliocentric distances, apart some cases that get into a hyperbolic orbit (this happens

with the narrowest close encounters with Mars after they begin to be Mars-crossers), and some have impacts with the Sun, also after only ~10 My of integration, but the majorities of them after 30 My, where the ν_6 secular resonance plays an important role.

During their evolution some escapers end their life with an impact, mostly with the Sun and the rest with the planets, in particular the terrestrial planets: the probability for these fugitives to hit the Earth and Mars in 100 My is respectively 0.7% and 1.1%. The highest one is for Venus, 2.5%.

We underline that the majority of the Hungaria escapers change their type-membership when they are NEAs, as it has been discussed in detail also by Milani et al. (1989), Dvorak and Pilat-Lohinger (1999), and Dvorak and Freistetter (2001) and we found that they have a mean life time equal to 0.27 My on average and their relative probabilities to be source of NEAs in 100 My is about 3.2% with 18% of these last ones colliding with the Sun.

The maximum release of NEAs by the escapers is at ~60 My after the initial conditions of the integration; instead if we look at inside the different NEA-types, we found that Atens and Apollos stop to increase at ~90 My. Their average life-time as NEAs is higher than the one coming from the Outer Main Belt, but the percentage of relative release is similar; instead this last one is smaller than sources like the ν_6 , the $J_3 : 1$ and in particular more than two times less than the *IMCs*. When they are NEAs they pass more time as Atens in 100 My of evolution after escaping from their proper family. If the lost of these family is constant, in case of no external supply, it will finish its own existence in about 3.125 Gy.

The majority of the Hungaria fugitives that becomes NEAs are Amors; then IEOs and Atens are more or less in equal number as population of Hungaria-NEAs.

Concerning their orbit on average, the semi-major axis continues to decrease, contrary to the eccentricity that is continuously growing, $\sim 2 \times 10^{-3} \text{ My}^{-1}$ with also increasing number of CEs and passing through MMRs with different planets and some secular resonances. CEs are especially with Mars, also many times just before being a NEA. We show also that after the Hungarias-NEAs are "cleaned" by impacts, the remaining ones keep the orbit constant (in semi-major axis and eccentricity) for an interval time < 10 My like the real ones.

About their initial inclination, we think that the former collision started from a period in which massive bodies (with diameters bigger than at least 30 km) collided inside the Main Belt region, presumably all started with an initial collision in the inner main belt region for a body with probably high inclination ($i \geq 23^\circ$).

This collision may have given birth to the E-belt (Bottke et al., 2011) and this last one gave origin to the present Hungarias and a great part of the NEAs.

The fugitives are Planet Crossing Asteroids (PCAs) at least in 91% of the cases in 100 My, their angles of deflection can be very high – rarely up to more than 90° (so retrograde orbits, after important CEs), even if on average it is less than 3°.

The duration of their close encounters is maximal for Mars, ~0.5 days, and minimal for Venus, ~0.25 days, somewhere in between for the Earth (~1/3 days). We could define a relation 2 : 3 : 4 (Venus:Earth:Mars) for the durations of close encounters with terrestrial planets, this is because the encounter velocities of the asteroids are very high for Venus and lower for Mars.

The Hungarias encounter velocities seem to be faster than the average values for the all the real asteroids that come close to the terrestrial planets, especially for the Earth and Venus; for this reason they probably do look like to cause craters bigger than the average at least less than 3% from the total population of impactors with terrestrial planets, but the most important contribution is toward the population which may impact Mars, ~2.8%.

Acknowledgments

We acknowledge funding from University of Vienna doctoral school IK-1045 and Austrian Science Foundation Grant P21821-N19.

Appendix A. Supplementary material

Supplementary data associated with this article can be found in the online version, at <http://dx.doi.org/10.1016/j.pss.2013.03.017>

References

- Bottke, W.F., Morbidelli, A., Jedicke, R., Petit, J.M., Levison, H.F., Michel, P., Metcalfe, T.S., 2002. Debiased orbital and absolute magnitude distribution of the near-Earth asteroids. *Icarus* 156, 399–433.
- Bottke, W.F., Vokrouhlický, D., Minton, D., Nesvorný, D., Morbidelli, A., Brasser, R., Simonson, B., 2011. The great archaic bombardment, or the late heavy bombardment. *Lunar and Planetary Institute Science Conference Abstracts* 42, 2591.
- Dvorak, R., Pilat-Lohinger, E., 1999. On the dynamical evolution of the Atens and the Apollos. *Planetary and Space Science* 47, 665–677.
- Dvorak, R., Freistetter, F., 2001. Dynamical evolution and collisions of asteroids with the earth. *Planetary and Space Science* 49, 803–809.
- Durda, D.D., Bottke, W.F., Enke, B.L., Asphaug, E., Richardson, D.C., Leinhardt, Z.M., 2004. The formation of asteroid satellites in catastrophic impacts: results from numerical simulations. *Icarus* 167, 382–396.
- Eggl, S., Dvorak, R., 2010. An introduction to common numerical integration codes used in dynamical astronomy. In: Souchay, J., Dvorak, R. (Eds.), *Dynamics of Small Solar System Bodies and Exoplanets*, Lecture Notes in Physics, vol. 790, pp. 431–480.
- Galiazzo, M.A., Souami, D., Eggl, S., Souchay, J., 2012. The vesta asteroid family: study of the family and close encounters with terrestrial planets and dynamical influences by (1) ceres and (4) vesta. *LPI* 43, 1424.
- Greenstreet, S., Ngo, H., Gladman, B., 2012. The orbital distribution of near-Earth objects inside Earth's orbit. *Icarus* 217, 355–366.
- Hanslmeier, A., Dvorak, R., 1984. Numerical integration with lie series. *A&A* 132, 203–207.
- Ivanov, B.A., Neukum, G., Bottke Jr., W.F., Hartmann, W.K., 2002. The comparison of size-frequency distributions of impact craters and asteroids and the planetary cratering rate. *Asteroids III*, 89–99.
- Lemaître, A., Morbidelli, A., 1994. Proper elements for highly inclined asteroidal orbits. *Celestial Mechanics and Dynamical Astronomy* 60, 29–56.
- Milani, A., Carpino, M., Hahn, G., Nobili, A.M., 1989. Dynamics of planet-crossing asteroids—classes of orbital behavior. *Icarus* 78, 212–269.
- Milani, A., Knežević, Z., Novaković, B., Cellino, A., 2010. Dynamics of the Hungaria asteroids. *Icarus* 207, 769–794.
- Morrison, D., 1977. Radiometric diameters for 84 asteroids from observations in 1974–1976. *The Astrophysical Journal* 214, 667–677.
- Pravec, P., et al., 2008. Spin rate distribution of small asteroids. *Icarus* 197, 497–504.
- Rossi, A., Marzari, F., Scheeres, D.J., 2009. Computing the effects of YORP on the spin rate distribution of the NEO population. *Icarus* 202, 95–103.
- Shoemaker, E.M., Williams, J.G., Helin, E.F., Wolfe, R.F., 1979. Earth-crossing asteroids: orbital classes collisions rates with Earth and origin. *Asteroids*, 253–282.
- Warner, B.D., Harris, A.W., 2007. Lightcurve studies of small asteroids. *BAAS* 39, 432.
- Warner, B.D., Harris, A.W., Vokrouhlický, D., Nesvorný, D., Bottke, W.F., 2009. Analysis of the Hungaria asteroid population. *Icarus* 204, 172–182.
- Zappalà, V., Cellino, A., Dell'Oro, A., Paolicchi, P., 2002. Physical and dynamical properties of asteroid families. In: Bottke, W.F., Cellino, A., Paolicchi, P., Binzel, R.P. (Eds.), *In Asteroids III*. University of Arizona Press, Tucson, p. 619.
- Zellner, B., Leake, M., Williams, J.G., Morrison, D., 1977. The E asteroids and the origin of the enstatite achondrites. *Geochimica et Cosmochimica Acta* 41, 1759–1767.

Chapter 3

The Hungaria Asteroids: Close encounters and impacts with terrestrial planets

The following article is a continuation of Galiazzo et al. (2013a), previous chapter. After the study of the orbital evolution of the Hungarias in the inner Main Belt, impacts with Terrestrial Planets are studied in details. This is the first time that the physics of an impact on the surface of a planet is inferred via the dynamical orbital evolution (and without photometric observations) of the impactor, its trajectory and speed during the atmospheric entry.

Authors: Mattia Alvisè Galiazzo, Akos Bazso and Rudolf Dvorak²⁵

Publication state: Submitted in May 2013. Probable publication: May 2014

Publication details: Memorie della Società Astronomica Italiana (10th Italian National Congress of Planetary Science), (9pp), 2014

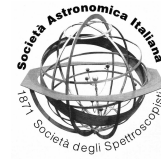
Contribution of the first author: The first author was responsible for the idea to investigate the impacts and their physical characterizations on the surface of the terrestrial planets of a region of the inner Main Belt, namely the Hungaria Group and combine numerical orbital evolution of the asteroids and physical evaluations of the impact craters, comparing them to the real ones on the terrestrial planets. The development, implementation and evaluation of the proposed methodology as well as the composition of the following article were performed by the first author.

Contribution of the co-authors: The resources necessary for the project's success were mostly supplied by the coauthors.

²⁵ Author affiliations are presented in the header of the following article.

*CHAPTER 3. HUNGARIAS: CLOSE ENCOUNTERS AND IMPACTS
WITH TERRESTRIAL PLANETS*

Furthermore, the coauthors' contributions encompassed a part of the “physical” numerical integration. Finally, the co-authors played partly a role in scientific discussions and in providing proposals for some improvements of the article.



The Hungaria Asteroids: Close encounters and impacts with terrestrial planets

M. A. Galiazzo¹, A. Bazso¹, and R. Dvorak¹

Institute of Astronomy, University of Vienna, Türkenschanzstr. 17, A-1180 Wien, Austria
e-mail: mattia.galiazzo@univie.ac.at

Abstract. The Hungaria asteroid family (Named after (434) Hungaria), which consists of more than 5000 members with semi-major axes between 1.78 and 2.03 AU and have inclinations of the order of 20° , is regarded as one source for Near-Earth Asteroids (NEAs). They are mainly perturbed by Jupiter and Mars, and are ejected because of mean motion and secular resonances with these planets and then become Mars-crossers; later they may even cross the orbits of Earth and Venus. We are interested to analyze the close encounters and possible impacts with these planets. For 200 selected objects which are on the edge of the group we integrated their orbits over 100 million years in a simplified model of the planetary system (Mars to Saturn) subject to only gravitational forces. We picked out a sample of 11 objects (each with 50 clones) with large variations in semi-major axis and some of them achieve high inclinations and eccentricities in connection with mean motion and secular resonances which then leads to relatively high velocity impacts on Venus, Earth and Mars. We report all close encounters and impacts with the terrestrial planets and statistically determine the mean life and the orbital distribution of the NEAs of these Hungarias.

Key words. Hungarias – asteroids – close encounters – impacts – NEAs – terrestrial planets

1. Introduction

The Hungaria group contains about 8000 asteroids, located in orbital element space¹ between $1.78 < a(\text{AU}) < 2.03$, $e < 0.19$ and $12^\circ < i < 31^\circ$, inside the ν_6 secular resonance (SR) and the mean motion resonances (MMRs) 4:1 with Jupiter (J4:1) and 3:4 with Mars (M3:4).

There is evidence from meteorites that members of the Hungaria group may reach the

terrestrial planets and be a source of impactors. In the first place this is deduced from the spectral type of the major component of the family, the E-type or Achondritic Enstatite (about 60%), which is consistent with the composition of some meteorites (aubrites, Zellner et al. (1977)) found on the Earth. Other Hungarias are also S-type (17.2%) and less C-types (6.0%) (Warner et al. 2009). The objects of the group are not very big in size compared to the other Main Belt Asteroids (MBAs), they have an average diameter of 1 km ranging up to 11.4 km, (434)Hungaria being the biggest member. The majority of Hungarias have a retrograde

Send offprint requests to: M. A. Galiazzo

¹ following in part a suggestion of Spratt (1990), so that our sample finally consisted of 8258 asteroids (August 2010)

rotation and similar spin rates (Pravec et al. 2008; Rossi et al. 2009).

The content of the paper is as follows:

- methods and details on the investigated bodies;
- statistical and analytical study on Hungarias path to be NEAs, impacts and close encounters with the Terrestrial planets;
- conclusions: discussion and summary on the previous described studies.

2. Methods and details

Hungaria asteroids was picked up from the database² of the Lowell observatory at Flagstaff, then a reasonable number of asteroids was taken for the orbital integrations: 200 out of the total Hungarias inside the group, the ones that have the higher deflection from the average of a metric d based on the osculating elements: $d = \left| \sqrt{\left(\frac{e}{\langle e \rangle}\right)^2 + \left(\frac{a}{\langle a \rangle}\right)^2 + \left(\frac{\sin i}{\langle \sin i \rangle}\right)^2} \right|$ (a , e and i are respectively the semi-major axis, the eccentricity and the inclination of the asteroids).

Firstly these first sample was integrated for 100 My with the Lie-integrator (Hanslmeier and Dvorak 1984; Egl and Dvorak 2010) in a simplified Solar system (planets from Mars to Saturn), enough³ for the scope of this first work, discovering the objects which escape from the group: 11 bodies (see table 1). They were discriminated considering only those ones who has a major deflection in the semi-major axis: $\Delta a > \Delta a_{group}/16 = 0.01563 AU$, with $\Delta a = a_{max} - a_{min}$: deviations from the group's mean semi-major axis of more than $\sim 7\%$ of the total width of the group.

Secondly the 11 fugitives were integrated again with the same initial conditions and together with 49 clones for each one of them inside these ranges: $a \pm 0.005 AU$, $e \pm 0.003$ and $i \pm 0.005^\circ$. This time in a Solar System which take in accounts all the planets from Venus to

Saturn, so taking in account also the terrestrial planets and all the close encounters. It is considered a close encounter when the asteroid crosses the following distances (close encounter radius, CER) from each planet: the average lunar distance 0.0025 AU for the Earth, and the lunar distances scaled to the respective Hill Sphere of the other 2 considered planets 0.00166 AU for Mars and 0.00170 AU for Venus.

3. Results

3.1. Statistical analysis of the dynamics of the Hungarias' Fugitives.

The 11 fugitives are also inside the Hungaria Family, so it is possible to speak about escapers from the family, a more restrictive definition of "group"; we remember here the definitions:

Group: a "group" of asteroids is defined by a range of osculating elements (see also Warner et al. (2009))

Family: a (dynamical) "family" of asteroids is defined by the use of the proper elements. Families are defined by a specific clustering method, which gives dynamically a homogeneous sample of asteroid in the Main Belt, the most well known are the Hierarchical Clustering Method (HCM, Zappalá et al. (1990)) and the Wavelet Analysis Method (WAM, Bendjoya et al. (1991)).

The orbit of the fugitives is rather chaotic after a close encounter as it can be seen in the case of (41577) 2000 SV₂ (Fig. 2). This asteroid become a Sungrazers in less than 100 Myrs, crossing the ν_6 secular resonance at $\sim 71 Myr$ and then after a very close encounter with Venus, it become a NEAs keeping a high value of eccentricity, always $e > 0.3$, finally after several close encounters with all the planets, it collides the Sun.

During the orbital evolution of 100 Myrs, all the Fugitives become Mars-crossers. 91 % of them (the clones) are planet crossing asteroids (PCAs) and 58% NEAs, in particular Amors and Apollos: Amors are the Earth-approaching NEAs with orbits exterior to the

² www2.lowell.edu/elgb

³ Integrations with the full Solar System from Mercury to Neptune shows the same general results.

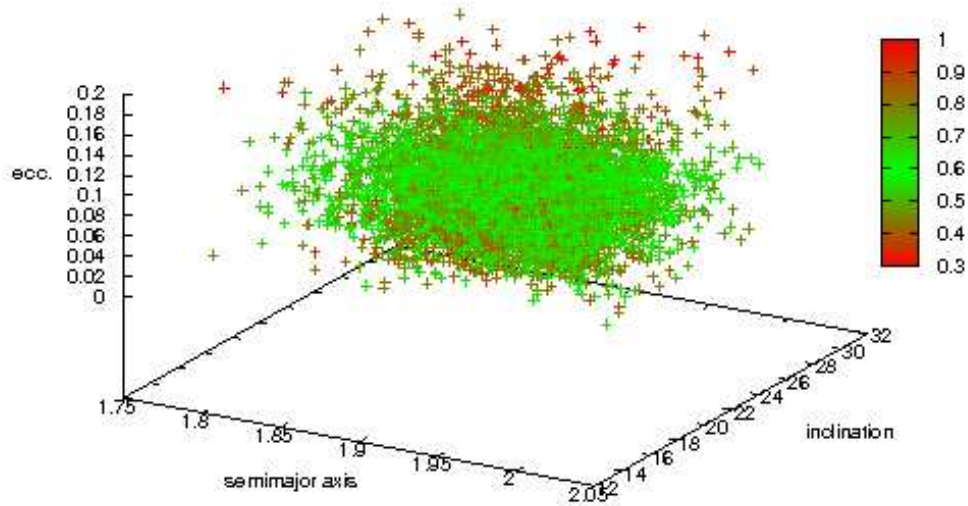


Fig. 1. The Hungaria group in the orbital space and the metric. Reddish crosses are for the asteroids with the most extreme value in the metric.

Earth's ($a > 1.0AU$ and $1.017(AU) < q < 1.3(AU)$); Apollos are Earth-crossing NEAs with semi-major axis larger than the Earth ($a > 1.0 AU$ and $q < 1.017 AU$, q is the perihelium), this means that 3.2% of all the Hungarias become NEAs in 100 Myrs. The average time-evolution of the Hungarias escapers is shown in Fig. 3, a Fugitive usually have a close encounter with Earth and Venus after becoming an Amor, an Apollo and an Aten.

The entry velocity at the *CER* for each planet it is 21.5 ± 2.3 km/s for the Earth, 27.8 ± 1.7 km/s for Venus and 10.8 ± 1.0 km/s for Mars.

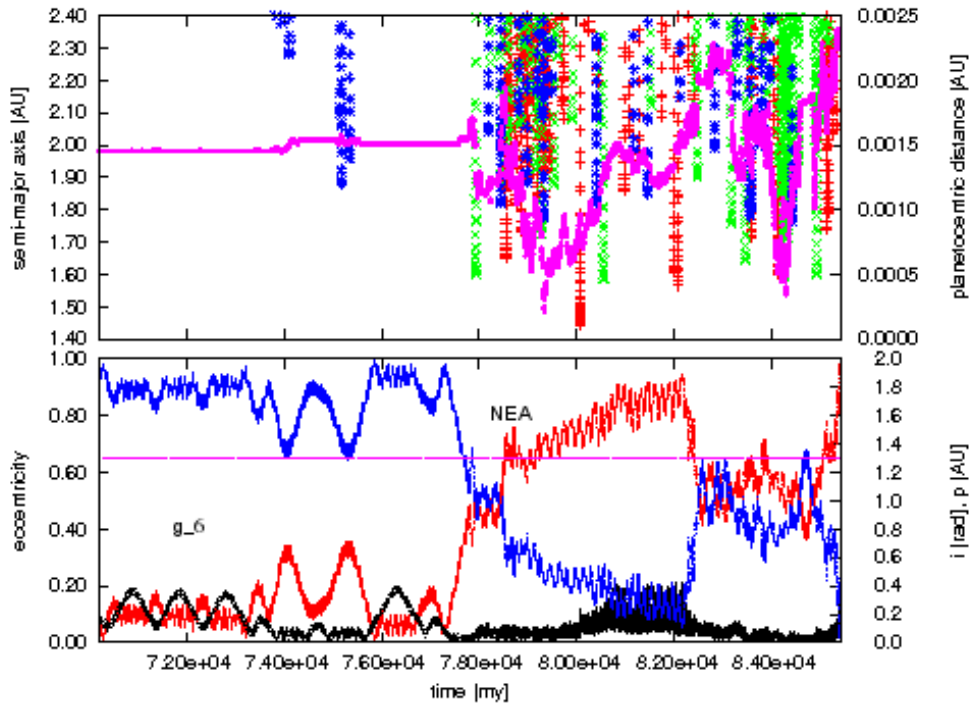


Fig. 2. Upper panel: semi-major axis and Planetocentric distance versus time. In blue, green and red, close encounters with respectively: Mars, Venus and Earth. Bottom panel: eccentricity (red), inclination (black) and perihelium (blue) versus time.

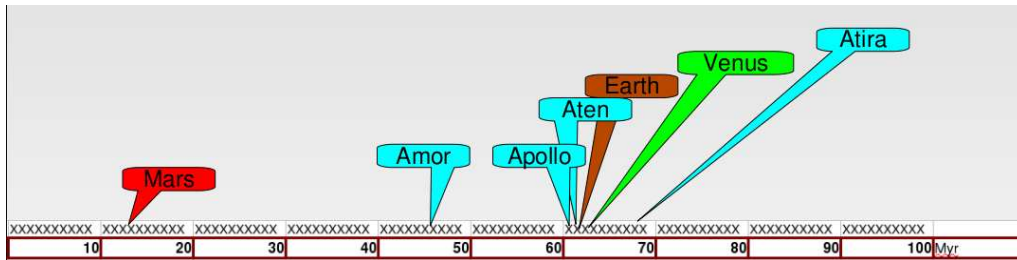


Fig. 3. Average time-evolution of a Fugitive. Each “x” represents 1 Myr. Atens are Earthcrossing NEAs with semimajor axis smaller than the Earth: $a < 1.0$ AU and $Q > 0.983$ AU (Q is the aphelion); Atiras have the orbit contained with the one of the Earth: $a < 1.0$ AU and $Q < 0.983$ AU.

3.2. Impacts

Some singular clones have an impact with a terrestrial planet. The percentage of the whole Hungaria's population having an impact with a terrestrial planet during 100 Myrs is: 0.7% for the Earth, 2.4% for Venus and 1.1% for Mars. It is possible to compute the diameter of the putative craters and some typical values concerning them. In order to make this the diameter of the asteroids is needed, see (table 1). They are computed with the equation of Fowler & Chillemi (1992), which gives a quite precise results, with an error, usually of second order (if the diameter is 220km the error is about of $20^1 km$, see Galiazzo (2009)): $D = \frac{1329}{\sqrt{\rho_v}} 10^{-H/5}$.

The estimates of the diameter of the Hungaria-impactors are based on the assumption that the asteroid has a spherical shape.

The known impact structures on Earth range from small circular bowls only a few hundred metres in diameter to large complex structures more than 200 km in diameter (French 1998), with ages as old as 2 Gyr. The biggest known craters on Earth are Vredefort and Sudbury craters, larger than 200 km in diameter. The “projectiles” capable of forming craters on the terrestrial planets today come primarily from three populations (Ivanov et al. 2002a):

1. asteroids from the main belt
2. Jupiter-family comets from the Kuiper Belt
3. long period comets from the Oort Cloud

Bottke et al. (2002) showed that the asteroids provide most of terrestrial impact craters coming from $a < 7.4$ AU orbits. Some hundreds of NEAs have a diameter ≥ 1 km similar to most of the known Hungarias. For the found fugitives the diameters range from approximately 1 km to ~ 2.5 km, see table 1.

3.3. Craters

During the integrations some clones have an impact with Terrestrial planets. The impact is assumed if the body surmounts the limit for the atmospheric entry (see fig. 1 of Westman et al. (2003)), for this cutoff⁴ it has been chosen in

⁴ see <http://neo.jpl.nasa.gov/news/2008tc3.html>

this work a value for the Earth equal to 65.4 km. For the other planets it has been derived an empirical equation using a constant k which depends on the scale height h_{atm} of the atmosphere, measured in astronomical units (1 AU = 149597870.7 km) and the (surface) density of each planet (for parameters see table 1):

$$k = \rho^{(E)} h_{tot}^{(E)} / h_{atm}^{(E)} \quad (1)$$

where

$$h_{tot}^{(E)} = r^{(E)} + h_{atm}^{(E)}. \quad (2)$$

Here $h_{atm}^{(E)}$ is the scale height of the Earth atmosphere, $\rho^{(E)}$ the density, and $r^{(E)}$ is the radius of the Earth (also in astronomical units). The atmospheric entry (r_{imp}) for Venus and Mars is given by the equation:

$$r_{imp} = r^{(P)} + h_{tot}^{(P)} \rho^{(P)} / k. \quad (3)$$

The probabilities computed from the results of the integrations confirm the trend and the values found in Ivanov et al. (2002a) for bodies with $H < 17$ mag, even if the value for Mars is very small compared to the results of this paper (0.21 compared to 0.34). This bias is due to the fact that here it is used a small sample and restricted to a special group of asteroids. Averaging on the fugitives which have impacts (9 out of 11), the average probability range from $(2.20 - 3.49) \times 10^{-8}$ /yr, meaning that a fugitive should orbit between 0.026 – 0.045 Gyr at its currently observed orbit before impacting one of the terrestrial planets⁵.

The impact angle is defined via the angle of the planetocentric velocity vector with the normal to the target's surface:

$$\cos(\theta_{norm}) = \frac{\mathbf{v} \cdot \mathbf{n}}{\|\mathbf{v}\| \cdot \|\mathbf{n}\|} \quad (4)$$

and so $\theta = 90^\circ - \theta_{norm}$. The diameter of the crater by means of the equations for the transient crater diameter (Collins et al. 2005):

$$D_{tc} = 1.161 \left(\frac{\rho_i}{\rho_t} \right)^{1/3} D_i^{0.78} v_i^{0.44} g^{-0.22} (\sin \theta)^{1/3}, \quad (5)$$

⁵ 0.040 Gyr for the Earth, meaning that impacts by Hungarias may happen since $\sim (0.46 - 0.92)$ Gyr ago. However this is only one of the probable suggestions, so caution may be advised before completely accepting these connections.

here D_i is the diameter of the impactor, ρ_i its density (for the Hungarias we chose $\rho_i = 1700 \text{ kg/m}^3$, McEachern et al. (2010)), and ρ_t is the density of the target. For the final crater diameter (McKinnon & Schenk 1985) it follows:

$$D_c = 1.17 \frac{D_{tc}^{1.13}}{D_*^{0.13}}, \quad (6)$$

with D_* the transition diameter inversely proportional to the surface gravity of the target (Melosh 1989), with the nominal value for the Moon of $D_{*,Moon} = 18 \text{ km}$ (Minton & Malhotra 2010):

$$D_* = 1.62 D_{*,Moon} / g^{(P)}. \quad (7)$$

Earth: Grieve & Shoemaker (1994) suggest that it is possible to distinguish two populations of craters: (i) craters with diameters between 24 to 39 km, the oldest being 115 Myr; and (ii) craters with diameters from 55 to 100 km, the oldest being 370 Myr. Ivanov et al. (2002a) assume that craters smaller than $\sim 20 \text{ km}$ belong to the younger set, so Hungarias should have formed craters younger than 115 Myr. This should be compared to the diameters found from our computations (see table 3,4 and 5), with the biggest crater formed by 2002 SV2 (20.89 km).

Mars: In the equatorial geologic-geomorphic units of Mars (latitude $\leq 35^\circ$), there are craters that range from 4 to 10 km (Condit 1978), similar to the putative crater made by a clone of 1996 VG9.

Venus: Looking at the Venus database⁶, also here a lot of craters has similar diameters to the ones found in these studies.

The impact energy, is computed via the equation given by Collins et al. (2005):

$$E = \frac{\pi}{12} \rho_{ast} D_{ast}^3 v_i^2 \quad (8)$$

This is the energy equivalent in megatons (Mt) if we consider the impactor's diameter D_{ast} expressed in meters, its velocity v_i in km/s and the density ρ_i in g/cm^3 . As can be seen the energy depends strongly on the diameter of the

impactor and on the impact velocity, which is computed by the equation given in Collins et al. (2005):

$$v_i = v_\infty \frac{\rho_i D_i}{\rho_i D_i + \frac{3 P_{pl}}{2 g_{pl} \sin \theta}}. \quad (9)$$

(using v_∞ as the speed of the asteroid before the atmospheric entry, D_i impactor diameter, P_{pl} atmospheric pressure). The maximum impact energy released for the Earth is $\approx 4.18 \times 10^5 \text{ Mt}$, more than forty thousand times the energy released to create the Meteor Crater in Arizona, USA (Shoemaker 1983). The impact energies for Venus are on average lower than on Mars.

Table 3, 4 and 5 summarize the data for the impacting asteroids, including the energy released by the “crash” of the impactor and the diameter of the crater⁷ on the two main types of the solid surfaces of the Earth (sedimentary rocks and crystalline rocks); two different surfaces for Venus (strong andesite and strong basalt), and one for Mars (andesite).

For each planet they are shown the maximum crater diameter made by the fugitives and the real craters on the terrestrial planets with similar diameter to the one made by the Hungarias. D_1 and D_2 are the crater diameters for a sedimentary surface (the bigger one) and for crystalline surface, for the Earth; strong andesite surface (the bigger diameter) and strong basaltic surface for Venus, and only feeble andesite surface for Mars. θ is the angle of impact; E , the energy released by the impact and $E_{Nord.Cr.}$ displays how many times we have the energy of the Nördlingen crater (the energy released by the impactor in the Ries Crater is ~ 15 megatons, see the impact database of the Planetary Space Science Centre), a thousand times the energy released at Hiroshima (15 kilotons, see <http://www.world-nuclear.org/info/inf52.html>) compared to the energy released by the Hungaria escapers. Then v_∞ is the velocity at the atmospheric entry, v_{imp} , the impact velocity and v_e is the relative escape velocity of the planet. There are also the orbital elements (a ,

⁷ All the diameters refer to an asteroid that does not suffer from fragmentation during its flight through the atmosphere.

⁶ <http://www.lpi.usra.edu/resources/vc/vcnames/>

e , i) at the border distance to be considered as a close encounter; the time of the impact t from the beginning of the integration and the disclosure time to arrive from the lunar distance to the target (to the limit of the atmospheric entry), Δt .

Asteroid (152648) 1997 UL₂₀ have the maximum number of impacts by its clones, 11 different ones.

The inclination at the atmospheric entry looks very high for Mars and contrary for the Earth, while the eccentricities continue to increase going interiorly the solar system. The average impact angle seems higher for the Earth and also the biggest craters appear here.

The impact velocity of the fugitives found for the Earth range from 14.2 to 30.18 km/s for the Earth. These values are larger than the results given by Ivanov & Hartmann (2002b); Chyba (1993) ($\langle v \rangle = 19.3$ km/s for an asteroid with $H_v < 17$ mag and $\langle v \rangle = 18.6$ km/s for $H_v < 15$ mag), even if that sample is for asteroids with $D < 50$ m. Hungarias seem to arrive faster on the average than other types of asteroids having close encounters with the Earth. Concerning Mars the range of velocities is from 9.32 to 23.42 km/s with the maximum value higher than for the average asteroids found in Ivanov & Hartmann (2002b), so the Hungarias arrive faster to Mars, too. On the other hand we find lower velocities for Venusian impactors, our results range from 5.24 to 24.57 km/s, against the average velocity of 24.2 km/s of Ivanov & Hartmann (2002b).

Some NEOs (in the JPL Small-Body Database Search Engine) fit well with the elements of the found impactors, also inside the ranges of the albedos and absolute magnitudes of the Hungarias, spectra types gave a good fitting, when they are present: (1620) Geographos, (2201) Oliato, (5751) Zao, (3551) Verenia, (5604) 1992 FE, an Amor asteroid of 2.3km (Delbó et al. 2003).

4. Conclusions

In 100 Myrs, 3.2% of all the Hungarias become NEAs and among these more than 90% are PCAs. Less than 1 % of them has an impact with Mars or the Earth, 2.4% of them with Venus and the rest end up as a Sun-grazer or stay still in a NEA's orbit; very rarely they are Jupiter crossers.

Found Hungaria fugitives which collide a planet create craters similar to the ones present on the terrestrial planets as dimension ($D < 30$ km). The biggest computed craters for them are 28 km for the Earth, 20 km for Venus and 23 km for Mars.

Some NEOs presents similar osculatory elements, size and spectral type (when it is available) to the fictitious fugitive-impactors: (1620) Geographos, (2201) Oliato, (5751) Zao, (3551) Verenia, (5604) 1992 FE.

Acknowledgements. We acknowledge funding from University of Vienna doctoral school IK-1045 and Austrian Science Foundation grant P21821-N19.

References

- Bendjoya, P., Slezak, E., Froeschle, C., The wavelet transform – A new tool for asteroid family determination, *Astron. Astrophys.* **251**, 312-330 (1991)
- Botke, W. F., Morbidelli, A., Jedicke, R., Petit, J. M., Levison, H. F., Michel, P., Metcalfe, T. S., Debaised orbital and absolute magnitude distribution of the near-Earth asteroids, *Icarus* **156**, 399-433 (2002)
- Chyba, C. F., Explosions of small Spacewatch objects in the Earth's atmosphere, *Nature* **363**, 701-703 (1993)
- Collins, G. S., Melosh, H. J., Marcus, R., Earth Impact Effects Program: A Web-based Computer Program for Calculating the Regional Environmental Consequences of a Meteoroid Impact on Earth, *MAPS* **6**, 817-840 (2005)
- Condit, C. D., Distribution and relations of 4- to 10-km-diameter craters to global geologic units of Mars, *Icarus* **34**, 465-478 (1978)
- Delbó, M., Harris, A. W., Binzel, R. P.; Pravec, P.; Davies, J. K., Keck observations of near-

- Earth asteroids in the thermal infrared, *Icarus* **166**, 116130(2003)
- Delva, M., "Integration of the elliptic restricted three-body problem with Lie series", *Celest. Mech.*, 34, 145-154, (1984)
- Dressler, B. O., Sharpton, V. L., Copeland, P., "Slate Islands, Lake Superior, Canada: A mid-size, complex impact structure", *Large Meteorite Impacts and Planetary Evolution II*, Editor B. O. Dressler, V. L. Sharpton, 109, (1999)
- Eggl, S. and Dvorak, R., "An Introduction to Common Numerical Integration Codes Used in Dynamical Astronomy", *Lect. Notes Phys.*, 790, 431-480, Souchay, J. J. and Dvorak, R. (Eds.), (2010)
- French, B. M., *Traces of Catastrophe: A Handbook of Shock-Metamorphic Effects in Terrestrial Meteorite Impact Structures*, Technical Report, LPI-Contrib-954, (1998)
- Fowler, J. W., Chillemi, J. R., IRAS asteroid data in processing, In: Tedesco, E.F., Veeder, G.J., Fowler, J.W., Chillemi, J.R. eds: *The IRAS Minor Planet Survey*, Technical Report PL-TR-92-2049, Phillips Laboratory, Hanscom AF base, MA.
- Grieve, R. A. F., Shoemaker, E. M., *The record of the past impacts on Earth*, In: *Hazards Due to Comets and Asteroids* (T. Gehrels, ed.), 417-462, Univ. of Arizona, Tucson.
- Hanslmeier, A. and Dvorak, R., "Numerical Integration with Lie Series", *A&A*, 132, 203-207, (1984)
- Galiazzo, M. A., *Fotometria di corpi minori del sistema solare esterno*, master-thesis at the Department of Astronomy, Univ. of Padova, Italy, (2009)
- Ivanov, B. A., Neukum, G., Bottke Jr., W. F., Hartmann, W. K., *The Comparison of Size-Frequency Distributions of Impact Craters and Asteroids and the Planetary Cratering Rate*, *Asteroids III*, 89-99, (2002)
- Ivanov, B. A., Hartmann, W. K., *Exogenic Dynamics Cratering and Surface ages*, Elsevier, (2002)
- Lichtenegger, H., "The dynamics of bodies with variable masses", *Celest. Mech.*, 34, 357-368, (1984)
- McEachern, F. M., Čuk, M., Stewart, S. T., *Dynamical evolution of the Hungaria asteroids*, *Icarus* **210**, 644-654 (2010)
- McKinnon, W. B., Schenk, P. M., *Ejecta blanket scaling on the Moon and - inference for projectile populations*, *Abstracts of the Lunar and Planetary Science Conference* **16**, 544 (1985)
- Melosh, H. J., *Impact Cratering: A geological process*, Oxford University press, New York, New York, USA, **245**, (1989)
- Minton, D. A., Malhotra, R., *Dynamical erosion of the asteroid belt and implications for large impacts in the inner solar system*, *Icarus* **207**, 744-757 (2010)
- Pravec, P., and 31 co-authors, *Spin rate distribution of small asteroids*, *Icarus* **197**, 497504 (2008)
- Rossi, A., Marzari, F., Scheeres, D. J., *Computing the effects of YORP on the spin rate distribution of the NEO population*, *Icarus* **202**, 95103 (2009)
- Shoemaker, E. M., *Asteroid and Comet Bombardment of the Earth*, *Annual Review of Earth and Planetary Sciences* **11**, 461-494 (1983)
- Spratt, C. E., *The Hungaria group of minor planets*, *Journal of the Royal Astronomical Society of Canada* **84**, 123-131 (1990)
- Turtle, E. P., Pierazzo, E., *Constraints on the site of the Vredefort impact crater from numerical modeling*, *Meteorites and Planetary Science* **33**, 483-490 (1998)
- Zappalá, V., Cellino, A., Farinella, P., *Hierarchical Clustering: How to Identify Asteroid Families and Assess their Reliability*, *Asteroids, Comets, Meteors III*, Lagerkvist, C. I., Rickman, H., Lindblad, B. A. (eds.), 211 (1990)
- Walker, G. W., Flanagan, F. J., Sutton Jr., A. L., Bastron, H., Berman, S., Dinnin, J. G., Jenkins, L. B., *Quartz latite (del-lenite), QLO-1, from Southeastern Oregon*, *Geological Survey U.S.* **840**, 15-20 (1976)
- Warner, B. D., Harris, A. W., Vokrouhlický, D., Nesvorný, D., Bottke, W. F., *Analysis of the Hungaria asteroid population*, *Icarus* **204**, 172-182 (2009)
- Westman, A., Wannberg, G., Pellinen-Wannberg, A., *Meteor head echo altitude distributions and the height cutoff effect studied with the EISCAT HPLA UHF and*

VHF radars, *Annales Geophysicae* **22**,
1575-1584 (2004)

Asteroid	H_V	G	D	ρ_v	Spec.-Type
(211279) 2002 RN ₁₃₇	16.9	0.15	1.01	0.3	Xe?
(41898) 2000 WN ₁₂₄	16.2	0.15	1.24	aver.	?
(39561) 1992 QA	15.3	0.15	1.88	aver.	?
(30935) Davasobel	14.7	0.15	2.48	aver.	S?
(175851) 1999 UF5	16.9	0.15	0.90	aver.	Xe?
(152648) 1997 UL ₂₀	15.8	0.15	1.49	aver.	?
(141096) 2001 XB ₄₈	16.2	0.15	1.24	aver.	?
(24883) 1996 VG ₉	15.3	0.15	1.88	aver.	?
(41577) 2000 SV ₂	14.9	0.15	2.26	aver.	?
(129450) 1991 JM	16.8	0.15	0.94	aver.	?
(171621) 2000 CR ₅₈	16.2	0.15	1.24	aver.	?

Table 1. Absolute magnitude in visual, slope parameter, diameter (km) and spectra types of the 11 fugitives. Data from the database “astorb.dat” of the Minor Body Center. Where not data are given for the visual albedo (ρ_v), the average (aver.) one, 0.38 (Warner et al. (2009), was taken. Question mark stands for no data available for the spectrum type.

Planet	radius R [km] pressure P [bar]	density ρ_1 [kg/m^3] h_{atm} [km]	density ρ_2 [kg/m^3] g [m/s]
Venus	6051.8 92	2800 15.9	3000 8.9
Earth	6371.0 1.01325	2500 8.5	2750 9.8
Mars	3396.2 0.00636	2500 11.11	– 3.71

Table 2. ρ_1^{Earth} and ρ_2^{Earth} are the densities of sedimentary and crystalline rock, respectively, (Collins et al. 2005); ρ_1^{Venus} is the (surface) density given by the fact sheet of NASA (<http://nssdc.gsfc.nasa.gov/planetary/factsheet/venusfact.html>) and ρ_2^{Venus} is the upper limit of basalt given in http://geology.about.com/cs/rock_types/a/aarockspecgrav.htm. ρ_1^{Mars} is the density for Mars: we have considered the lower value for andesite (see the link mentioned just before). For the scale heights of the atmospheres (h_{atm}) we have chosen for the Earth the value mentioned at <http://neo.jpl.nasa.gov/news/948tc3.html>. All the other parameters come from the NASA fact-sheets for each planet.

Asteroid	D_1 [km]	D_2 [km]	θ	
Energy [Mt $\times 10^5$]	$E_{Nord.Cr.}$	v_∞ [km/s]	v_{imp} [km/s]	v_e [km/s]
semi-major axis [AU]	eccentricity	inclination [deg]	time [Myr]	Δt [h]
Earth craters				
Davasobel	27.47	26.61	55	
4.181	15.48	15.23	16.05	11.20
0.8020	0.3918	6.10	89.182	9.5
Crater	Diameter ⁸	v_{imp} ⁹	Age ¹⁰ [Ma]	
Slate Islands	30.00	~ 20 km/s	436	–

Table 3. Earth-impacts

Venus craters				
2000 SV2	19.60	19.15	43	
4.851	17.965	31.21	19.88	10.2
0.9269	0.3755	46.47	97.403	3.87
Crater	Diameter ¹¹	v_{imp}	Age [Ma]	
Rowena	19.6	–	–	–

Table 4. Venus-impacts.

Mars craters				
2000 SV2	22.85		53	
2.689	9.958	14.57	14.80	5
Crater	Diameter ¹²	v_{imp}	Age [Ma]	
Endeavour	22.0	–	–	–

Table 5. Mars-impacts.

Chapter 4

Lunar effects on close encounters of Hungaria asteroids and Near-Earth Asteroids with the Earth

The numerical integrations used in the previous two articles are used to evaluate directly the close encounters of the Hungaria-NEAs. In addition a study on the orbital evolutions of a large sample of *NEAs* in all its own types was performed. All this work was done to evaluate the Lunar perturbation on the asteroid close encounters. Considering the binary system disjointed and not simplified as the previous work in only one single massive body (which encompass both the masses of the Earth and of the Moon) placed on their point for the central mass. This work is a continuation of the previous two in order to see if the presence of the Moon disjointed by the Earth could create important differences in the statistics, but it does not significant ones.

Authors: Akos Bazso and Mattia Galiazzo²⁶

Publication state: Published in 2011

Publication details: Proceeding of the Journées 2011

Contribution of the first author: The first author was responsible for the basic idea to evaluate the perturbation of the Moon in front of the *NEAs*, estimating the number of close encounter and impacts of the real *NEAs*. The whole text of the paper has been written by the first author.

²⁶ Author affiliations are presented in the header of the following article.

Contribution of the co-authors: The idea to investigate the Hungarias was given by the second author, who fully performed the integrations of the Hungarias and estimate the number of close encounter and impacts of the fictitious Hungaria-NEAs with and without the Moon present in the orbital integration. In addition, corrections and suggestions on the text of the paper was given by the second author.

LUNAR EFFECTS ON CLOSE ENCOUNTERS OF HUNGARIA ASTEROIDS AND NEAR-EARTH ASTEROIDS WITH THE EARTH

A. BAZSÓ, M. GALIAZZO

Institute for Astronomy, University of Vienna
Türkenschanzstraße 17, A-1180 Vienna, Austria
e-mail: akos.bazso@univie.ac.at, mattia.galiazzo@univie.ac.at

ABSTRACT. The Earth is target to many celestial objects, among them Near Earth Asteroids (NEA) play a significant role. Different dynamical groups have been found, the source of these asteroids is mainly the main belt and, in particular the Hungaria group. We carry out a statistical investigation by numerical integration of the motion of real asteroids and their hypothetical clones in a simplified dynamical model of the solar system up to 100 My. In a first part we present integrations of existing Hungaria asteroids to determine which of them could become NEAs. Then the influence of the Moon on the orbits of these NEAs is investigated. The main goal is to find the frequency of close encounters and deflection angles due to them, possible impacts and the strength of deflection by the Moon.

1. INTRODUCTION

The population of Main-Belt Asteroids (MBA) was found by Hirayama (1918) to be clustered into “families” of asteroids, which share similar orbital elements (i.e. semi-major axis a , eccentricity e , inclination i). Later it turned out that the families can also be discriminated by spectroscopic properties (taxonomic classification by Tholen). These groups and families originated presumably by collisional break-up of larger objects, a process which is still ongoing in the solar system.

One of these groups is the Hungaria group, named after the biggest object (434) Hungaria, located at the inner edge of the main-belt at approximately 2 AU (astronomical units). The Hungaria group is an interesting case to study the dynamics of MBAs, since it is surrounded by several mean-motion resonances (MMR) and secular resonances (SR). On the outer edge the J4:1 MMR with Jupiter effectively removes asteroids, while the inner edge is shaped by Mars encounters at perihelion, additionally the M3:4 MMR acts inside the orbital parameter region of the Hungarias, and the ν_6 secular resonance limits the maximum inclination of the group’s members (Milani et al., 2010).

All these constraints lead to the conclusion, that since the scattering of objects from the Hungaria group preferably happens towards the inner solar system (Galiazzo & Bazsó, 2011), there must be an exchange of asteroids between the Hungaria group and the Near Earth Asteroids (NEAs). The spectra of Enstatite achondrite meteorites (McSween, 1999) studied on Earth give indirect evidence for a link to Hungaria asteroids, as they show similar features like the E-type spectral class, and approximately 60% of the Hungaria population belongs to this class (Warner et al., 2009).

To confirm this link we started a study of the dynamics of the Hungaria group with the aim to find out more about the evolution to Near-Earth asteroids and their long-time behaviour. The main point is the investigation of close-encounters to the Earth, where also the influence of the Moon needs to be taken into account. Domingos et al. (2004) verified that the orbits of NEAs can be significantly affected by the Moon at low relative velocities. The gravitational influence of the Moon results in a twofold effect: on one hand the Moon prevents the Earth from collisions, but on the other hand it can enhance the collision rates.

2. DESCRIPTION OF THE MODELS AND METHODS

This study consists of two complementary parts:

1. In the first part from a selection of 200 real asteroids we found 11 Mars-crossing objects that subsequently become NEAs (“escapers”, see Table 1 of Galiazzo & Bazsó, 2011). These 11 Hungarias

were cloned, i.e. their initial conditions (orbital elements a, e, i) were slightly modified, to enhance the statistics of close encounters. The dynamical model consisted of the planets Venus to Saturn, the integrations were carried out for 100 million years with the Lie N-body integrator (Hanslmeier & Dvorak, 1984; Egl & Dvorak, 2010), which is capable of treating close encounters accurately by using an adaptive step-size.

In our sample of Hungarias we have chosen objects that fall into the following intervals of osculating elements: $1.78 \leq a[\text{AU}] \leq 2.03$, $0 \leq e \leq 0.19$, $12 \leq i[\text{deg}] \leq 31$. Their typical diameters range from $\approx 0.5 - 2.5$ km, which is not too distinct from the NEA sizes.

The primary goals were to establish the number of close encounters and impacts, the impact probability and relations between different encounter related parameters.

2. The following part concentrates on the NEAs, as we have previously seen that many Hungarias can evolve into orbits typical for NEAs. We investigate each of the three NEA groups in detail by selecting some hundred objects (100 Atens, 200 Apollos, and 300 Amors) and running numerical integrations for 10 million years using the same code as above. The integration time here is shorter than for the Hungarias, since due to their typically smaller semi-major axes the orbital evolution of NEAs is faster, and additionally the median lifetime of NEAs is of the same order as our integration time (Gladman et al., 1997).

We compare the evolution of NEAs in two models, model 1 (M1) is the spatial elliptic restricted three body problem Sun–Earth–NEA, and model 2 (M2) the spatial restricted four body problem Sun–Earth–Moon–NEA (i.e. we always consider the NEAs to be massless). In this way we can compare the results for close encounters without Moon in M1 with those in M2 with the Moon’s contribution added.

For each close encounter¹ of every asteroid we collect data like the minimum distance to the Earth, the relative velocities, the time spent inside the lunar orbit, and the magnitude of deviation from the unperturbed orbit during fly-by. The latter is expressed by the “deflection angle”, by which we mean the angle formed by the velocity vectors at the time instants of begin and end of the close encounter. The deflection angle depends on the minimum distance to Earth, the closer the asteroid approaches the higher the angle gets since the trajectory is strongly influenced.

3. RESULTS

The data for close encounters (see Table 1) are at first glance as expected. The Amor group asteroids with typically relatively large semi-major axes ($a \geq 1.5$ AU) have the fewest encounters with Earth. On the contrary there is a sharp increase for both the Apollos ($a \geq 1$ AU) and Atens ($a < 1$ AU), as both are Earth orbit crossing populations, whereas the Amors only approach Earth at their perihelia. The table also shows that there is a difference in the relative velocities for Amors vs. Apollos/Atens, although the average velocity for Amors (M2) is almost as high as for the other NEA groups. The other velocities do not exhibit such big differences, for each group the values lie within the $1 - \sigma$ interval. Considering the deflection angles it is obvious that a lower relative velocity result in a higher deflection, if the asteroids pass close enough by the Earth or Moon.

The number of close encounters is not given for the Hungarias in Table 1, because the numbers depend strongly on the clones chosen, and that would make an average very unreliable. There are even clones completely lacking close encounters, which are derived from an object that itself does have close encounters, thus showing how sensitive the results are with respect to the initial conditions, and that the reliable orbit determination after a close encounter is not trivial. Higher relative velocities for Hungarias in the table are due to the fact, that they first increase their eccentricities to leave the main belt and become Mars crossers, then having Mars encounters further increases the eccentricity. So when they finally evolve into Earth orbit crossing asteroids they quite often have a higher mean eccentricity than other NEAs.

For the deflection angle we find a quite simple relation to the minimal distance. When both are plotted as in Figure 1 a fitting function of the form $y = a/x^b + c$ can be used, where the exponent $b \approx 1$. This fit also holds in the case of NEAs, with the angles being larger, reaching up to more than 90° in extreme

¹We define a “close encounter” of an asteroid to the Earth, if the mutual distance of the two bodies is less than 0.0025 AU, which is the average lunar distance of 384400 km.

group (model)	total number of encounters	relative velocity [km/s]	deflection angle [deg]	duration [days]
Amors (M1)	296	10.5	6.77	0.54
Amors (M2)	315	14.0	7.71	0.36
Apollos (M1)	10789	14.7	1.83	0.43
Apollos (M2)	12558	13.5	2.06	0.46
Atens (M1)	25258	14.4	1.45	0.44
Atens (M2)	26425	15.1	1.37	0.42
Hungarias (M1)	—	20.3	0.8	0.35
Hungarias (M2)	—	20.1	12.8	0.34

Table 1: Summary of the close encounter count with direct comparison between the two models M1/M2 for NEAs (The numbers for Hungaria escapers are not given, see text for explanation). For every group the total (absolute) number of encounters within 0.0025 AU is shown, first for model 1 where there is no influence by the Moon, and second for model 2 including the additional gravitational effect caused by the Moon. Also shown are the averaged values for the relative velocity, deflection angles and durations, i.e. the time elapsed between entering and exiting the region inside 0.0025 AU.

cases where there would be an impact. The scattering of points in the plot is a natural consequence of the variation in encounter velocity, which itself depends on the osculating elements (eccentricity, inclination) at the given time. Apart from the values shown in the table, when considering all the clones, the duration of close encounters seems to be shorter (or at most similar) in the case of model 1 (without Moon), while the deflections angles are systematically larger in model 2 (with Moon).

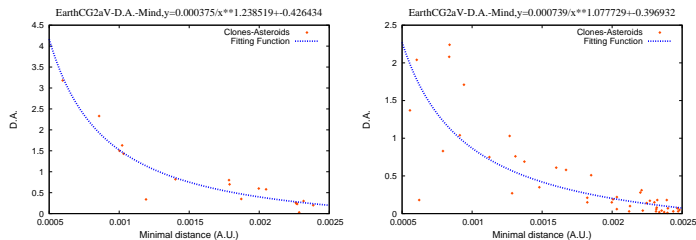


Figure 1: Dependence of the deflection angle on the minimal distance to Earth for close encounters with velocities less than 11.2 km/s. Every point in the plot corresponds to a separate close encounter event. The left figure shows the case for a Hungaria asteroid without the Moon, on the right the same object with the Moon.

In the integrations the majority of close encounters takes place at a rather large distance, so most of the time only “shallow encounters” occur. This behaviour is well visible in Figure 2, where the highest fraction of events (around 70%) falls into the right-most bin, representing minimal encounter distances just below the lunar distance. Here qualitatively no difference between Hungarias and NEAs is found, in any case one can observe a linear trend in these log-log plots (minimal distance vs. number).

For the two selected Hungaria asteroids shown in the right part of Figure 2 there were no impacts, so the minimal distances are well above the “critical” value of 6400 km, while for the NEAs the figures show several cases with impacts, that fall either into the bin at 3.5 or 3.8. It is also visible that the fraction (relative number of cases) is systematically higher for the lowest distance bins in model 2 (including the Moon) compared to model 1. When computing the impact probability P_c for the Hungarias using the method of Dvorak & Pilat-Lohinger (1999) we get for M1 $P_{c,1} = 9.7 \times 10^{-8}$ /year, and for M2 $P_{c,2} = 1.1 \times 10^{-8}$ /year. Here we see that the impact probability is higher without the Moon.

4. CONCLUSIONS

Considering the data presented we argue, that the Moon does have a non-negligible effect on close

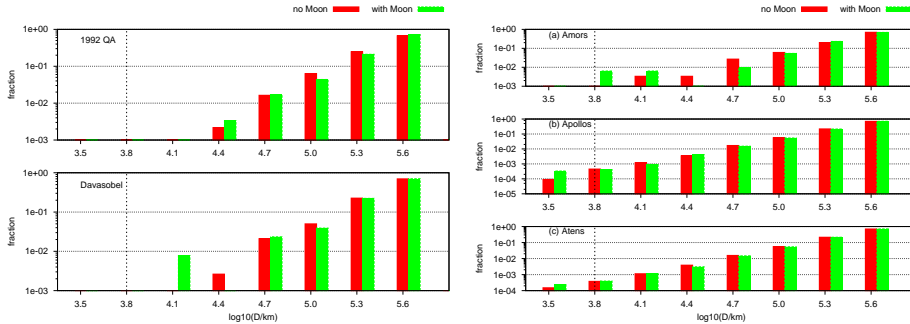


Figure 2: Histograms for the distribution of the distances for two selected Hungarias (left) and the NEA groups (right). The bars represent the fraction of cases (number per bin normalised by the total number of close encounters) for the distance D being lower than a certain value. The red (left) resp. right (green) bars indicate model 1 resp. model 2. Note that the distance is on a logarithmic scale, i.e. the plot range corresponds to an interval of $3200 < D < 400000$ km. The vertical lines at 3.8 indicate the collision distance of approximately one Earth radius, $D = 10^{3.8} \approx 6300$ km.

encounters of both Hungarias and Near Earth asteroids. We have shown that there are distinct differences whether or not the Moon’s gravitational influence is taken into account. The number of close encounters is similar in both models, and is only comparable for objects belonging to the same group of NEAs. Although the absolute numbers depend on the arbitrary choice of the limit distance (for a larger value of 0.01 AU instead of 0.0025 AU the number of close encounters increases by an order of magnitude at least), a normalisation still gives good results. The deflection angles and impact probabilities indicate that in the Moon’s presence incoming asteroids are more effectively scattered, which is why the first values are higher and the latter lower. The interesting shift of minimal encounter distances to lower values in model 2 gives rise to additional questions, that we need to tackle in future work. We will continue our work to better understand the role of the Moon, but we are aware that we need more data to draw decisive conclusions.

5. REFERENCES

- Domingos, R. C., Winter, O. C., Neto, E. V., 2004, “Collisions with the Earth: the Moon’s contribution”, *Advances in Space Research*, 33, pp. 1534–1538
- Dvorak, R. and Pilat-Lohinger, E., 1999, “On the dynamical evolution of the Atens and the Apollos”, *Planetary and Space Science*, 47, pp. 665–677
- Eggl, S. and Dvorak, R., 2010, “An Introduction to Common Numerical Integration Codes Used in Dynamical Astronomy”, In: *Lecture Notes in Physics*, Berlin Springer Verlag, 790, J. Souchay & R. Dvorak (Eds.), pp. 431–480
- Galiazzo, M. and Bazzó, Á., 2011, “The Hungaria Asteroids: Close encounters and impacts to terrestrial planets”, *Celest. Mech. Dyn. Astr.*, submitted
- Gladman, B. J., Migliorini, F., Morbidelli, A., Zappala, V., Michel, P., Cellino, A., Froeschle, C., Levison, H. F., Bailey, M., Duncan, M., 1997, “Dynamical lifetimes of objects injected into asteroid belt resonances”, *Science*, 277, pp. 197–201
- Hanslmeier, A. and Dvorak, R., 1984, “Numerical Integration with Lie Series”, *A&A*, 132, pp. 203–208
- Hirayama, K., 1918, “Groups of asteroids probably of common origin”, *AJ*, 31, pp. 185–188
- McSween, H. Y., 1999, “Meteorites and their parent planets”, Cambridge University Press, Cambridge, UK, pp. 168.
- Milani, A., Knežević, Z., Novaković, B., Cellino, A., 2010, “Dynamics of the Hungaria asteroids”, *Icarus*, 207, pp. 769–794
- Warner, B. D., Harris, A. W., Vokrouhlický, D., Nesvorný, D., Bottke, W. F., 2009, “Analysis of the Hungaria asteroid population”, *Icarus*, 204, pp. 172–182

Chapter 5

Water delivery in the early Solar System

The following article studies with a numerical and statistical investigation the possibility that asteroids from the inner Main Belt, namely the Hungaria region, can be a source for Near-Earth Asteroids and in particular a source of water for the Earth and the other Terrestrial Planets.

Authors: Rudolf Dvorak, Siegfried Eggl, Áron Süli, Zsolt Sándor, Mattia Galiazzo and Elke Pilat-Lohinger²⁷

Publication state: Published 26 June - 10 July , 2011

Publication details: AIP Conference Proceeding, 1468 (10pp), 2011

Contribution of the fourth author: The fourth co-author provided proposals for some improvements of the article and indicated the spectroscopic composition of the Hungaria asteroids, specifying the probable poor content of water in E-type asteroids, despite a certain percentage contain water, being C-type in a smaller fraction (Assandri & Gil-Hutton, 2008).

Contribution of the other co-authors: The idea to investigate in particular the Hungaria group (following the results of the work of Galiazzo, Bazso & Dvorak (2013a), which was in progress at that time) as well as the resources necessary for the project' success were mostly supplied by the other coauthors.

Furthermore, the coauthors' contributions encompassed the whole "physical" numerical integration. Finally, they construct the whole paper and played a vital role in the statistical evaluation plus a scientific discussions and in providing proposals for some improvements of the article.

²⁷ Author affiliations are presented in the header of the following article.

Water delivery in the Early Solar System

Rudolf Dvorak*, Siegfried Egg1*, Áron Süli*,†, Zsolt Sándor*, Mattia Galiazzo* and Elke Pilat-Lohinger*

**Universitätssternwarte Wien, Türkenschanzstr. 17, 1180, Wien, Austria*

†*Department of Astronomy, Eötvös Loránd University, Pázmány Péter sétány 1/A, 1117 Budapest*

Abstract. As part of the national scientific network 'Pathways to Habitable Worlds' the delivery of water onto terrestrial planets is a key question since water is essential for the development of life as we know it. After summarizing the state of the art we show some first results of the transport of water in the early Solar System for scattered main belt objects. Hereby we investigate the questions whether planetesimals and planetesimal fragments which have gained considerable inclination due to the strong dynamical interactions in the main belt region around 2 AU can be efficient water transporting vessels. The Hungaria asteroid group is the best example that such scenarios are realistic. Assuming that the gas giants and the terrestrial planets are already formed, we monitor the collisions of scattered small bodies containing water (in the order of a few percent) with the terrestrial planets. Thus we are able to give a first estimate concerning the respective contribution of such bodies to the actual water content in the crust of the Earth.

Keywords: Early-Solar-System, Water-Transport, Hungaria-asteroids

PACS: 96.12.Bc, 96.30.Ys

INTRODUCTION

The presence of liquid water on the surface of a terrestrial planet is a basic requirement for habitability in planetary systems. The questions one needs to answer in this connection are

- When the terrestrial planets formed how much was their content of water?
- Why don't we find water in the same quantities on the other terrestrial planets?
- What happened to the water when a mars-sized object hit the Earth and the Moon formed?
- What happened during the Late Heavy Bombardement (LHB)
- Where from came water after the LHB?
- What is the role of the comets from the Oort Cloud?

A main problem in this context is to find out where the water came from in the early stages on the one hand; on the other hand, when water was lost during special phases in later stages one needs to explain how it was replenished on the surface. At the end one should explain also how it could stay liquid on a terrestrial planet in the habitable zone for times up to billions of years. A central question in this respect is the collisional behaviour of small bodies regarding their content of water; it has to be modelled with specially designed effective programs like the well known SPH (Smooth Particle Hydrodynamics) codes.

The possible water loss of terrestrial like planets in our Solar System (SS) and in Extrasolar Planetary system (EPS) in general should be set in context with geophysical processes like the stop of outgassing due to rapid mantle and core cooling or lack of atmospheric protection by a planetary magnetosphere

- the stellar radiative environment of young active stars (SS and EPS)
- collisions of protoplanetary objects in general (SS and EPS),
- the Late Heavy Bombardement (SS)
- the formation of the Moon (SS)

After the early stage the transport mechanisms in our SS from the main belt and also the Edgeworth-Kuiper-Belt can adequately be computed taking into account the important role of all sorts of resonances: mean motion resonances, secular resonances and three body resonances. The water delivery of the comets from the Oort cloud can be investigated statistically although it can only account for a fraction of the water on Earth regarding their different D/H ratio. Comets may have been brought into the inner SS by orbital changes due to passing stars, interstellar clouds and galactic tides leading to comet showers. Although the water transport is the central question it is of fundamental interest to investigate how organic (carbon-containing) material could be delivered which then lead or may have lead to the development of life on Earth-like planets in habitable zones.

Different scenaria will have formed very different architectures of the planets in an extra solar planetary system compared to our own system. The observed, close-in, Jupiter like planets, which evolved into such orbits via migration processes, make it difficult to explain the continuous existence of terrestrial planets on stable orbits within the habitable zone. Together with theoretical investigations on habitable planets, results from the existing satellite missions (CoRoT, KEPLER and Herschel) as well as future ones (Plato, James Webb, Gaia) combined with the progress in Earth-bound observations (Alma, ESO) will help to clarify the origin and presence of water (and organic materials) as a basis for life.

STATE OF THE ART

From many articles concerning the formation of terrestrial planets and their content of water (e.g. [16, 22, 19, 2, 23]) we can draw a coherent picture of those phases of planet-formation where the debris disk and a giant planet were already present. Following current models, most of a planet's water-content can be regarded as being produced by collisions between the growing protoplanet and Moon to Mars-sized planetesimals originating from the asteroid belt. According to [15] and also [22] the accretion of planetary embryos from distant regions (outside the snowline) by terrestrial planets could have happened also without the presence of a Jupiter-sized object. Other studies claim that the early Earth as well as the terrestrial planets were dry, just as the asteroids in the region of their formation, because only in the cold outer part of the early SS gas and water were present in big quantities ([26]). But in these phases collision events ([7, 8]) as well as the EUV radiation from the early star could have reduced the water content

in these regions (e.g. [5, 6, 13]). At any rate during a later stage water was brought onto the surfaces of the terrestrial planets and, whereas Venus and Mars could not keep their water on the surface, the Earth's magnetosphere anticipated water loss (e.g. [13]). Many scenarios try to explain the water transport onto Earth; the most plausible seems to be that the C-asteroids from the outer main belt of asteroids, main belt comets ([3]) and small bodies from outer regions of the SS up to the scattered disk, consisting in big parts of frozen water contributed to the water content on Earth.

Given the discovery of water and a subsurface ice reservoir on the asteroid 24 Themis ([4]), and comet-like activity of several small asteroids it is clear that water is in fact abundant in many solar system bodies and may even lie well hidden inside a crust. Collision probabilities, impact velocities and size distributions depend crucially on the orbits of the colliding objects as well as the perturbations of the planets on their motion respectively. Regarding these topics, namely

- formation and early development of Earth-like planets with respect to their water content,
- the possible loss of water through collisions with other celestial bodies (e.g. the impact of a Mars-like body onto the Earth with subsequent formation of the Moon, ([20], [25]) and
- late water transport,

cannot be modelled by pure gravitational N-body simulations, but with sophisticated codes including accretion, the role of the disks, the collisional growth etc.([10]). Numerous simulations concerning the formation of planets in the early Solar System have been performed where the early formation of a gas giant (Jupiter) is assumed. Hereby the giant planets are playing a key role; they formed when still there was a considerable amount of helium and hydrogen present in the early Solar nebula. Later accretion of terrestrial planets is closely connected to the perturbations due to these planets on planetesimals within the inner part of the disk ([22], [2]). The process of accretion of embryos by terrestrial planets may be possible for different giant planet configurations, and even without gas giants present in the system (e.g. [15] and [22]). Although most of the discovered EPS host at least one big planet – due to a biased sample because of the constraints in our observations – this may not be the rule for the formation of planetary systems in general (e.g. CoRoT-7b,c¹).

A crucial factor for water-delivery scenarios onto terrestrial planets is the so-called 'snowline' which is due to the outward diffusion of gas charged with vapour that condenses on existing particles during the period when its temperature changes. This change acts on the accumulation of particles that originate from further radial distances and have a faster inward migration because of their small sizes. As a consequence, water can be present as water ice bound in icy planetary embryos in the outer parts (respectively beyond the snowline) of the protoplanetary disc. Accretion of water from these bodies is a stochastic process, therefore planets may have different water content due to their

¹ CoRoT-7 is a planetary system (consisting of at least two planets) which was discovered by the space mission CoRoT (details in [12])

different histories ([19]). In this article it is also claimed that such contributions to water on terrestrial planets may be minor because of the perturbations of Jupiter. There exist quantitative estimates for the impact erosion of atmospheres and condensed oceans of planets during the LHB ([7]). But also the delivery of prebiotic organic matter (C, H, O, N and P) together with water by main belt comets and also comets from the Oort Cloud([21]) has been established via hydrodynamic simulations. According to recent results of computations by [1] some small amount of amino acids could even survive low impact velocities as subsurface habitats.

TRANSPORT OF WATER TO THE TERRESTRIAL PLANETS FROM THE HUNGARIA MAIN BELT REGION

One expects that the main source for water delivery to the Earth are asteroids in the main belt between Mars and Jupiter (as well as comets from the Oort cloud). A water gradient in the protoplanetary disk such that at 1 AU bodies were dry, whereas bodies at 2.5 AU contain 5 percent of water is the usual assumption. It is well known ([18]) that asteroid groups in the main belt with high inclination to the ecliptic plane can evolve to become Mars crossers. Such configurations seem promising candidates, if one was to look for possible mechanisms that can uphold a constant supply of material into the inner Solar System.

In our preliminary approach we took a sample of fictitious small bodies in the region where now the Hungaria family of asteroids is located. This family is believed to originate from a violent dynamical event ([18], [27]) about 0.5 Gyrs ago that caused an injection of the Hungaria predecessors into orbits with an inclination of about 20 degrees. Another interesting point is the proximity of these asteroids to the 4:1 mean motion resonance with Jupiter as well as several secular resonances as their semimajor axes are mostly between 1.8 and 2 AU). Nowadays the Hungaria group consists of more than 8000 known members with the largest objects with sizes up to 12 km. The membership of asteroids within this group to one or more families is still in debate ([18]). However, for our purposes, the existence of such bodies will be taken as a reasonable argument, that during dynamically more violent times in the late stages of the Solar System's formation, planetesimals could have been proliferated to this region of the main belt.

We have undertaken numerical simulations up to 40 million years, in order to investigate the number of possible close encounters respectively impacts of our test population with the terrestrial planets in the inner Solar System. As a dynamical model we chose to include the Venus-Earth-Mars-Jupiter-Saturn system as it is now, with exception that we did not consider the moon explicitly.

Using results by [11] 300 planetesimals were distributed in a phase space region of the Hungaria group which has been shown to lead to an increased number of close encounters. Another 648 were placed in the groups enclosing resonances. The goal was to see how quickly the respective populations become so-called Near-Earth-Asteroids, where every now and then one might have close encounters respectively impacts on the Earth (and also Mars and Venus). The four different chosen regions, where the initial

conditions for the four different samples were chosen, are given below:

- **S1**: 300 Hungarias clones with three different semimajor axes $a = 1.90792307, 1.91027822, 1.90508465$ AU and equally distributed eccentricities in the range $0.18 < e < 0.19$ and inclinations in the range of $17^\circ < i < 27^\circ$.
- **S2**: 216 clones close to the ν_{16} secular resonance² equally distributed with slightly larger semimajor axes than the Hungarias $1.9 < a < 2.1$ AU and the eccentricities and inclinations like in **S1**.
- **S3**: 216 clones close to the ν_5 secular resonance³ equally distributed with slightly smaller semimajor axes than the Hungarias $1.8 < a < 1.9$ AU and the eccentricities and inclinations like in **S1**.
- **S4**: 216 clones in the region of the ν_5 secular resonance with semimajor axes $1.85 < a < 1.95$ AU, the eccentricities like in the range of **S1** but with significantly larger inclinations $27^\circ < i < 35^\circ$.

In Fig.1 we depict the region of Hungaria family in an plot $\sin(i)$ versus the semimajor axes. Note that the bodies in samples **S1**, **S2** and **S3** have the same inclinations but their initial conditions are shifted to larger respectively smaller semimajor axes. The initial orbital elements for the fictitious bodies of **S4** are distributed in semimajor axes $1.85 < a < 1.95$ and have large initial inclinations (around 30°). of the figure).

Close Encounters with the Planets

The results for the four different planetesimal samples are summarized in the following graphs 2-5. We note that during our integrations the mutual perturbations between planetesimals was neglected and only close encounters with the planets were reported.

Depending on the close encounters we could extrapolate collision timescales which are crucial for estimates for a possible water transport onto the terrestrial planets; we estimated the water content to be three percent of the small bodies' masses.

Fig.2 shows the number of close encounters within the so-called Hill's sphere⁴. We note that for Venus the results do not agree with other studies with respect to the frequency of close encounters (e.g.[11], [9]). This is because of the relatively short integration time in our investigations. The transport of the asteroids from the Hungaria region to the inner regions of the planetary system takes longer (about several tenth of million years) than for Mars and the Earth. In Fig.3 we compare the closest encounters during the integrations for the four samples for all planets. One can see that counted in planetary radii only one real collision occurred and that is one with Jupiter. Although no collisions are reported for the terrestrial planets we can extrapolate these results of the

² where the secular nodal motion of the massless body equals the nodal motion of Saturn

³ where the secular perihelion motion of the massless body equals the perihelion motion of Jupiter

⁴ This sphere around a planet is defined as $r_H = (\frac{\mu}{3})^{\frac{1}{3}}$ where μ is the mass of the planet in Solar masses. It can be regarded as a sphere of influence where inside the gravitation of the planet is larger than the one of the Sun

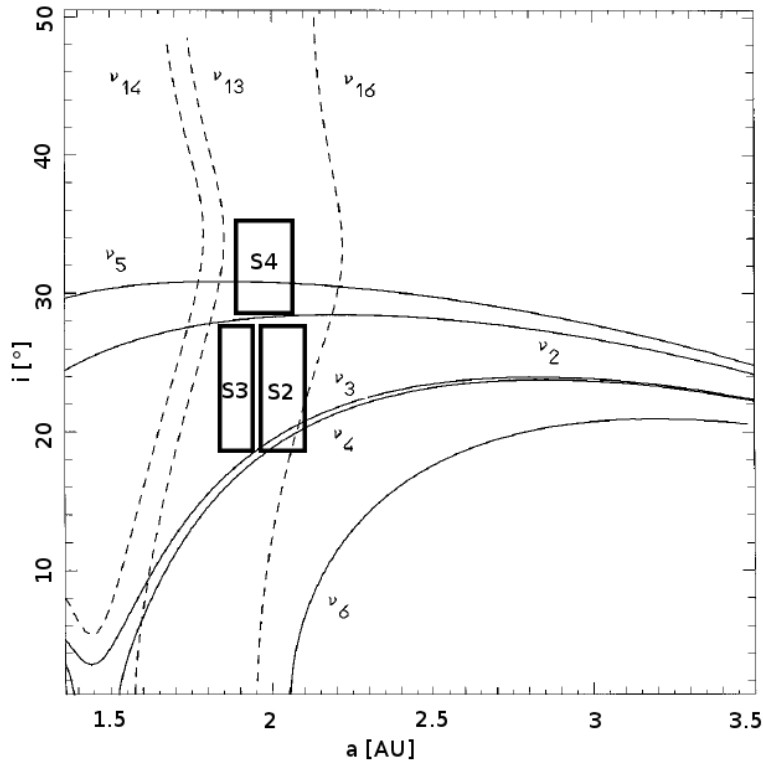


FIGURE 1. The Hungaria asteroid region in a inclination versus semimajor axes diagramm. The locations of the initial conditions of the samples **S2**, **S3** and **S4** are shown in the rectangular boxes. The initial conditions for the sample **S1**, just inside the Hungaria region, are between **S2** and **S3**. The dashed lines indicate the secular resonances involving the longitudes, the solid lines involving the perihelion longitudes between a small body and a planet. The numbers '2' - '6' stand for the planets Venus to Saturn. (after [17]).

frequency of the close encounters and find (see next chapter) an estimation of the time interval of a single Hungaria clone for an encounter. It is also visible from the graph that the (biased, see former remark about the integration time) tendency for collisions is getting larger from Venus to Jupiter; this reflects the results shown in Fig.2 where one can see the increasing number of close encounters from Venus to Jupiter. The larger values for the closest distances to Saturn in planetary radii reflects also the smaller number of encounters to this planet.

The Impacts

We need to say that in all our samples 'real' collisions were very rare! We used the results of the many encounters to the planets to derive from there a value for possible impacts (see Figs. 4 to 6). Binned values of the encounters were plotted versus the number of such events. A logarithmic least square fit provided us with the desired value

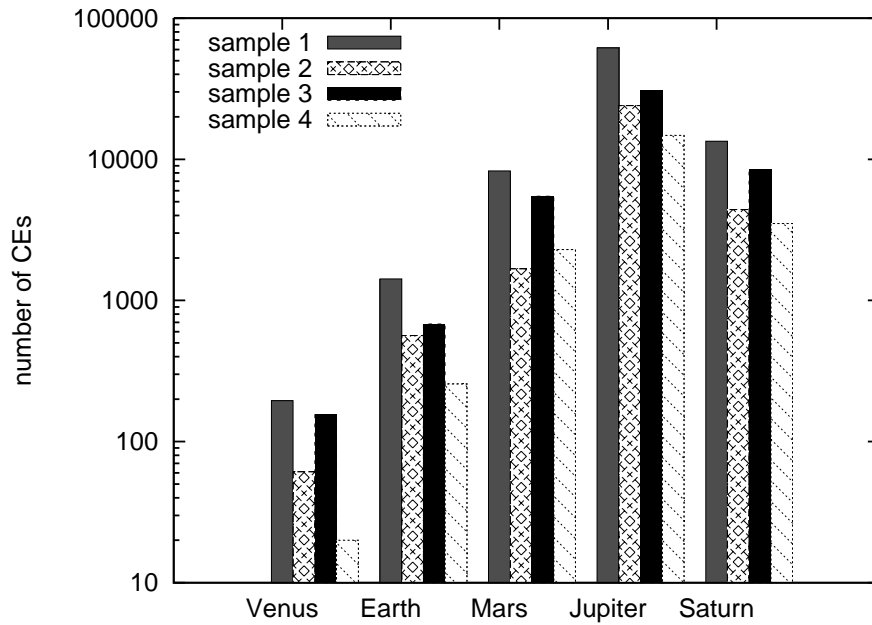


FIGURE 2. Logarithmic plot of the number of close encounters of the fictitious objects with the planets within its Hill's sphere (for more see in the text) for all the planets involved. We separate the results for the four different samples

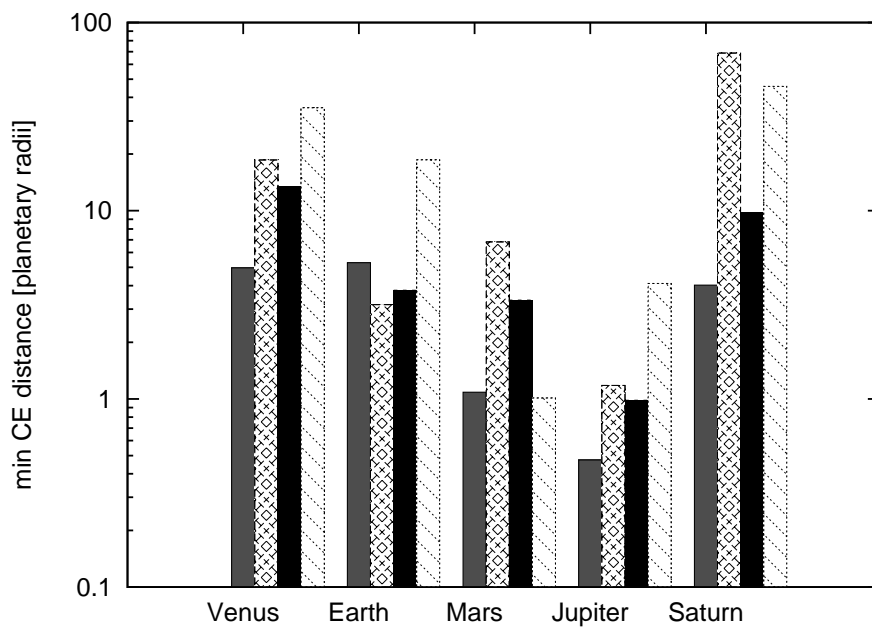


FIGURE 3. Logarithmic plot of the closest encounters to the planets in units of the radii of the planets. Detailed description in the text

TABLE 1. Impact times for the samples **S1** -**S4** (columns 3-6) onto the terrestrial planets within 1 Gyr

Planet	Radius[AU ⁻⁵]	S1	S2	S3	S4
Mars	2.25939	800.69	819.275	258.348	10.6991
Earth	4.25875	442.778	12.3894	30.3799	4.29435
Venus	4.04484	1.49954	71.7986	20.3137	0.655851

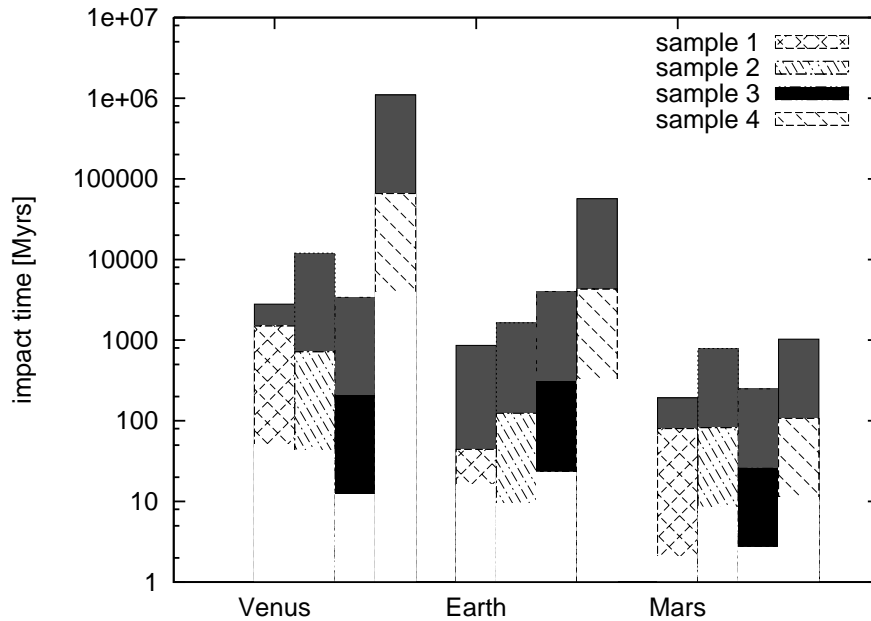


FIGURE 4. Impact time scales for Hungaria like planetesimals in the samples **S1** to **S4** on the terrestrial planets. For detail see text.

for the probability of collisions. We do not show this fit for Venus because the results are biased because of the small number of events.

It is evident that Mars – as closest to the Hungarias – suffers from impacts first of all, whereas Venus globally is the planet with the least such events (due to the relatively short time scales of integrations). Most impacts of the fictitious objects occurred in **S1**, which is a somewhat surprising fact, because shifting versus the secular resonances (**S2** and **S3**) should cause more perturbations on a body located there. Totally insignificant for the transport of small bodies to the inner system seems to be the group **S4**, which is probably due to the large inclinations we have chosen for the initial conditions.

In Fig.4 we plotted the mean values of the impact time scales which are the intersecting lines between the patterned and full bar segments. The mean values plus one standard deviation are denoted by the top of the bars, mean values minus one standard deviation by the bottom end of the patterned region. The large errors (especially for Venus and for all planets in **S4** are caused by the poor statistics due to the choice of the integration time respectively the initial conditions.

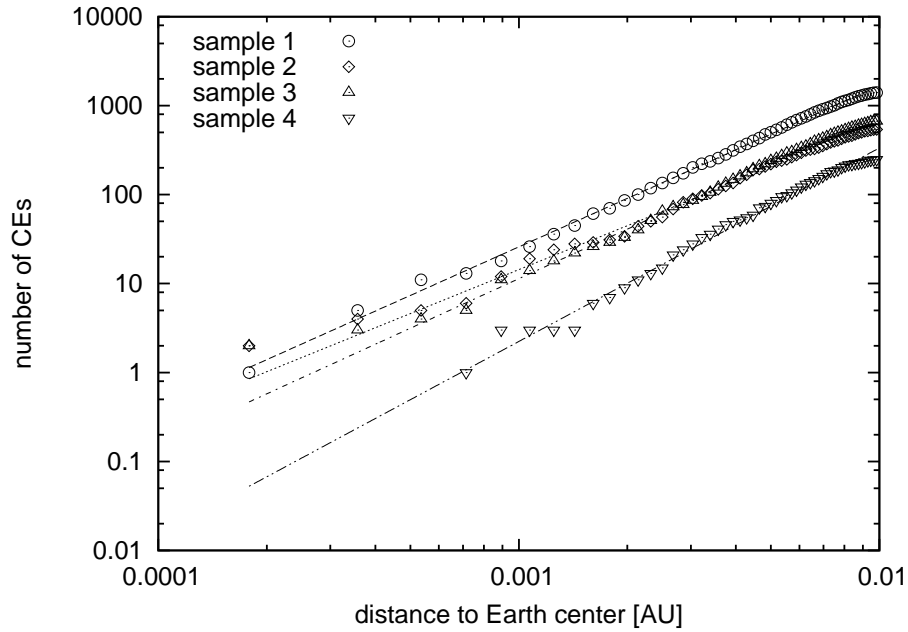


FIGURE 5. Logarithmic least square fit for the encounters with Earth using the results of samples **S1** to **S4**

In addition to the former results we have undertaken numerical experiments with a fictitious planetary system consisting of more massive terrestrial bodies comparable to a recent study by [24]. In our new study of the sample **S1**, also for 300 clones representing small bodies, we have taken five times large masses⁵ for these planets; we expected many more impacts because of the higher gravitational perturbations. In fact in contrary to the former results for the 'real' SS where only 1 'real' collision (namely with Jupiter) was reported in this investigation the results are the following ones:

- 5 with Venus at 8.9, 8.58, 19.1, 34.7 and 38.6 myrs
- 3 with Earth at 33.9, 43.13 and 46 myr
- 2 with Mars 18.1 37.8 myr
- 1 with Jupiter at 37.7 myr

These results agree much better with the ones we mentioned above, namely that Venus is suffering the most of collisions. We can explain this – expected result – that the time scales of transport of the 'planetesimals' to the inner SS are much faster in the case with $\kappa = 5$.

⁵ like in the former mentioned paper we define a multiplication factor κ for the terrestrial planets

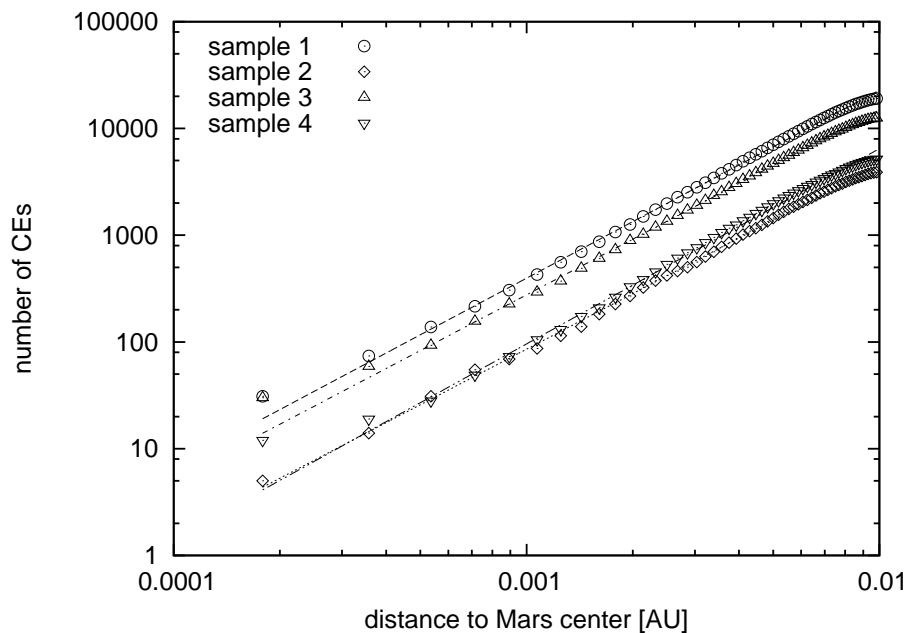


FIGURE 6. Logarithmic least square fit for the encounters with Mars using the results of samples **S1** to **S4**

CONCLUSIONS: WATER FROM HUNGARIA LIKE PLANETESIMALS?

The values from the former Tab.1 can now be used to estimate not only the how many bodies from this region may hit the Earth, it can also be used to estimate – in principle – how much water was transported from this region in the SS to our planet. Because of the very small number of impacts (see Tab.1) the contribution to the water in the crust of the Earth (estimated to be several $10^{-4}M_{Earth}$) is for sure insignificant!

Another result is of interest in this context: by far Mars suffers from most of such impacts and thus received a lot of more water even than Earth. But where is the water now? New results show that man structures on the surface of Mars are due to floating water. During the development of the Solar System this planet lost most of its water because the thin atmosphere, the much lower gravitation field and the absence of a protecting magnetosphere ([14])

For the water on Earth we can summarize that the phase space region around the Hungaria asteroid group is capable of injecting planetesimals into the inner Solar System but the total number is in fact far to low. The timescales necessary for a considerable number of impacts are too large to constitute an efficient water transport mechanism and to contribute to our actual water on our planet and thus this region can be excluded as source for water delivery to the Earth.

This preliminary study can be understood as a first step of investigation of the whole phase space between Mars and Jupiter with respect to the transport to terrestrial planet crossing regions (region of Near Earth Asteroids) and thus to possible collisions of

small bodies with different water content on these planets, especially on the Earth.

ACKNOWLEDGMENTS

The authors R.D., A.S., Z.S. and E.P.L. need to thank the NFN (Nationales Forschungsnetzwerk) 'Pathways to Habitable worlds' from the Fonds zur Förderung der Wissenschaft Nr. S 11603-N16 and S-11608-N16, S. Eggl would like to acknowledge the support of University of Vienna's Forschungsstipendium 2012; M.Galiazzo has to thank the Doctoral School at the University of Vienna 'From Asteroids to Impact Craters'

REFERENCES

1. Abramov, O., Mojzsis, S. J., *Nature*, **459**, pp. 419–422 (2009)
2. Alibert, Y., Mordasini, C., Benz, W. and Naef, D., “Testing planet formation models against observations,” in *EAS Publications Series*, edited by K. Goździewski et al., pp. 209–225 (2010).
3. Bertini, I., *Planetary and Space Science*, **59**, pp. 365–377 (2011).
4. Campins, H., Hargrove, K., Pinilla-Alonso, N., Howell, E. S., Kelley, M. S., Licandro, J., Mothé-Diniz, T., Fernández, Y. and Ziffer, J., *Nature*, **464**, pp. 1320–1321 (2010).
5. Chassefière, E., *Journal of Geophysical Research*, **101**, pp. 26039–26056, (1996).
6. Chassefière, E., *Icarus*, **124**, pp. 537–552, (1996).
7. Chyba, C. F. *Nature*, **348**, pp. 113–114 (1990a)
8. Chyba, C. F., *Nature*, **343**, pp. 129–133 (1990b)
9. Dvorak, R. and Pilat-Lohinger, E., *Planetary and Space Science*, **47**, pp. 665–677 (1999)
10. Eggl, S. and Dvorak, R., *Lecture Notes in Physics*, **790**, pp.431–480 (2010).
11. Galiazzo, M., Bazso, A. and Dvorak, R. (in preparation)
12. Hatzes, A. P., Dvorak, R., Wuchterl, G., Guterman, P., Hartmann, M., Fridlund, M., Gandolfi, D., Guenther, E. and Pätzold, M., *Astronomy and Astrophysics*, **520**, (2010),
13. Lammer, H., Eybl, V., Kislyakova, K. G., Weingrill, J., Holmström, M., Khodachenko, M. L., Kulikov, Y. N., Reiners, A., Leitzinger, M., Odert, P., Xiang Grüss, M., Dorner, B., Güdel, M. and Hanslmeier, A., *Astrophysics and Space Science*, **69**, (2011).
14. Lammer H. et al. (submitted to Space Science Library)
15. Levison, H. F. and Agnor, C., *Astronomical Journal*, **125**, pp. 2692–2713 (2003).
16. Lunine, J. I., Chambers, J., Morbidelli, A. and Leshin, L. A., *Icarus*, **165**, pp. 1–8 (2003).
17. Michel, P. and Froeschlé, Ch. *Icarus*, **128**, pp. 230–240 (1997)
18. Milani, A., Knežević, Z., Novaković, B. and Cellino, A., *Icarus*, **207**, pp. 769–794 (2010)
19. Morbidelli, A., Chambers, J., Lunine, J. I., Petit, J. M., Robert, F., Valsecchi, G. B. and Cyr, K. E., *Meteoritics and Planetary Science*, **35**, pp. 1309–1320 (2000).
20. Pahlevan, K. and Stevenson, D. J., *Earth and Planetary Science Letters*, **262**, pp. 438, (2007).
21. Pierazzo, E. and Chyba, C.F., *Advances in Astrobiology and Biogeophysics*, pp. 137, (2006)
22. Raymond, S. N., Quinn, T. and Lunine, J. I., *Icarus*, **168**, pp. 1–17 (2004).
23. Raymond, S. N., Armitage, P. J., Moro-Martin, A., Booth, M., Wyatt, M. C., Armstrong, J. C., Mandell, A. M., Selsis, F. and West, A. A. *ArXiv e-prints*, (2011).
24. Süli, Á and Dvorak, R., *Astronomische Nachrichten*, **328**, pp. 4–9 (2007)
25. Taylor, J. *American Geophysical Union, Fall Meeting 2010*, (2010).
26. Trigo-Rodríguez, J. M. and Martín-Torres, F. J., *ArXiv e-prints*, (2011).
27. Warner, B. D., Harris, A. W., Vokrouhlický, D., **204**, pp. 172–182 (2009)

Chapter 6

Other sources of PCAs

6.1 V-type asteroids: impacts and close encounter with Terrestrial Planets

This paper is in preparation and it continues under the frame of Galiazzo et al. (2013a, 2014a), but with a different group of asteroids, the V-types *NEAs*, which are thought to be originated mainly by the Vesta Family (Asphaug , 1997; Marchi et al. , 2004, 2005; Fulvio et al. , 2012). Close encounters and impacts with Terrestrial Planets will be statistically studied, considered the possible gravitational perturbations of 4 Vesta and 1 Ceres, too.

Authors: Mattia Alvisè Galiazzo¹, Siegfried Eggl², David Bancelin^{1,2}, Damya Souami³

Publication state: submission expected in December, 2013

Publication details²⁸: Monthly Notices of the Royal Astronomical Society, 2014

Contribution of the first author: The first author was responsible for the entire idea to study the V-types asteroids as a special source of close encounters and impactors on Terrestrial Planets. All the “physical” numerical integration was done by the first author. The statistical analysis, computations and writing the part of the paper in this thesis was done by the first author.

Contribution of the co-authors: An important role in scientific discussion and suggestions were given by the co-authors.

²⁸Much probable journal and year of publication.

Affiliations:

1. Institute for Astrophysics (IfA), University of Vienna, Turkenschantstr. 17, 1180 Vienna, Austria
2. IMCEE, Observatoire de Paris, UPMC, UMR 8028 CNRS, 77 avenue Denfer-Rocherau, 75014, Paris, France
3. SYRTE, Observatoire de Paris, Systèmes de Référence Temps Espace, CNRS/UMR 8630, UPMC, 75014 Paris, France

V-types asteroids (See Appendix B and Table B.2) are spread from the Main Belt to the inner Solar system. They can have many close encounters and eventually impacts with terrestrial planets. Most of the known asteroids seem to be fragments from the crust of Asteroid (4) Vesta (Asphaug, 1997; Marchi et al., 2004, 2005; Duffard et al., 2006; Fulvio et al., 2012), but possibly some of them come from other sources, also *HED* (Howardite-Eucrite-Diogenite) meteorites are ejecta which not come from Vesta directly but went out of surface of V-type asteroids such as V-type *NEAs*. This study is done via a statistical investigation on the V-type *NEAs*' close approach to the planets and considering the possible influence of two most massive asteroids in the Main Belt, i.e. 4 Vesta and 1 Ceres. In order to integrate²⁹ the orbits of the V-type asteroids (27 bodies found via JPL Small-Body Database Search Engine, http://ssd.jpl.nasa.gov/sbdb_query.cgi#x, see Table 6.1), the full Solar System from Mercury to Neptune, with the Pluto system and also the Moon are considered.

In this case the computation is done for shorter time than the Hungarias, because *NEAs* have a much shorter life-time than *MBAs*. In fact they have an impact with terrestrial planets or the Sun even in less than 5 Myrs. Close encounters and impacts are found in the ranges described on Table 1.2.

Because V-types asteroids are thought to be originated mainly by the Vesta family, even if some of them are thought to be originated by the Eunomia one (Carruba et al., 2005; Carruba, Michtchenko & Lazzaro, 2007; Migliorini et al., 1997), this might be thought as a study on the origin of *NEAs* from the Middle Main Belt, and in particular the Vesta family, too.

6.1.1 Results

Close encounters

After the analysis of the results from the integrations, it has been found that 33% (9) of the asteroids have close encounters with Venus, 52% (14) with Earth and 37.0% (10) with Mars; so assuming these results, V-types have close encounters preferentially with the Earth. Mars and Venus seem to have similar rates of *CEs*.

The mean durations of close encounters are different from the ones found from the Hungaria's *NEAs* (Galiazzo et al., 2013a, see Chapter 2) apart for Venus. It is higher for the Earth and it is about the half time for Mars: 0.30 ± 0.25 d for Venus, 0.93 ± 0.67 d for Earth and 0.26 ± 0.11 d for Mars. V-types asteroids stay longer near the Earth during close encounters than Venus and Mars.

The V-types seem to have more close encounters, considering the total number of *CEs* per each asteroid with the Earth, than the other planets (similarly to the Hungaria's *NEAs*). In fact the average number of close encounters by each asteroid for each terrestrial planet in 5 My of orbit-evolution is: 9 for Mars, 30 for the Earth and 4 for Venus.

²⁹using the Lie-integrator program (Hanslmeier & Dvorak, 1984; Eggl & Dvorak, 2010)

6.1. V-TYPES ASTEROIDS AND CLOSE ENCOUNTERS

Table 6.1: V-types asteroids considered in this work: their initial osculating elements and their diameter (D).

Asteroid	a (au)	e	i	D (km)
1997 GL ₃	2.28	0.78	6.69	0.162
1999 RB ₃₂	2.43	0.57	3.88	0.270
2000 DO ₁	1.43	0.68	3.45	0.215
(1981) Midas	1.78	0.65	39.83	3.400
(3551) Verenia	2.09	0.49	9.5	0.900
(3908) Nyx	1.93	0.46	2.18	1.000
(4055) Magellan	1.82	0.33	23.24	2.490
(4688) 1980 WF	2.24	0.52	6.38	0.600
(6611) 1993 VW	1.70	0.48	8.7	1.235
(7889) 1994 LX	1.26	0.35	36.91	2.146
(137052) Tjelvar	1.25	0.81	14.94	1.075
(162157) 1999 CV ₈	1.30	0.35	15.26	0.296
(192563) 1998 WZ ₆	1.45	0.41	24.76	0.854
(5381) Sekhmet	0.95	0.30	48.97	1.410
(8566) 1996 EN	1.51	0.43	37.96	1.300
(137924) 2000 BD ₁₉	0.87	0.89	25.69	0.910
(138404) 2000 HA ₂₄	1.14	0.32	2.17	0.373
(143947) 2003 YQ ₁₁₇	2.18	0.66	21.01	2.146
(163697) 2003 EF ₅₄	1.61	0.47	2.95	0.246
(238063) 2003 EG	1.74	0.71	31.75	1.305
1996 JA ₁	2.56	0.70	21.83	0.200
1999 RB ₃₂	2.43	0.57	3.88	0.266
2003 FT ₃	2.67	0.57	4.32	0.501
2003 FU ₃	0.86	0.39	13.04	0.163
2003 GJ ₂₁	1.81	0.40	7.07	0.067
2004 FG ₁₁	1.59	0.72	3.11	0.155
2008 BT ₁₈	2.22	0.60	8.11	0.539

The average deflection angle Θ is small ($< 1^\circ$) for the Earth and Mars, similar to the ones found for the Hungarias (Chapter 2), apart for Venus where the deflection is higher on average (3.6° for V-types).

The mean entry velocity of the V-types, for each terrestrial planet (Table 6.2), seems much bigger compared with the ones of the Hungaria's *NEAs*.

Planet	\bar{v}_{en}	$\bar{v}_{en,max}$	$\bar{v}_{en,min}$
Venus	25.50 ± 8.03	34.73	16.32
Earth	26.12 ± 5.49	42.25	11.08
Mars	23.74 ± 8.78	32.88	13.85

Table 6.2: Data of the planetary close encounters for some of the 27 V-types. All the velocities are measured at the distance for an encounter relative to the planet ($2.50 \cdot 10^{-2}$ AU for the Earth, $1.70 \cdot 10^{-2}$ AU for Venus and $1.66 \cdot 10^{-2}$ AU for Mars, as defined in Section 1.5): \bar{v}_{en} is the mean entry velocity, $\bar{v}_{en,max}$ is the mean maximum entry velocity, $\bar{v}_{en,min}$ is the mean minimum entry velocity. Exit velocity is always equal to the entry velocity inside a range of $0.01km/s$.

Planet	\bar{i}_{en}	$\bar{i}_{en,max}$	$\bar{i}_{en,min}$	\bar{i}_{ex}	$\bar{i}_{ex,max}$	$\bar{i}_{ex,min}$
Venus	15.01 ± 12.76	24.97	11.46	14.96 ± 12.76	24.82	11.44
Earth	19.47 ± 13.54	35.55	11.47	19.45 ± 13.57	35.47	11.51
Mars	28.15 ± 14.38	43.34	16.67	28.18 ± 14.36	43.36	16.81

Table 6.3: Data of the planetary close encounters for the 27 V-types. All the inclinations was measured at the distance for an encounter relative to the planet ($2.50 \cdot 10^{-2}$ au for the Earth, $1.70 \cdot 10^{-2}$ au for Venus and $1.66 \cdot 10^{-2}$ au for Mars, as defined in Section 1.5): \bar{i}_{en} is the mean entry inclination, $\bar{i}_{en,max}$ is the mean maximum entry inclination and $\bar{i}_{en,min}$ is the mean minimum entry inclination over all clones, \bar{i}_{ex} is the mean exit inclination, $\bar{i}_{ex,max}$ is the mean maximum exit inclination, $\bar{i}_{ex,min}$ is the mean minimum exit inclination.

6.1. V-TYPES ASTEROIDS AND CLOSE ENCOUNTERS

Sun or Planet	I.N./5My	%/5My	$\langle t_{imp} \rangle$ (My)	$t_{imp,i}$ (My)
Sun	5	19	1.554	0.321 1996JA ₁
Venus	3	11	2.148	0.403 2003EF ₅₄
Earth	1	4	0.375	0.375 2003FU ₃

Table 6.4: This table show the impact rate with each terrestrial planet and the Sun. “I.N.” is the number of impact with the bodies and next there is the percentage to the total of integrated *NEAs* (%). $\langle t_{imp} \rangle$ is the average time of impact over all ones and $t_{imp,i}$ is the first time when a V-type asteroid has an impact with the relative planet, next to this number there is the name of the impactor. Mars and Mercury have no impact.

Impacts

31% of V-types end their life in 5 Myrs, the majority of them collides with the Sun and Venus, confirming that these two last bodies set the destiny of the *NEAs*. Mars has no impact, see Table 6.4. However, at this rate, it seems that the V-types asteroids would disappear in ~ 15 Myrs, confirming in part the average lifetime of *NEAs* found by Gladman et al. (1997). As it was done in Galiazzo et al. (2014a) (see Chapter3), it is possible to compute the diameter of the putative craters and the most important physical parameters concerning an impact like the impact velocity, the impact angle and the impact energy. The majority of the impacts between the terrestrial planets are with Venus (Table 6.4), but with smaller craters (Table 6.5) than the Hungaria’s ones (see Chapter 3), despite higher impact velocities on average. Probably this difference in crater size is due to an observational bias, because among *NEAs*, the smaller size objects are really more, but on the other hand it is easier to observe them in front of small sized ($D < 1$ km) asteroids in the Main Belt. Then collisions happen soon, in the first half of the considered 5 million years of integration time.

In Table 6.5 are reported only the biggest crater made on the planets (craters’ dimension were computed assuming an average density for the V-types asteroid equal to 2.0 kg/m^3 , considering the basaltic asteroids, with an higher density, the highest value in Opeil, Consolmagno & Britt (2010). In case of the Earth only one collision is found and a relative small crater. In Table 6.4, a real crater of similar dimension in North America is shown.

The energy released in these impacts are also smaller than the impact energies of the Hungarias, again mainly because of the smaller size of the V-type asteroids, even if they are denser than the Hungaria’s asteroids.

This work will be completed after this doctorate.

Asteroid	D_1 [km]	D_2 [km]	θ
Energy [Mt $\times 10^5$]	$E_{Nord.Cr.}$	v_{imp} [km/s]	v_e [km/s]
semi-major axis [au]	eccentricity	inclination [deg]	time [Myr]
Earth craters			
2003 UF_3	3.32	3.2	38
0.004	0.015	27.3	11.20
0.6968	0.4737	29.94	0.375
Crater	Diameter	v_{imp}	Age[Ma]
Newporte	3.2	~ 20 km/s	< 500
Venus craters			
(5604) 1992 $_{FE}$	4.44	4.33	24
0.015	54.60	8.4	10.2
0.5387	0.4896	10.60	3.474
Crater	Diameter	v_{imp}	Age [Ma]
Oivit	4.3	–	–

Table 6.5: Earth- and Venus-impacts. The meaning of the values are described in Chapter 3. Source of the diameters of Newporte crater and Oivit Crater are respectively www.passc.net/EarthImpactDatabase/newporte.html and www.lpi.usra.edu/resources/vcvcinfo?refnum=873. The impact velocity for Newporte crater is assumed to be the average impact velocity on the Earth.

6.2 Centaurs (Inner Centaurs) close encounters with terrestrial planets

This paper is in preparation and it continues the frame of Galiazzo et al. (2013a, 2014a), but with a different group of asteroids, the inner region of the Centaurs (between the orbits of Jupiter and Saturn). The majority of them evolve inside the *NEAs*' region (Levison , 1996; Bottke et al. , 2002; Horner, Evans & Bailey , 2004a,b) and possibly encounter terrestrial planets.

Authors: Mattia Alvise Galiazzo¹

Publication state: submission expected in January, 2014

Publication details³⁰: Planetary and Space Science, 2014

Affiliation: Institute for Astrophysics (IfA), University of Vienna, Turken-
schantstr. 17, 1180 Vienna, Austria

³⁰Much probable journal and year of publication.

Centaur asteroids are asteroids and comets, usually of larger sizes than the bodies in the Main Belt. Their orbits lie between the Giant planets, having a semi-major axis between 5.2 au and 30 au. This study (Galiazzo et al. , 2014b) consider the evolution of the orbit of the inner Centaurs, between the orbit of Jupiter and Saturn, so bodies with a semimajor axis in this range: $5.2(\text{au}) < a < 9.5(\text{au})$. Computations of the orbit were performed using all the planets from Mercury to Neptune, considering also the Pluto system and in addition the most 3 massive known centaurs (10199) Chariklo (1997 CU₂₆) (mass equal to $0.62564410^{-12}M_{\odot}$), 1995 SN₅₅ (mass equal to $1.902400 \cdot 10^{-11}M_{\odot}$) and 2002 GZ₃₂, (mass equal to $0.616151 \cdot 10^{-11}M_{\odot}$) and for 1 Myrs. 84 known centaurs are integrated as massless bodies. Results from the orbital integrations of these works show that a lot of these objects go in the inner Solar System and many ones in cometary orbit, this cometary behavior was found by Horner, Evans & Bailey (2004a,b), too. Despite this, none of them has been found in this work having close encounters in the range used in the previous chapters ($d < 2.5 \cdot 10^{-2}$ au for the Earth, $1.7 \cdot 10^{-3}$ au for Venus and $1.66 \cdot 10^{-3}$ au for Mars) even if some centaurs like 2007 SA₂₄ ($a_0 = 6.27$ au, $e_0 = 0.57$ and $i_0 = 17.09^\circ$, its initial osculating elements) which becomes a sun-grazer, arrives at a distance of the order of 10^{-3} au from the Earth, before colliding with the Sun (due to several close encounters with Jupiter because it is captured by it, see Fig. 6.1), close encounters of same order of distance happen also for Venus and Mars. 37 % end out as sun-grazers, a little percentage of them, instead exits out of the Solar System in 1 Myr, mainly due to close encounters with Jupiter, even if some close encounters with (10199) Chariklo (1997 CU₂₆) was found too.

It is interesting to know that many Centaurs'PCAs arrive at high eccentric orbits, from parabolic to hyperbolic or even elliptic ones with very eccentricities next to 1; someone after important close encounters with Jupiter, and/or also with some other massive asteroids like (10199) Chariklo (1997 CU₂₆). After these CEs, Centaurs reach cometary orbits and sometimes retrograde orbits, too.

Typical orbits are shown in Table 6.6:

typically ECAs of Centaurs' origin seem to be Hyperbolic comets, sometimes Halley-type ones or Apollos too. Comet C/2008 J₄ McNaught and the Apollo 2007 GT₃ seem of Centaur origin.

6.2. CENTAURS (INNER CENTAURS) CLOSE ENCOUNTERS WITH TERRESTRIAL PLANETS

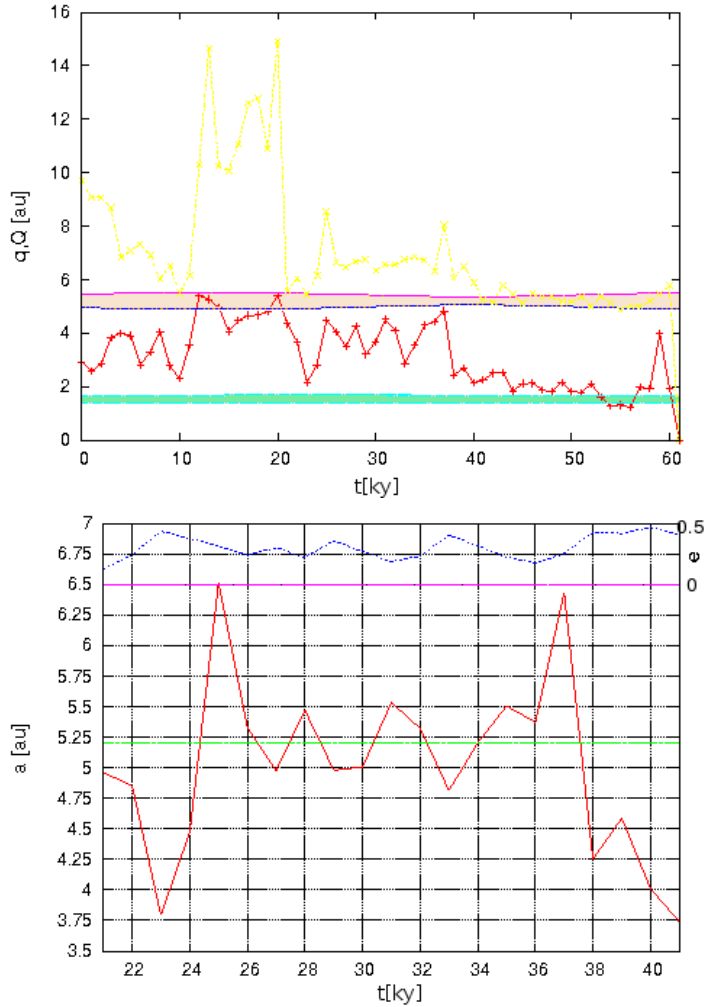


Figure 6.1: Orbital evolution of the Centaur sungrazer 2007 SA₂₄. Upper panel: Aphelion or perihelion of the body (y-axis) versus time (x-axis). Zone crossed by Jupiter, light pink area between 2 lines which are the perihelion and the aphelion of Jupiter. Zone crossed by Mars, light blue, between the perihelion and the aphelion of Mars. Red dotted line is the perihelion of the centaur 2007 SA₂₄ and the yellow dotted line is its aphelion. Bottom panel: Capture of centaur 2007 SA₂₄, semimajor axis in red, by Jupiter, semimajor axis in green. Semimajor axis (left y-axis) versus time. In the upper part of this panel, it is plotted the eccentricity (right y-axis) versus time of the 2007 SA₂₄.

Table 6.6: Summary of some typical orbit (osculating elements) of Centaurs crossing the Earth orbits, *ECAs*, divided in 5 typical region found between the results of the integrations in this work. “ID Real” is the code name of the Comet. In each third row of the object it is given the real name “Name” (first column) and the Comet Type (last column).

Regions	a (au)	e	i°	T_j
ID Real	a (au)	e	i°	T_j
Name				Comet Type
Centaurs A	-12.05	1	90	-0.43
<i>C/2008 J₄</i> (McNaught)	-15.88	1.03	87.4	-0.29
				Hyperbolic
Centaurs B	$-60 < a < -40$	1.02	$110 < i < 111$	$-0.58 < T_j < -0.51$
<i>C/1980 E₁</i> (Bowell)	-58.5	1.056	1.7	2.22
				Hyperbolic
Centaurs C	$1.92 < a < 2.2$	1.00	$23 < i < 27$	$2.42 < T_j < 2.79$
2007 <i>GT₃</i>	1.99	0.94	25.4	3
				Apollo
Centaurs D	$9.3 < a < 9.31$	0.99	$93 < i < 94$	$0.53 < T_j < 0.54$
<i>P/2005 T₄</i> (SWAN)	9.32	0.93	160.4	-0.37
				Hyperbolic
Centaurs E	-2.44	1.381	$2 < i < 3$	0.83
<i>C/1999 U₂</i> (SOHO)	-2.02	1.02	26.8	-2.33
				Hyperbolic

Chapter 7

A statistical dynamical study of meteorite impactors: a case study based on parameters derived from the Bosumtwi impact event

This paper perform a statistically study in order to find the most probable origin of the impactor of a paleo-impact event such as the Bosumtwi Crater and it is the first one trying to solve this problem. This work unites two fields, planetary science (and geology) and astronomy (celestial mechanics). The statistical study is done from results given by backward numerical integrations, “launching” back the asteroids from the points on the Earth where the impact has happened, during a politely deduced past instant of time, which fits with the impact discovered time by Koeberl et al. (1997a). Physical data of the impact was found via Artemieva, Karp & Milkereit (2004). A methodology is given and describes how is possible to use a more complete statics in case more physical data are known (both for the impact event and for the impactor, i.e. its composition, so spectral type).

Authors: Mattia Alvisè Galiazzo, Akos Bazso, Matthew Huber, Anna Losjak, Rudolf Dvorak and Christian Koeberl¹

Publication state: Accepted. Publication expected in in October, 2013

Publication details: Astronomical Notes, Issue 9, (4pp), 2013

¹Author affiliations are presented in the header of the following article.

Contribution of the first author: The first author was responsible for the entire idea to study the origin of the impactor of the Bosumtwi crater and also the methodology. Half of the “physical” numerical integration was done by the first author. The statistical analysis, computations and writing down the paper was done by the first author.

Contribution of the co-authors: Vital contribution on the geological input and information about the crater site was given by the co-authors, also an important role in scientific discussions in the developing of the work and vital hints in the editing of the paper. In addition half of the “physical” numerical integration was performed by the co-authors.

A statistical dynamical study of meteorite impactors: a case study based on parameters derived from the Bosumtwi impact event

M. A. Galiazzo^{1,*}, Á. Bzszó¹, M. S. Huber², A. Losiak², R. Dvorak¹, and C. Koeberl^{2,3}

¹ Institute for Astrophysics, University of Vienna, Türkenschanzstraße 17, A-1180 Vienna, Austria

² Department of Lithospheric Research, University of Vienna, Althanstraße 14, A-1090 Vienna, Austria

³ Naturhistorisches Museum Wien, Burgring 7, 1010 Vienna, Austria

The dates of receipt and acceptance should be inserted later

Key words impact craters – celestial mechanics – minor planets, asteroids – methods: N-body simulations – methods: statistical

The study of meteorite craters on Earth provides information about the dynamic evolution of bodies within the Solar System. Bosumtwi crater is a well studied, 10.5 km in diameter, ca. 1.07 Ma old impact structure located in Ghana. The impactor was ~ 1 km in diameter, an ordinary chondrite and struck the Earth with an angle between 30° and 45° from the horizontal. We have used a two phase backward integration to constrain the most probable parent region of the impactor. We find that the most likely source region is a high inclination object from the Middle Main Belt.

© 2013 WILEY-VCH Verlag GmbH & Co. KGaA, Weinheim

1 Introduction

When studying impact craters, it is sometimes possible to determine the properties of the impactor that produced the crater, but the source where the impactor originated in the Solar System is more difficult to determine. Recently, the Almahata Sitta fall was observed by astronomers, tracked by satellites as it entered the atmosphere, and collected soon after striking Sudan. In this case, dynamical models were combined with detailed information about the meteorite type to track the impactor back to the Inner Main Belt (Jenniskens et al., 2010). For older impacts, the same precision cannot be achieved because of the lack of detailed information on orbital parameters. However, based on the geological constraints on the dynamic nature of the impactor, a statistical model can be used to suggest the most probable region from which the impactor could have originated. The aim of this study is to statistically constrain the most probable parent region of the impactor that formed the Bosumtwi impact crater.

1.1 Bosumtwi crater: Geological background

The Bosumtwi impact crater was chosen for this study because of its relatively young age and unusually good constraints on the direction of the impactor. The Bosumtwi impact crater is a 10.5 km in diameter complex meteorite impact crater located in the Ashanti Province of southern Ghana. It is 1.07 ± 0.11 Ma old and relatively well preserved (e.g., Koeberl et al., 1997a). The Bosumtwi structure is currently filled by the closed-basin Lake Bosumtwi that is 8 km

in diameter and up to 72.5 m deep. It is considered to be the largest, relatively young, confirmed impact structure on the Earth. Bosumtwi is a unique crater, since it is one of just three craters in the world that are associated with a tektite strewn field (e.g., Koeberl, 1994). Tektites are centimeter-sized pieces of natural glass formed during a hypervelocity impact event by ejection of molten target-surface material and occurring in strewn fields (e.g., Koeberl, 1994). Based on the distribution of tektites around Bosumtwi crater it is possible to constrain the direction of travel of the bolide prior to the impact. Based on the Cr isotope composition of the tektites derived from Bosumtwi, Koeberl et al. (2007b) established that the impactor that formed Bosumtwi crater was most probably an ordinary chondrite (while carbonaceous and enstatite chondrites were excluded). The properties of the impactor that formed the crater have been constrained by numerical modeling. According to Artemieva et al. (2004), the Bosumtwi structure was formed by an impactor 0.75 to 1 km in diameter, moving with a velocity higher than 15 km/s, and most probably 20 km/s. Due to association of the Bosumtwi crater with the Ivory Coast tektite strewn field, the direction of the incoming impactor was estimated to be from N-NE to S-SW and the angle of impact is thought to be between 30° and 45° (Artemieva et al., 2004).

2 Model & Methods

This study uses a statistical approach to constrain the parent region of the Bosumtwi impactor, using $a - i$ space (a and i for semi-major axis and orbital inclination, respectively) and the absolute magnitude (H_v) distribution inside the defined regions of the Solar System. First, we made a back-

* Corresponding author: e-mail: mattia.galiazzo@univie.ac.at

ward integration¹ from the present to the time of impact. The integration used the Radau integrator, included relativity, and all the planets plus Pluto, the Moon, Vesta, Ceres, Pallas and Juno. The integration considered the positions of the Earth between 0.96 and 1.18 Ma (1.07 ± 0.11 Ma) in order to find the possible position of the Earth during the time when the impact occurred, accounting for the error of the impact age measurement. Then, we made another backward integration using the Lie-integrator (Eggl and Dvorak, 2010) without Mercury, Pluto and the 4 asteroids, from the time of the impact to 100 Ma, simulating the orbital evolutions of 924 fictitious Bosumtwi impactors beginning at the calculated location of the Earth. Two cases were considered for this integration:

1) Fixed case (FC): we started the integration at the location of the Earth (as calculated in the initial integration) exactly at 1.07 Ma. Then, 384 particles, with a gaussian distribution of impact velocities (v_i) around 20 km/s were launched with 32 different velocities. Those velocities correspond to the average value for Earth-impactors, as well as the most likely velocities indicated by numerical modeling for the Bosumtwi impactor (Artemieva et al., 2004). Velocities have a Gaussian distribution in the range of 11.2 to 40 km/s, which are the escape velocity from the Earth and cometary speed, respectively. Then, 4 impact angles were considered using random values among $\Theta = 37.5^\circ \pm 7.5^\circ$ for each velocity and 3 different directions ($\Omega_1 = 67.5 \pm 3.5^\circ$, $\Omega_2 = 78.75 \pm 3.5^\circ$ and $\Omega_3 = 56.25 \pm 3.5^\circ$ from east) for each angle. The launch position is the present latitude and longitude of the Bosumtwi crater site.

2) General case (GC): 540 particles were integrated using combinations of the following properties to account for the lack of knowledge of the exact position of the Earth at the time of the impact: 3 different orbital positions of the Earth, corresponding to the minimum, average and maximum aphelion (at 3 different times) in the Solar System; 3 different directions of the impactor ($\Omega_1 = 67.5 \pm 3.5^\circ$, $\Omega_2 = 78.75 \pm 3.5^\circ$ and $\Omega_3 = 56.25 \pm 3.5^\circ$ from east); and 60 different sections of the Earth along lines of longitude every 6° for each position of the Earth. For each of the 540 particles, impact angle and latitude² were distributed randomly, and v_i had a gaussian distribution like in the FC. Once data were generated, analysis was done on two levels. First, regions were defined as in Table 1, where only the semimajor axis was considered. Then, for those particles which fell into the Main Belt, more specific constraints were necessary because of the much higher population. Assuming the impactor was an ordinary chondrite (Koeberl et al.,

¹ Due to the fact that a backward integration could be distorted by chaotic motion in close encounters, we have looked for a measure that is as simple as possible and is expressed in terms of orbital elements, since these are familiar indices of orbit differences. Because there should be preferential orbits in the regions far from the Earth, we can use a statistical approach. We stopped the integration for a particular body whenever the asteroids overcome an eccentricity equal to 0.985 or have had a close encounter with a planet less than $\sim 10^{-5}$ AU.

² varying $\pm 1.3^\circ$ (Neron deSurgy & Laskar, 1995) from the present one, to account for the variance of the obliquity.

2007b) and from the numerical results of Artemieva et al.³ (2004), we can exclude the possibility of a cometary orbit, such as NEOs (Near-Earth objects) with orbits of $Q > 4.5$ AU (Fernández et al., 2002).

REGIONS (Table 1): At the end of the integration, the particles are examined to determine the probability that they fall into a defined region based on the semi-major axis range (called $P(a)$). The orbital properties of the particles were derived from the time intervals between close encounters where they show little variance. The average time between close encounters with planets was determined to be 284 ky.

MAIN BELT GROUPS (Table 2): Asteroids in the Main Belt were subdivided into 3 regions and with these 3 constraints: (1) $1.5264 < a < 5.05$ AU, $Q < 5.46$ AU (aphelion of Hilda family from Broz and Vokrouhlicky, 2008), (2) $q > 1.0017$ AU (the average semi-major axis of the Earth after 100 Myr of integration) and (3) the NEAs with $Q < 4.35$ and $q > 1.0302$.

Then, each of these 3 groups was divided into 2 sub-groups: the low inclination group (*LIG*) and the high inclination group (*HIG*), the border between the two regions being $i = 17.16$ (Novaković et al., 2011). The regions with the highest densities of particles were then determined. For these the Tisserand parameter with respect to Jupiter⁴ was calculated to test whether or not the properties correspond to known families in the Main Belt.

2.1 Absolute magnitude and spectroscopy

Ordinary chondrites, thought to be responsible for the Bosumtwi impact, are associated with the taxonomical S-group: S, L, A, K, R, Q and intermediate types Sl, Sa, Sk, Sr, Sq (Bus & Binzel, 2002). Surveys have also revealed that the NEA population is dominated by objects belonging to the taxonomic classes *S* and *Q* (25% as Q-type and 40% as S-type, Bus et al., 2004). When corrected for observational biases, about 40% of the NEA population belong to one of these two taxonomic classes. In the case of Mars crossers, 65% belong to the S class (de León et al., 2010). To compute the absolute magnitude of our impactor, we used the equation of Fowler and Chillemi (1992): $H_v = -5 \log(\frac{D_p^{1/2}}{1329})$. Using the average albedo for the S-group asteroids, 0.197 (Pravec et al. 2012), and considering the likely size range of the Bosumtwi impactor, its absolute magnitude ranged from 17.4 to 18.0 mag. The absolute magnitude of the impactor can be used to calculate the probability (called $P(H_V)$) that the impactor originated from a particular region based on the likelihood of objects of similar absolute magnitude originating in a particular region,

³ see also their Table 2 where the fit between the diameter of the crater and the impact velocity is in agreement with impact velocities typical of asteroids.

⁴ $T_j = \frac{a_j}{a} + 2\sqrt{\frac{a}{a_j}(1-e^2)} \cos i$, where a_j is the semi-major axis of Jupiter, a , e and i are the actions of the osculatory elements of the asteroid.

Reg.	Orb.	$P(H_v)$	$P_{FC}(a)$	$P_{GC}(a)$
IMB	$1.78^* \leq a \leq 2.06$	0.3737	0.0924	0.0404
MMB	$2.06 < a < 3.28$	0.2870	0.1036	0.1030
OMB	$3.28 < a < 5.05$	0.0232	0.0112	0.0121
TRO	$5.05 < a < 5.35$	♣	0.0056	0.0000
CEN	$5.35 < a < 30.00$	♣	0.056	0.0646
TNO	$a > 30.00$	♣	0.0112	0.0020

Table 1 Regions are defined by the a that corresponds to strong perturbative Mean Motion Resonance (2.06 AU for $J_4 : 1$ and 3.28 for $J_2 : 1$), apart for the inner border of the (IMB) equal to the aphelion of Mars. The borders of the Jupiter Trojans (TRO) as in Tsiganis et al. (2005) and for the TNOs, the standard definition is used. MMB, OMB, CEN stand respectively for Middle Main Belt, Outer Main Belt and Centaurs. Orb. stands for semi-major axis borders of the region. For the lower border of the IMB (*), we take the minimum a for the innermost group of asteroids (see Galiazzi et al. 2012). The “♣” means that H_v are biased for the absence of a small bodies survey, so no significative computation is possible. $P_{FC}(a)$ and $P_{GC}(a)$ stands respectively for probability to find the origin in the region through the a in the FC and in the GC.

i.e., from the IMB, $11.21 < H_{vIMB} < 27.60$. The spectral properties of ordinary chondrites exclude the possibility that this object come from a family such as Vesta or Hungaria, but it favours the Flora, Ariadne, Nysa, Maria, Eunomia, Mersia, Walsonia, Coelestina, Hellona, Agnia, Gefion and Koronis groups (Cellino et al., 2002) for the LIG; Barcelona and Hansa for the HIG (Novaković, et al., 2011).

3 Results and discussion

The final backward integration of 100 My shows that particles which survived the integration tend to converge on the Main Belt (Figure 1), and that only a negligible number of them is found in cometary orbits with an initial aphelion greater than Jupiter’s one, with a $v_i > 27$ km/s; then a very negligible part in hyperbolic orbits with a $v_i > 33$ km/s. This suggests that the impactor most likely originated in the Main Belt.

REGIONS: The results are listed in Table 1, where $P(H_v)$ shows that on the basis of the absolute magnitude, the object most likely originated from the Main Belt, with a 37% probability of originating from the IMB and a 29% probability of originating in the MMB. The integration performed in this work shows that the majority of backwards integrated particles fall into the IMB and MMB, with $\sim 10\%$ of objects in the FC falling into each of these. The GC, however, resulted in the majority of objects originating from the MMB, again with $\sim 10\%$ of objects, and only $\sim 4\%$ of objects originating from the IMB.

MAIN BELT: Results are given in Table 2, subdivided in 2 rows. In the upper row we have the LIG and the lower one, the HIG: $P(a, i)$ is the probability to find the asteroid at high or low inclinations in the regions defined via

Reg. Low	$P_F(H_v)$	$P_F(a, i)$	$P_G(a, i)$
Reg. High	$P_F(H_v)$	$P_F(a, i)$	$P_G(a, i)$
IMB Low	0.234	0.006	0.000
IMB High	0.420	0.006	0.018
MMB Low	0.307	0.000	0.010
MMB High	0.113	0.020	0.022
OMB Low	0.023	0.003	0.000
OMB High	0.019	0.000	0.004

Table 2 MBAs group have the same subdivision per semi-major axis, as in Table 1, apart for the IMB: $1.53 < a < 2.06$ where the lower limit is the average aphelion of Mars in 100 Myr from the impact time. “Low”= Low inclined orbit ($i < 17.16$) and “High”= High inclined orbit. $P_F(a, i)$ and $P_G(a, i)$ stands respectively for probability to find the origin in the region defined by semi-major axis, and inclination too, in the FC and in the GC.

semi-major axis, G and F stands respectively for GC and FC.

FC: The most probable source region of the Bosumtwi impactor based on the fixed case integration falls within the Main Belt at high inclination, with the most likely group being the MMB at high inclination, with 2% of the population falling into this group. The objects have highly inclined orbits (up to $\sim 75^\circ$), and the most populated zone at $2.42 \pm 0.03 < T_j < 2.84 \pm 0.25$.

GC: The most probable source region of the Bosumtwi impactor based on the general case is from the MMB with high inclination: $i > 36.9$ (Fig. 2) and $2.42 \pm 0.05 < T_j < 2.79 \pm 0.09$. However, low inclination MMB is also possible, together with high inclination IMB.

4 Conclusions

The Bosumtwi impactor probably originated in the MMB at orbital inclinations greater than 35° with a possible initial T_j equal to 2.63 ± 0.25 . These values are based only on our numerical integrations (the highest values⁵ in $P_G(a, i)$ and $P_G(a)$ found in the GC, see Table 1 and 2 and Figure 2.) and not considering the spectroscopical type too, because we do not have yet any significant number of measure in this zone of the Main Belt (Cellino et al. 2002). Also this zone is still not well studied and so we could not identify a particular family as the most likely source. Asteroids with similar orbital parameters to the modeled Bosumtwi impactor are: 2002 MO₃, 2009 XF₈, 2002 SU and 2010 RR₃₀. There could be a cluster of asteroids at very high inclined orbits as shown by these results, something that we are planning to study after this work. This method should be improved to

⁵ Because of close encounters, some integrations were stopped before 100 My, so less orbits end their evolution in the Main belt, see Fig. 1. These ones are the missing percentage from the results, a part still happen to be as NEAs, a part reach our maximum tolerance value for eccentricity (0.95) and another small fraction has again impacts during the backward integration.

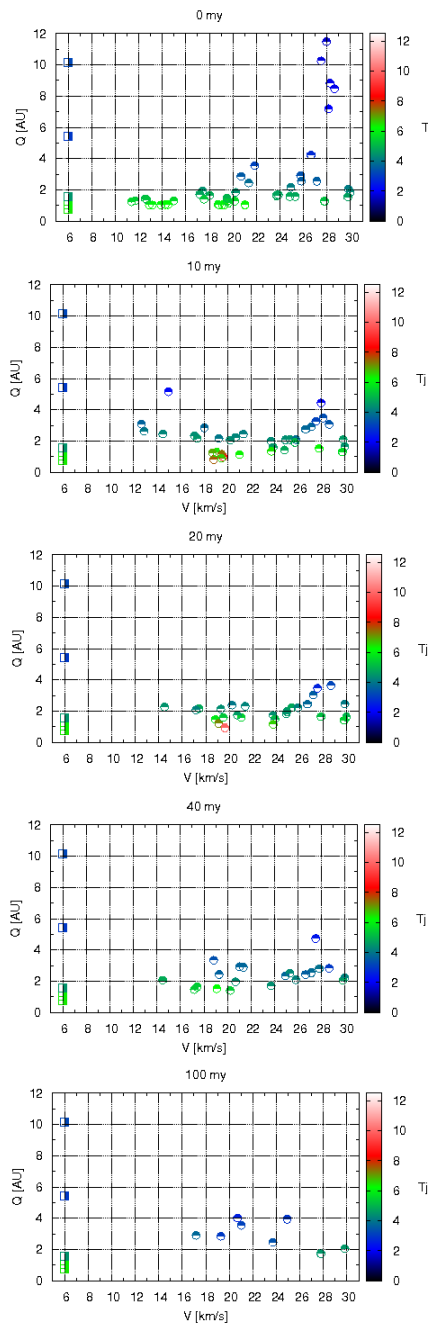


Fig. 1 Evolution of a sample, through the different ranges of admitted velocities, of fictitious asteroids (impactors) over the total integration time. In colours the Tisserand Parameter, on the x-axis, the impact velocity in km/s and on the y-axis the aphelion in AU. On the left, at a fictitious and non-real velocity of 6 km/s we have the planets as reference, from top to the bottom: Saturn, Jupiter, Mars, Earth, and Venus. The T_j shows that the particles tend to achieve the values of the MBAs (see the plot at 100 my).

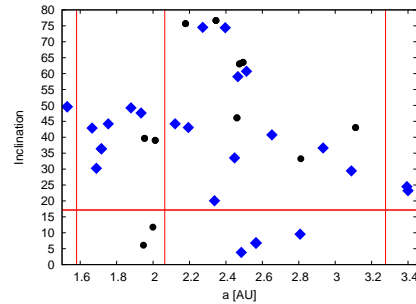


Fig. 2 $a - i$ space. Vertical lines define the border of the regions in semi-major axis, as in Table 1, and the horizontal line discriminate *HIG* and *LIG*. Diamonds for *GC* and circles for *FC*.

find more consistent probabilities (i.e. with more fictitious particles and larger integration times) and it can potentially be applied to other old impact craters with well constrained impactor properties, and even to impacts on other planets.

References

- Artemieva, N., Karp, T., Milkereit, B.: 2004, GGG 5, 11016
 Broz, M., Vokrouhlicky, D.: 2008, MNRS 390, 715
 Bus, S. J., Binzel, R. P., Volquardsen, E. L., Berghuis, J. L.: 2004, BAAS 36, 1140
 Bus, S. J., Binzel, R. P.: 2002, Icar 158, 146
 Cellino, A. and Bus, S. J. and Doressoundiram, A. and Lazzaro, D.: 2002, Asteroids III, 633
 de León, J., Licandro, J. and 3 coauthors, Serra-Ricart, M., Pinilla-Alonso, N., Campins, H.: 2010, A&A 517, A23
 Dvorak, R., Pilat-Lohinger, E., Schwarz, R., Freistetter, F.: 2004, A&A 426, L37
 Eggl, S., Dvorak, R.: 2010, LNP 790, 431
 Fernández, J. A., Gallardo, T., Brunini, A.: 2002, Icar 159, 358
 Fowler, B., Chillemi, B.: 1992, MNRAS 423, 3074
 Galiazzo M. A., Bazzo, A., Dvorak R.: 2013, P&SS 84, 5
 Koberl, C.: 1994, GSA Special Paper 293, 133
 Koberl, C., Bottomley, R., Glass, B. P., Storzer, D.: 1997a, GeCoA 61, 1745
 Koberl, C.; Milkereit, B., Overpeck, J. T., and 9 coauthors: 2007a, M&PS 42, 483
 Koberl, C., Shukolyukov, A., Lugmair, G. W., Guenter, W.: 2007b, E&PSL 256, 534
 Jenniskens, P., Vaubaillon, J., Binzel, R. P. and 13 coauthors: 2010, M&PS 45, 1590
 Neron de Surgy, O., Laskar, J.: 1995, BAAS 27, 1172
 Novaković, B., Cellino, A., Knezević, Z.: 2011, Icar 216, 69
 Pravec, P., Harris, A. W., Kusnirák, P. Galád, A. and Hornoch, K.: 2012, Icar 221, 365
 Tsiganis, K., Varvoglis, H. and Dvorak, R.: 2005, CeMDA 92, 71

Chapter 8

Photometry of Comet *C/2012 S1* (ISON)

Many asteroids and comets have been discovered in these years, both for improved devices: new powerful telescopes on the Earth and in the space and new unpredicted objects that had close encounters and impacts too with terrestrial planets. Unexpected was the event in Russia, Chelyabinsk (see Appendix B). New comets will arrive (i.e. Comet *C/2013 N4* Borisov, discovered very recently, in July, 2013), and some probable “super-bright” (i.e. Comet *C/2012 S1* Ison) and some has just arrived in the inner solar system like *C/2011 L4 Pan – STARRS*, visible at naked eyes in both hemispheres.

The following article is a photometric study in BVRI-band on comet *C/2012 S1* Ison, called the comet of the Century, using frames from observation of M.A. Galiazzo and W. W. Zeilinger via the Austrian national telescope: Figl Observatory. In addition some computation of the minimal distance to the planets and perihelion, plus a brief show on the orbit was given.

Authors: Mattia Alvisè Galiazzo, Werner W. Zeilinger¹

Publication state: Published in June 2013.

Publication details: ALPO, “The Strolling Astronomers”, US, (3pp), 2013

Contribution of the first author: The first author was responsible of the observations of the comet, photometric and computations of the close encounters with Terrestrial Planets and Sun. In addition he was the principal writer of the paper.

Contribution of the co-author: The resources necessary for the observation

¹ Author affiliations are presented in the header of the following article.

were given by the co-author who let the first-author observing in remote-control. Vital contribution in correcting some constraints in the reduction of the frames. Important suggestions on the speed of the comet and its photometry.

Feature Story:

Photometry of Comet C/2012 S1 (ISON)

M. A. Galiazzo, Department of Astrophysics at the University of Vienna

mattia.galiazzo@univie.ac.at

W. W. Zeilinger, Department of Astrophysics at the University of Vienna

Biographical Information

MSc M. A. Galiazzo

Titles:

- MSc at the University of Padova, Italy
- PhD student at the Department of Astrophysics at the University of Vienna, Austria: "*Planetology: From Asteroids to Impact Craters (NEO asteroids and Impact Crater Studies)*"

Collaborations with: Dr. Carraro (ESO – Chile), photometry of minor bodies (Centaur and KBOs) and Prof. J. Souchay (Observatoire de Paris – France), dynamics of asteroids.

Research areas: asteroids and minor bodies of the Solar System (photometry and celestial mechanics)

Prof. W. W. Zeilinger:

Titles:

- Ph.D. at the University of Vienna, Austria
- Fellowships at University of Padova, Italy and ESO
- Associate professor at the Department of Astrophysics at the University of Vienna

Research areas: structure and evolution of galaxies, dark matter in galaxies, stellar populations, astronomical instrumentation, astronomical software development

Introduction

(Editor's Note: Comet ISON was discovered on September 21, 2012, by

two amateur astronomers in Russia, using a reflecting telescope at an observatory of the International Scientific Optical Network. Source: <http://www.voanews.com/content/astronomers-await-comet-ison-year-end-spectacular/1663642.html>)

Comet C/2012 S1 (ISON) presently shows unusually strong activity despite being far from the sun. The comet was observed with 1.5m RC telescope of the Leopold Figl – Observatorium für Astrophysik on April 10, 2013 UT when it was at geocentric distance of 4.1389 AU and heliocentric distance of 5.7844 AU. We report the result of Bessel VRI imaging photometry.

Methods

Images in the Bessel VRI photometric bands were obtained using a f/6.3 focal reducer and a peltier-cooled CCD camera yielding a field of view 5.6x4.8

arcmin² with a scale of 0.307 arcsec pixel⁻¹.

The comet was observed under photometric sky conditions with an average seeing of about 2.0 arcsec FWHM. The data were calibrated using standard IRAF procedures for bias and flat field correction.

The photometric calibration was performed with Landolt photometric standard stars (airmass 1.43) observed on April 10, 2013 UT. The photometric analysis, including corrections for airmass and extinction, was carried out using IRAF and Daophot II software. PSF-photometry was performed with an aperture radius of 32.12 arcsec and a fitting radius of 42.83 arcsec (equal for all photometric bands), selecting the best stars for fitting.

(Continued on page 19)

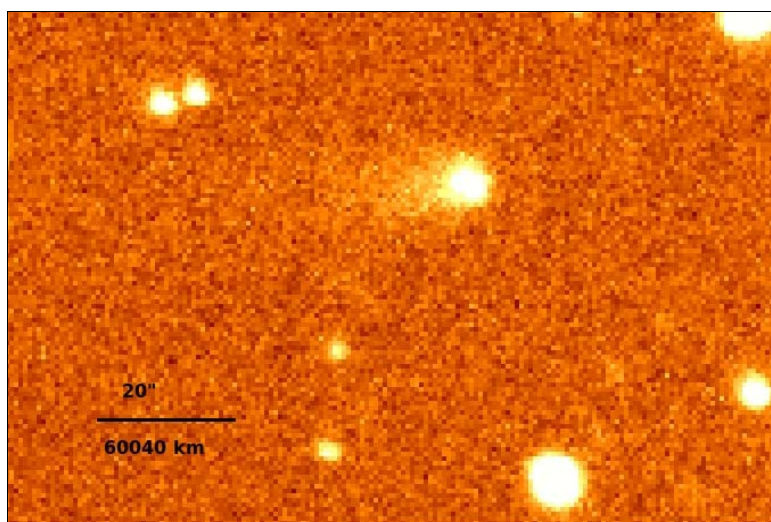


Figure 1. False color image of C/2012 S1 (ISON). The image was obtained by stacking all R band images (total exposure time: 1260s).

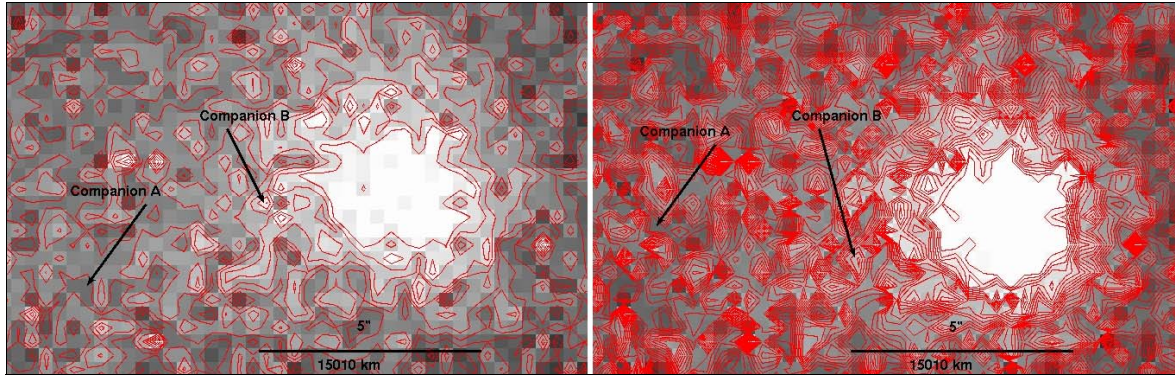


Figure 2. False color R band images of C/2012 S1 (ISON) obtained at 20:43:54 UT (left) and 20:49:45 UT (right). The positions of the candidate sources A and B are indicated.

Table 1. Photometric Results of Comet C/2013 S1 (ISON) from the Individual Images

Body	UT	Coordinates	F	Exp	A.M.	Ph.A.	Mag.
Comet	20:23:56	06:37:12.081 +30:12:51.14	R	120	1.54	8.0710	16.62±0.04
Comet	20:33:13	06:37:12.082 +30:12:49.81	R	120	1.59	8.0710	16.86±0.04
Comet	20:43:54	06:37:12.082 +30:12:48.65	R	300	1.65	8.0710	16.76±0.03
Comet	20:49:45	06:37:12.082 +30:12:47.94	R	360	1.69	8.0710	16.81±0.03
Comet	20:57:00	06:37:11.983 +30:12:47.44	R	360	1.74	8.0709	17.04±0.05
Comet	20:27:38	06:37:12.029 +30:12:49.60	V	120	1.57	8.0710	17.03±0.04
Comet	20:37:03	06:37:12.039 +30:12:49.60	V	120	1.62	8.0710	17.15±0.05
Comet	21:26:04	06:37:11.964 +30:12:44.20	I	300	2.01	8.0709	15.12±0.04

NOTE: Column UT indicates the respective universal time. Columns F, Exp, A.M., Ph.A. and Mag. contain the filter, airmass, phase angle and derived apparent magnitude respectively.

Table 2. Photometric Results of the Candidate Sources A and B in the Neighborhood of Comet C/2013 S1 (ISON)

Body	UT	Coordinates	F	Exp	A.M.	Ph.A.	Mag.
B	20:23:56	06:37:12.313 +30:12:49.21	R	120	1.54	8.0710	17.88±0.08
A	20:33:13	06:37:13.032 +30:12:49.58	R	120	1.59	8.0710	18.95±0.24
B	20:33:13	06:37:12.267 +30:12:50.07	R	120	1.59	8.0710	17.55±0.07
A	20:43:54	06:37:12.645 +30:12:47.00	R	300	1.65	8.0710	18.26±0.09
B	20:43:54	06:37:12.327 +30:12:48.36	R	300	1.65	8.0710	17.57±0.05
A	20:49:45	06:37:12.681 +30:12:48.34	R	360	1.69	8.0710	18.71±0.11
B	20:49:45	06:37:12.352 +30:12:47.51	R	360	1.69	8.0710	18.02±0.07
A	20:57:00	06:37:12.696 +30:12:46.43	R	360	1.74	8.0709	18.45±0.09
B	20:57:00	06:37:12.375 +30:12:47.94	R	360	1.74	8.0709	18.15±0.07
A	20:37:03	06:37:13.150 +30:12:47.99	V	120	1.62	8.0710	19.33±0.37
B	20:37:03	06:37:12.334 +30:12:48.57	V	120	1.62	8.0710	18.88±0.16
A	21:26:04	06:37:13.234 +30:12:39.60	I	300	2.01	8.0709	18.06±0.33
B	21:26:04	06:37:12.039 +30:12:43.67	I	300	2.01	8.0709	16.23±0.09

NOTE: The columns are the same as described in Table 1.

(Continued from page 17)

Results

During this run of observations, the brightness decreased with an amplitude of 0.32 R magnitudes, ranging between apparent magnitude: 16.62 (R mag) and 17.04 (R mag), see Table 1. The computed color indices are $V-R = +0.42 \pm 0.07$ mag and $V-I \approx +2.69 \pm 0.08$ mag; the individual measurements have a maximum error of 0.05 mag.

Signatures of possible comet fragments and/or companions were detected in the images (see Table 2 and Figure 2) within about 10 arc seconds of the comet by applying PSF-photometry which uses the fitted profiles of reference stars to detect sources even at sub-seeing resolutions.

The photometric signatures of two sources are consistently present in all frames. The photometric results are presented in Table 2. We derive V-R color-indices of $+0.88 \pm 0.52$ and $+0.43 \pm 0.40$ mag for sources A and B respectively. Further deep observations are needed to confirm these detections.

The size of the projection of the tail (SPT) from the center of the coma and the approximate diameter of the coma (ARC) is computed from the stacked R band image (see Fig. 3): $SPT \approx 9.21''$ (corresponding to 60,700 km) and $2.5 \text{ arcsec} (7,740 \text{ km}) < ARC < 5.5 \text{ arcsec} (9,960 \text{ km})$.

The real length of the tail can be much larger than the projection observing the

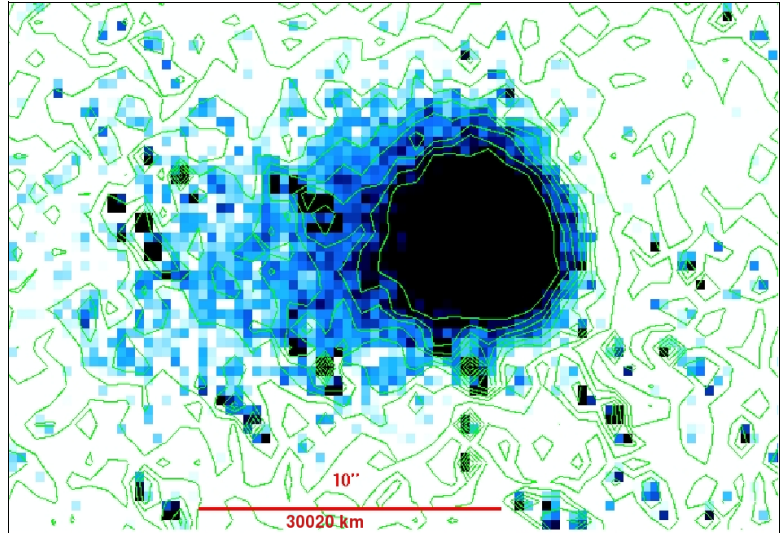


Figure 3. Coma and tail of C/2012 S1 (ISON). The image is a contrast enhancement of the stacked R band image of Figure 1.

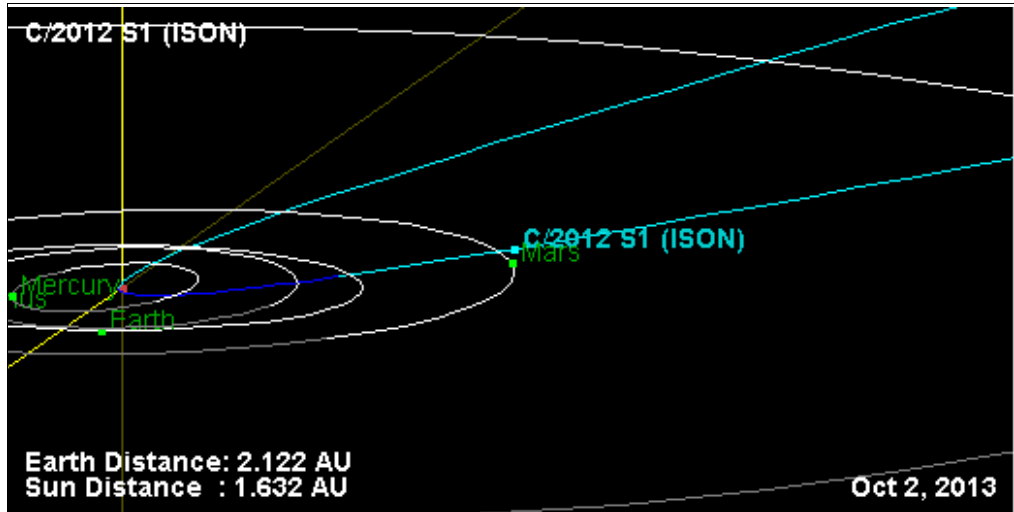


Figure 4. Orbit and position of Comet Ison at October 2, 2013 at the Periareion (Image made via JPL-horizon orbit diagram).

direction of the comet (cyan vector) and the point where the Sun is indicated by the yellow vector).

The comet was observed when it was pretty well over the ecliptic. Important closest approaches are expected with

some bodies of the inner Solar System and they are in order: October 2, 2013, with Mars (0.0729 AU, see Figure 4); November 28, 2013 with the Sun (0.013 AU), and if the comet survives, December 28, 2013 with the Earth, but relatively far away (0.427 AU).

Chapter 9

Conclusions

The threat of *NEA* impacts is underlined by this study and it shows that the Earth can be impacted by asteroids from one of the three sources once every 5 Myrs. The asteroids that might collide with the terrestrial planets range from a few hundred meters in diameter to a few kilometers (even more than 100 km if Centaurs are considered). Their orbits are driven by multiple crossings of strong resonances, i.e. the secular resonance ν_6 and the resonances with Jupiter, in particular J3:1. On the other hand, this work shows that also resonances with smaller planets play a significant role. Noticeable examples are the resonances M7:9 and E5:12. Also three-body mean motion resonances (with Jupiter and Saturn together, as perturbing bodies, i.e. J7:S-5:-1), excite the eccentricities, resulting in more close encounters. Perturbations and close encounters enhance the chances of impacts between the asteroids and the inner bodies of the Solar System, i.e. the Sun and the terrestrial planets.

The majority of *NEAs* finish their lives colliding with the Sun or Venus. Some turn out to be Sun-grazing objects or also asteroids that formerly were comets, so it is possible to speak about extinct-comets. An example of this could be comet C/2012 S1 ISON (Chapter 8). After its perihelium (or even before), it could fragment. The fragments will continue their lives as *NEAs*. Even its nucleus could “switch off” and become a new *NEA*, at least while it stays in the proximity of the terrestrial planets. At the moment it has a semi-parabolic orbit with an eccentricity, $e = 1.0000020$ (computed from MPEC2013-H38, observations of comets till July 24, 2013. See www.minorplanetcenter.net/mpec/K13/K13H38.html). It will maintain this orbit until it is perturbed by the gravity of other objects during close encounters.

9.1 *NEAs*' origin

Hungarias asteroids are source of all types of *NEAs*, whereas Centaurs seem to be sources of Apollos and of hyperbolic and Halley comets. In particular:

Hungarias' origin (143409) 2003 BQ₄₆, (249595) 1997 CH₂₈, (285625) 2000 RD₄, (1620) Geographos, (2001) Oliato, (5751) Zao and 5604 1992 FE;

Centaurs' origin³¹ Apollo NEAs: 2007 GT₃^{*}. Hyperbolic comets: C/2008 J₄ (McNaught)^{*}, C/1999 U₂ (SOHO)[♣], C/1980 E₁ (Bowell)[♣]. Halley type comets: P/2005 T₄ (SWAN)[♣].

Further investigation of the orbits of these asteroids would be important in order to better understand their origins and confirm the results of this thesis.

Another important result of this work is the discovery of the most probable origins of paleo-impact events and the description of a new statistical method. In particular, the Bosumtwi crater case, via astrodynamics and geology methods, was tackled. The results of this study indicate that the origin of this recent crater is an asteroid coming from the Middle Main Belt at high inclinations ($i > 35^\circ$) with a possible initial T_j equal to 2.63 ± 0.25 . The real existence of asteroids with similar orbits such as 2002 MO₃, which suggest that real asteroids are present in this region, support this result.

9.2 Close encounters with the terrestrial planets

Thanks to the work on the Hungaria group, V-types asteroids and the inner Centaurs region between Jupiter and Saturn, it is now possible to compare the data from 3 different source regions or sources of Planet Crossing Asteroids. No close encounters were detected (hence no impacts neither), for Centaurs in the range established (Table 1.1). This means that it is possible to compare only Hungarias and V-types.

To compare the data of different groups of asteroids (Table 9.1) the following normalized amplitudes have been chosen: one normalized by integrational time, $N_{e_T, norm}$ (e stands for event³²), and one normalized by total number of bodies multiplied by the integrational time, $N_{e_T, ast, norm}$, in the sample respectively to each analyzed group:

- in the case of the V-type, the normalized number of events, i.e. the close encounters ($N_{CE, norm}$) (or impacts, $N_{imp, norm}$), is the ratio between the total number of events ($N_{e, tot}$) and the total number of bodies multiplied by the integrational time (T in My):

$$N_{CE_T, norm} = \frac{N_{CE, tot}}{T} \quad (9.1)$$

³²An event could be an impact (*imp*) or a close encounter (*CE*)

and

$$N_{CE_T,ast,norm} = \frac{N_{CE,tot}}{T \cdot N_{ast}} \quad (9.2)$$

where N_{ast} is the number of asteroids that are integrated as *NEAs* in each calculation, i.e. 11 for the Hungarias and 27 for the V-types;

- in the case of the Hungarias, the time when they become *NEAs* is considered, namely the average time for the fugitives to become *NEAs* for the first time (see Chapter 2). It is defined: $T = 100 - \bar{T}_{NEA} = 100 - 46.67 = 53.33 \text{ My} = T'$, so $N_{CE_t,norm} = \frac{N'_{CE,tot}}{T'}$ and $N_{CE_t,ast,norm} = \frac{N'_{CE,tot}}{T' \cdot N_{ast}}$, where $N'_{CE,tot} = \frac{N_{ast} N_{CE,tot}}{N_{tot,clones}}$ and $N_{tot,clones}$ is the total number of clones of the Hungarias fugitives (550), so in the end $N_{CE_T,ast,norm} = \frac{N_{CE,tot}}{T' \cdot N_{tot,clones}}$. (From now on, for economy of writing, $N_{CE_T,ast,norm} = \bar{N}_{CE(T,a)}$, $N_{CE_T,norm} = \bar{N}_{CE(T)}$, $N_{imp_T,ast,norm} = \bar{N}_{i(T,a)}$ and $N_{imp_T,norm} = \bar{N}_{i(T)\cdot}$).

Table 9.1: Summary of close encounters (of the number of asteroids for each planet) with the terrestrial planets for 2 groups of asteroids studied in this thesis. *H* and *V* means respectively Hungaria Group and V-types group. The asterisk indicates a difference in the quality of the statistics between the two groups: the number of close encounters with Mars is biased for the Hungarias by the fact that it is considered also the quantity computed when the Hungarias are still non-NEAs. *All* is the total normalized number of close encounter with terrestrial planets and *All** are *CEs* with Venus and the Earth only.

Planets	$\bar{N}_{CE(t)}(H)$	$\bar{N}_{CE(t)}(V)$	$\bar{N}_{CE(t,a)}(H)$	$\bar{N}_{CE(t,a)}(V)$
Venus	0.050	2.000	0.005	0.074
Earth	0.059	2.800	0.005	0.104
Mars	0.160*	1.800	0.015*	0.067
All*	0.109	4.800	0.010	0.178
All	0.269	6.600	0.024	0.244

Results in Table 9.1 show that, V-types have many more asteroids which have close encounters than E-types (Hungarias) and V-types have also more close encounters by each asteroids than E-types (Table 9.2). Therefore if V-types are thought to originated from 4 Vesta, this will mean that the Vesta family will have more *CEs* with the terrestrial planets than Hungarias, both individually ($N_{CE_t,ast,norm}$) and as a whole $N_{CE_t,norm}(H)$. Considering both *NEAs* from Hungarias and V-types (Table 9.1 and 9.2) as one sample, the Earth is the planet most encountered (both by single asteroids and by whole groups).

9.2. CLOSE ENCOUNTERS WITH THE TERRESTRIAL PLANETS

Table 9.2: Summary of the total number of close encounters (by each asteroid for each planet) with the terrestrial planets for V-types and Hungarias studied in this thesis. The number of close encountered with Mars is biased, as explained in Table 9.1.

Planets	$N_{CE(t)}$	$N_{CE(t,a)}$
Venus	0.079	2.050
Earth	0.109	2.859
Mars	0.082*	1.867*

It has been shown that the gravitational perturbation of the Moon does not change significantly the number of close encounters. Although the absolute numbers depend on the arbitrary choice of the limit distance (for a larger value of 0.01 au instead of 0.0025 au the number of close encounters increases by an order of magnitude at least), a normalization still gives good results (Chapter 4). So it is still possible to compare orbital integrations that take into account the evolution of *NEAs* coming from different regions of the Solar System, with and without the Moon. Therefore, it is legitimate to think that the number of close encounters and impacts with Hungaria-, V-type- and Centaur-*NEAs* is not affected by the presence of the Moon.

The mean durations of *CEs* between Hungaria and V-type asteroids are different, apart for in the case of Venus (see Chapter 2 and Section 6.1), V-types asteroids stay near (in the *CE*-region, see Fig. 9.1) the Earth about ~ 2.5 times longer than Hungarias and near Mars about half as long as Hungarias.

V-type asteroids stay longer near the Earth during close encounters than they do during close encounters with Venus and Mars, which is different to the Hungarias that have a relation $t_{Venus} : t_{Earth} : t_{Mars} = 2 : 3 : 4$, meaning that Hungaria *PCAs* stay half as long in the *CE*-region of Venus than in the *CE*-region of Mars.

The average deflection angle Θ is small ($< 1^\circ$) for the Earth and Mars both for V-types and Hungarias (Section 6.1). For Venus, instead, the deflection of the V-types *PCAs* is higher on average (3.6°) than the deflection of the Hungarias ($< 1^\circ$).

Finally, an empirical equation (Eqn. 1.6) has been found for the rotational angle which fits very well with the correlation between the minimum distance of the asteroid to the planet and the deflection angle. This equation depends on three constants (defined as a and b and c , see Eqn. 1.6). Analyzing this equation for different asteroids, it is possible to infer empirically the rotational angles of the asteroids at the time when they are beginning their close encounters with a planet, knowing in advance their minimal distance with the planet and its osculating elements (see Chapter 2). For instance, the computed constants relative to Mars for the Hungaria asteroid (30935) Davaşobel are $a = -16.06307$, $b = -0.04237$

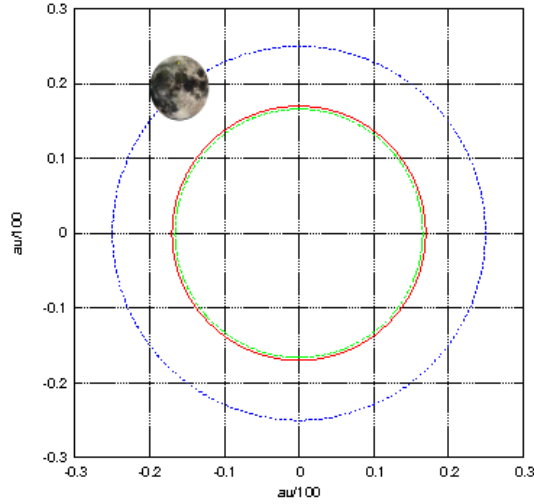


Figure 9.1: Projection on a x-y plain of the CE-region for the 3 major terrestrial planets (the border is the relative circle). From the smallest circle to the biggest: Mars CE-region (CE radius, $r_{CE} = 0.166 \cdot 10^{-2} au$), Venus CE-region ($r_{CE} = 0.170 \cdot 10^{-2} au$) and the Earth CE-region ($r_{CE} = 0.250 \cdot 10^{-2} au$). The Moon is shown to underline that the radius of the Earth CE-region is the average Lunar distance (0.0025 au). The point (0,0) is the center of the relative planet.

and $c = 12.19940$; so using Eqn. 1.6 and these three constants, and supposing the perigeum is known before its approach to the region for a CE, and it is half the average close encounter radius distance for Mars (0.00083 au), the rotational angle will be 0.31° . This method could be useful if a good statistical study of close encounters is performed for each terrestrial planet. More integrations considering close encounters are needed in order to create a statistical table of CEs with their osculating elements at the entrance of the sphere for close encounters and the three computed parameters a , b and c for the relative orbit of the approaching asteroid. This could be an important tool to compute in advance the real orbit of the asteroids after a close encounter and obviously by how much its trajectory will be deflected.

9.3 Impacts

9.3.1 Impacts with terrestrial planets and the Sun

Among the three analyzed group, the V-types have the highest number of impacts with terrestrial planets in respect to the other 2 studied regions, and only the

Centaurs experience no collisions. However, the considered integration time for the Centaurs is probably too short and with longer integration times, a number of collisions might be expected, even if probably still a negligible number if compared with the number of impacts of V-types and Hungarias. The number of impacts is summarized in Table 9.3 with normalized quantities as described in Section 9.2.

Table 9.3: Summary of impacts with the terrestrial planets for the 3 groups of asteroids studied in this thesis. H, V and C mean respectively Hungaria Group, V-types group, Centaurs. Sun-grazing Centaurs are also considered as impacts, and, considering their very high eccentric orbits, will all end up colliding with the Sun. The meaning of the asterisk is the same one explained in Table 9.1.

Bodies	$\bar{N}_{i(T)}(H)$	$\bar{N}_{i(T)}(V)$	$\bar{N}_{i(T)}(C)$	$\bar{N}_{i(T,a)}(H)$	$\bar{N}_{i(T,a)}(V)$	$\bar{N}_{i(T,a)}(C)$
Sun	0.074	1.000	> 31.000*	0.007	0.0369	> 0.370*
Venus	0.005	0.600	0.000	< 0.001	0.022	0.000
Earth	0.002	0.202	0.000	< 0.001	0.007	0.000
Mars	0.002*	0.000	0.000	< 0.001*	0.000	0.000

Table 9.4: Summary of total number of impacts with the terrestrial planets and the Sun for V-types, Hungarias and Centaurs, studied in this thesis. The meaning of the asterisk is the same one explained in Table 9.1.

Bodies	$\bar{N}_{i(T)}$	$\bar{N}_{i(T,a)}$
Sun	> 31.074	> 0.413
Venus	0.605	0.022
Earth	0.204	0.007
Mars	0.002*	0.001*

The mortality of the Centaurs due to collisions with the Sun is very high (more than 31 asteroids every 1 Myr) and it is higher than the other 2 groups (Hungarias and V-types). The planet that collides with the most asteroids is Venus (~ 3 times the rate for the Earth) for Hungarias and V-types. These results are in accordance with Ivanov et al. (2002), who computed the number of impacts in 1 Gyr for all of the asteroids with an absolute magnitude in visual smaller than 17. Asteroids with this brightness have diameters ranging from 0.75 to 2.4 km, depending on their albedo (see www.minorplanetcenter.net/iau/Sizes.html).

Ivanov et al. (2002) also found that Venus has the highest rate of impacts with asteroids among the terrestrial planets and is second only to the Sun. V-types NEAs seem to affect much more (by two order of magnitude) the terrestrial planets than E-types Hungaria-NEAs. These results demonstrate that the terrestrial

planets suffer collisions with more asteroids of Vestian origin than of Hungaria origin, thus impacts with asteroids with a basaltic composition are privileged. This material is connected to the *HED*, that is thought of Vestian origins (Section 6.1 and Appendix B).

In fact, the ratio between the sample of *HED* meteorites and the enstatite chondrites on the Earth (Burbine et al. (2002a); see also Fig. 1.19), confirms the disproportion between V-type impacts and E-type (of Hungaria region origin) impacts.

The number of collisions with Mars for the Hungarias is biased for the reasons explained in Section 9.2. When the Moon was considered (i.e. in the V-types asteroids, Section 6.1, and in the Hungarias, Chapter 4), no impacts were detected with the Moon, so even here the contribution of the Moon was negligible.

Two important conclusions should be mentioned about the Hungaria asteroids: (1) they cannot be an important source of water for terrestrial planets due to the small rate of impacts (see Chapter 5), though it is worth recalling that the considered integration time was small and larger integrations times would produce more impacts; (2) considering their initial inclination, it is plausible (see Chapter 2) that the collision that created the Hungaria family happened during a period in which massive bodies (with diameters bigger than at least 30 km) collided inside the Main belt region. Presumably all Hungaria asteroids were created in an initial collision in the *IMB* region for a body that probably had a high inclination: $i \geq 23^\circ$.

Hungaria craters are the largest found on the Earth in this work, with possible diameters³³ $D \lesssim 30$ km (Chapter 3). These are much larger than the V-types craters with $D \lesssim 5$ km (consequently the impact energy is 1-2 order less). No craters due to impacts with Centaurs are found during the integrational time for the study of their orbits (Chapter 6.2). Centaurs even have no close encounters inside the cutoff limit considered in this work. On the other hand, a hypothetical impact with Centaurs would certainly be catastrophic and would create the biggest crater on the surface of a terrestrial planet. What is interesting is that V-types *NEA* impact velocities seem³⁴ higher than the Hungaria impact velocities. V-type close encounter velocities also seems higher, i.e. for the Earth, the V-type average encounter velocity is 26.12 km/s as opposed to the highest velocity for the Hungaris of 22.32 km/s.

A question arises from all this work. How could the Earth keep such biological diversity with this sort of impact rate? Is the amount of water in the right quantity to keep the incredible atmosphere in its present condition and allow the surface so unique? Is the activity of the Earth so different from the other planets? The

³³The maximum diameter for a crater made by a Hungaria asteroid in this work is ~ 30 km.

³⁴The statistics are poor and it might be that the detected V-type asteroid is faster than all the Hungarias' impactor speed found.

presence of intelligent beings on Earth seems to be a unique thing over at least 1 Ly of distance (roughly the radius of the Solar system when you consider the trailing edge of the Oort cloud, Morbidelli et al., 2006). But if we consider only an asteroid impact as the unique cause of extinction (among the possible others), so an asteroid which has a radius larger than 2 km, <http://impcat.arc.nasa.gov/intro.cfm> and Morrison et al. (2002), the Earth will experience an extinction of “intelligent-life”, much probable, this will occur every 30-70 million years (Morrison et al. , 2002), and so only for in this interval of time, a planet could host and keep intelligent beings alive. Assuming that the number of impacts is similar in other extrasolar planetary systems, the impact rate found in the Solar system could justify the fact that other intelligent life forms are not visible, because they are already extinct or because they are still to be formed again in the future, given that intelligent life has existed for a few hundred thousand years (at least looking at human-beings’ science progress, and traces of that, on the Earth and also outside, i.e. Pioneers and Voyagers satellites or electrogmanetical signals beyond the atmosphere, i.e. radio signals etc.).

The present thesis gives some important little pieces of the answer to this vital question. Also suggestions and ideas are given for future research concerning small bodies and their impacts in the Solar System.

This work will be extended in the future in order to achieve more precise results, using also the contributions of non-gravitational forces. When the physical parameters of the asteroids are found and confirmed in more detail using present and future astronomical missions with satellites that transport tools for observations.

Appendix A

Influence of the secular resonances for the asteroids

Let us consider the perturbing influence of n -planets of mass m_i on the orbit of an asteroids. Considering the alternative elements $h = e \sin \bar{\omega}$, $k = e \cos \bar{\omega}$, $p = \sin i \sin \Omega$, and $q \sin i \cos \Omega$. Let the asteroid have the standard osculating elements $a, \lambda_0, e, i, \bar{\omega}, \Omega$ and, likewise, the eight planets of the Solar System, $a_j, \lambda_{0j}, e_j, i_j, \bar{\omega}_j, \Omega_j$, for $j = 1, 8$. Then it is needed also to define the next parameters:

$$\alpha_i = \begin{cases} a/a_i & a_i > a \\ a_i/a & a_i < a \end{cases} \quad (\text{A.1})$$

and

$$\bar{\alpha}_i = \begin{cases} a/a_i & a_i > a \\ 1 & a_i < a \end{cases} \quad (\text{A.2})$$

as well as $\epsilon_i = \frac{m_i}{M}$, where M is the mass of the Sun.

Analog to the secular evolution of the planetary orbits, the secular terms in the disturbing function of the asteroids generated by the perturbing influence of the planets,

$$\mathcal{R} = \mu' \sum_i^n S(a, a_i, e, e_i, I, I_i) \cos \phi \quad i = 1, 2, \dots, n \quad (\text{A.3})$$

cause the asteroid's osculating orbital elements to evolve in time:

$$h(t) = e_{free} \sin(At + \beta_{free}) + h_{forced}(t) \quad (\text{A.4})$$

$$k(t) = e_{free} \sin(At + \beta_{free}) + k_{forced}(t) \quad (\text{A.5})$$

$$p(t) = \sin I_{free} \sin(Bt + \gamma_{free}) + p_{forced}(t) \quad (\text{A.6})$$

and

$$q(t) = \sin I_{free} \sin(Bt + \gamma_{free}) + q_{forced}(t) \quad (\text{A.7})$$

where

$$A = \sum_{i=1,8}^n \frac{\epsilon_i \alpha_i \bar{\alpha}_i b_{3/2}^1(\alpha_i)}{4} \quad (\text{A.8})$$

$$B = -A \quad (\text{A.9})$$

$$h_{forced} = - \sum_{i=1,8} \frac{\nu_l}{A - g_l} \sin(g_l t + \beta_l) \quad (\text{A.10})$$

$$k_{forced} = - \sum_{i=1,8} \frac{\nu_l}{A - g_l} \cos(g_l t + \beta_l) \quad (\text{A.11})$$

$$p_{forced} = - \sum_{i=1,8} \frac{\nu_l}{A - f_l} \sin(f_l t + \gamma_l) \quad (\text{A.12})$$

and

$$q_{forced} = - \sum_{i=1,8} \frac{\nu_l}{B - f_l} \cos(f_l t + \gamma_l) \quad (\text{A.13})$$

The eigenvalues g_l and f_l can be solved via standard numerical techniques (Press et al. 1992). The phase angles γ_l and β_l can be found by demanding that, at $t = 0$, equations A.10, A.11, A.12 and A.13 lead to the right osculating elements.

as well as

$$\nu_l = \sum_{i=1,8} A_i e_{il} \quad (\text{A.14})$$

$$\mu_l = \sum_{i=1,8} B_i I_{il} \quad (\text{A.15})$$

The parameters e_{free} and I_{free} appearing in the previous equations are the eccentricity and the inclination, respectively, that the asteroid orbit would possess were it not for the perturbing influence of the planets. These are usually called the *free*, or *proper*, eccentricity and inclination, respectively. Roughly speaking, the planetary perturbations cause the osculating eccentricity, $e = (h^2 + k^2)$, and inclination, $I = \sin^{-1}[(p^2 + q^2)^{1/2}]$, to oscillate about the corresponding free quantities, e_{free} and I_{free} , respectively (from Fitzpatrick, 2012 and Murray & Dermott 1999).

Appendix B

Meteorites, Parent Bodies and connections

B.1 Meteorites

Groups are subdivided in subgroups depending on their petrological type, e.g. CO3 (Moss meteorite fallen in Norway, July 14, 2016 and in Russia, 1937) and CV3 (Allende meteorite, the largest carbonaceous meteorite ever found on Earth, February 8, 1969, in Mexico). The number 3 in the nominative means lack of secondary heating effects. Table B.4 describes the group of meteorites (with their relative percentage of falling down to the Earth) and their relation to their most probable parent body (asteroid). ast.= means asteroids, Subs = subgroups, Ord. = Ordinary, Diff. = Differentiated, Prim. = Primitive, Enst. = Enstatite, Carb. = Carbonaceous, St. = stony, Ch. = Chondrites and Ach. = Achondrites. Minerals or components are listed in decreasing order of average abundance. ol = olivine, px = piroxene, opx = orthopyroxene, pig = pigeonite, enst = enstatite, aug = augite, cpx = clinopyroxene, plag = plagioclase, mag = magnetite, met = metallic iron, sul = sulfides, phy = phyllosilicates, toch = tochilinite, graph = graphite, CAIs = Ca-Al-rich refractory inclusions, schreib = schreibesite, she = shergottite, nak = nakhite, cha = chassignite, feld-reg = feldspathic regolith, incl = inclusions, \pm = may be present and Mesosider. = Mesosiderites.

One of the most recent case of meteorites on the Earth is the case of Chelyabinsk meteor. An asteroid (meteor) of about ~ 17 m entered in our atmosphere with a speed of ~ 18 km/s and exploded next the city of Chelyabinsk (Russia), releasing micro-ejecta bodies (meteorites) around. In the day of the impact one other asteroid 2012 DA₁₄ came very close to planet Earth, but as it can be visible from their orbits (Fig. B.1) they seems not related, despite it is very unusual to have such a close encounter, like 2012 DA₁₄ and even less a meteor of such size that give rise to injuries too!

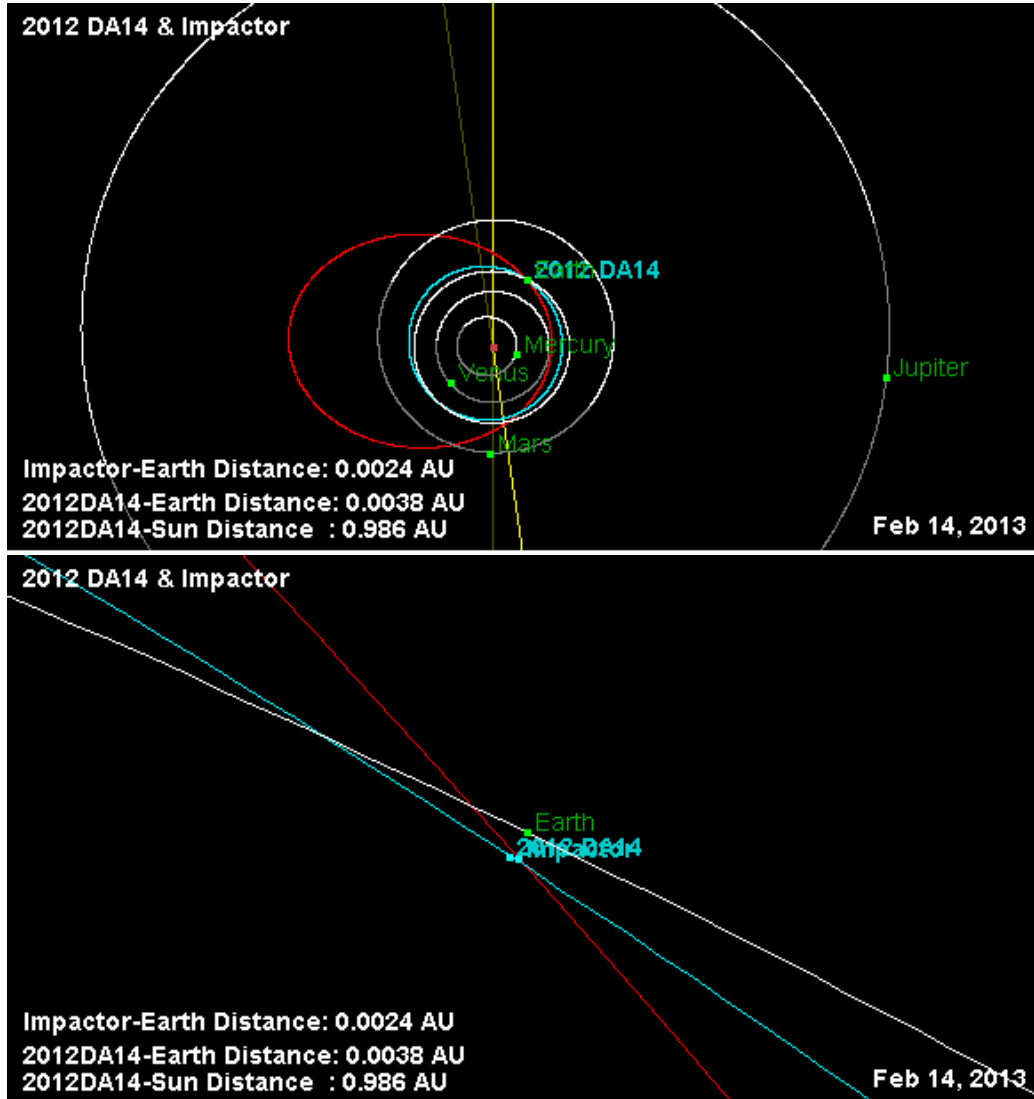


Figure B.1: Comparison of the orbits of the asteroid 2012 DA₁₄, $a = 0.9103$ au, $e = 0.0984$ and $i = 11.61$, in light green and of the Chelyabinsk meteor $a = 1.60$ au, $e = 0.53$ and $i = 4.07$, see http://www.aiaahouston.org/wp-content/uploads/2012/07/Horizons_2013.03.04_page.28_and.29_Adamo.3_of.3.pdf

APPENDIX B. METEORITES, PARENT BODIES AND
CONNECTIONS

Group	Subs	Composition	Fall %	Source
<i>Ord. Ch.</i>	L	ol,px,plag,met,sul	38.0	$S_{(IV)}$ ast.
<i>Ord. Ch.</i>	H	ol,px,met,plag,sul	34.1	6 Hebe[$S_{(IV)}$]
<i>Ord. Ch.</i>	LL	ol,px,plag,met,sul	7.91	$S_{(IV)}$ ast.
<i>Irons</i>		met,sul,-ol,-px, -plag,-schreib,-SiO ₂	4.2	M ast.
<i>Diff. Ach.</i>	Eucrites	pig,plag	2.7	4 Vesta(V)
<i>Diff. Ach.</i>	Howardites	eucritic-diogenitic breccia	2.1	4 Vesta(V)
<i>Carb. Ch.</i>	CM	phy,toch,ol	1.7	19 Fortuna
<i>Diff. Ach.</i>	Diogenites	opx	1.2	4 Vesta(V)
<i>Diff. Ach.</i>	Aubrites	enst,sul	1.0	3103 Eger
<i>Enst. Ch.</i>	EH	enst,met,sul,plag, \pm ol	0.8	M ast.
<i>Enst. Ch.</i>	EL	enst,met,sul,plag	0.7	M ast.
<i>St. irons</i>	Mesosider.	basalt-melt breccia	0.7	M ast.
<i>Carb. Ch.</i>	CV	ol,px,CAIs	0.6	K ast.
<i>Carb. Ch.</i>	CI	phy,mag	0.5	C ast.
<i>Carb. Ch.</i>	CO	ol,px,CAIs,met	0.5	221 Eos
<i>St. Irons</i>	Pallasites	ol,met	0.5	A ast.
<i>Diff. Ach.</i>	Ureilites	ol,px,graph	0.5	S ast.
<i>Ach.</i>	"Martian"	she,nak,cha, opx,basaltic-breccias	0.4	Mars
<i>Carb. Ch.</i>	CR	phy,px,ol,met	0.3	C ast.
<i>Carb. Ch.</i>	CK	ol,CAIs	0.3	C ast.
<i>Prim. Ach.</i>	Acapulcoites	px,ol,plag,met,sul	0.1	S ast.
<i>Diff. Ach.</i>	Angrites	TiO ₂ -rich aug,ol,plag	0.1	S ast.
<i>Prim. Ach.</i>	Lodranites	px,ol,met, \pm plag, \pm sul	0.1	S ast.
<i>R Ch.</i>	R	ol,px,plag,sul	0.1	A/S ast.
<i>Prim. Ach.</i>	Winonaites	ol,px,plag,met	0.1	S ast.
<i>Carb. Ch.</i>	Tagish Lake		0.1	D ast.
<i>Diff. Ach.</i>	Brachinites	ol,cpx, \pm plag	\ll 0.1	A ast.
<i>Carb. Ch.</i>	CH	px,met,ol	\ll 0.1	C/M ast.
<i>Ach.</i>	"Lunar"	feld-reg-breccia	\ll 0.1	Moon

Table B.1: Meteorites groups, their postulated parent body or source bodies, their fall percentage and their compositional characteristics.

B.2 Spectral Type classification of asteroids

Hartmann et al. (1987) found that various asteroids in comet-like orbits were classified in the low-albedo spectral classes D, P and C; cometary nuclei tend also to have low albedos. Moreover, *NEAs* in non-cometary orbits (typically with only moderate eccentricities) tend to be of S-type, as expected for the inner main belt. Surveys have also revealed that the *NEA* population is dominated by objects belonging to the taxonomic classes *S* (“rocky asteroids”) and *Q* (25% as Q-type and 40 % as S-type, (Binzel et al., 2004) and when corrected for discovery biases, about 40% of the *NEA* population belong to on of these two taxonomic classes. In the case of Mars-Crossers, 65% belong to the S class (de León et al., 2010). In the Main belt from 2.0 to 2.5 AU there are signes of mafic silicates and these minerals are also the most abundant class of meteorites (80% of the falls), the ordinary chondrites (*OCs*). Therefore, given the dominance of S-type among the *NEA* population and the ordinary chondrites among the meteorites, it has been generally and widely assumed that they are connected, and that *NEAs* are the most likely parent bodies of the *OCs*.

Some asteroid’s families¹ are associated with some meteorites (as parent families, Cellino et al., 2002 and Novakovic et al., 2012):

Flora family is associated with meteorite-types *L3*, *L4*, *L5* and *LL*;

Vesta family with *HED* type;

Maria Family with *O.C.* type²;

Eos family with *CO/CV* type;

Watsonia family with *CO3/CV3* type.

¹see Table B.3 and B.4. Bapt.= Baptistina, Theob.= Theobalda, Mel.= Meliboea, Erig.= Erigone, Mass.= Massalia, Eun.= Eunomia, Nem.= Nemesis, Chl.= Chloris, Bra.= Brasilia, Kor.= Koronis and Ver.= Veritas. Age0 means age < 0.1 Gyr. * = computed via Fowler & Chillemi (1992).

²Ordinary Chondrite

APPENDIX B. METEORITES, PARENT BODIES AND
CONNECTIONS

Table B.2: Summary of asteroid taxonomic classes (Cellino et al. , 2002).
Mod. = Moderate.

Tholen Class	Bus Class/SMASS	Albedo	Spectral Features
A	A	Mod.	Very steep red slope shortward of 0.75 μm ; moderately deep absorption feature longward of 0.75 μm .
B, C, F, G	B, C, C_b , C_h , C_g , C_{hg}	Low	Linear, generally featureless spectra. Differences in UV absorption features and presence/absence of narrow absorption feature near 0.7 μm .
D	D	Low	Relatively featureless spectrum with very steep red slope.
E, M, P	X, X_c , X_e , X_k	From low (P) to very high (E)	Generally featureless spectrum with reddish slope; differences in subtle absorption features and/or spectral curvature and/or peak relative reflectance.
Q	Q	Mod.	Reddish slope shortward of 0.7 μm ; deep, rounded absorption feature longward of 0.75 μm .
R	R	Mod.	Mod. reddish slope downward of 0.7 μm ; deep, absorption longward of 0.75 μm .
S	S, S_a , S_k , S_l , S_q , S_r	Mod.	Moderately steep reddish slope downward of 0.7 μm ; moderate to steep absorption longward of 0.75 μm ; peak of reflectance at 0.73 μm . Bus subgroups intermediate between S and A, K, L, Q, R classes
T	T	Low	Moderately reddish shortward of 0.75 μm ; flat afterward.
V	V	Mod.	Reddish shortward of 0.7 μm ; extremely deep absorption longward of 0.75 μm .
—	K	Mod.	Moderately steep red slope shortward of 0.75 μm ; smoothly angled maximum and flat to bluish longward of 0.75 μm with little or no curvature.
—	L, L_d	Mod.	Very steep red slope shortward of 0.75 μm ; flat longward of 0.75 μm ; differences in level.
—	O	—	Peculiar trend, known so far only for asteroid 3628.

B.2. SPECTRAL TYPE CLASSIFICATION OF ASTEROIDS

All the data shown in the Table B.3 and B.4 come from Cellino et al. (2002); Nesvorný et al. (2005); Bendjoya P. & Zappalá et al. (2002); Carry (2012) and Novaković, Cellino & Knežević (2011).

Table B.4 shows the most important data/properties of the most well recognized asteroid families at high inclinations ($i > 17^\circ$) in the Main Belt. Only the approximate age of Hungaria Family is known (0.5 Gy) among these families. Hungaria Family is not shown because it has been just well described in Chapter 2, 3 and 5, and also Lorre Family that still has to be confirmed ($a = 2.74$, $e = 0.28$ and $i = 26.6$ with a diameter of 33.5 km).

APPENDIX B. METEORITES, PARENT BODIES AND
CONNECTIONS

Table B.3: Summary data of the most well recognized asteroid families in the Main Belt at inclinations, $i < 17^\circ$: a , e and i (the osculating elements); the size (km) and the density (g/cm^3) of their major body, the principal taxonomic class and the approximate age (Gyrs).

Family	a	e	i	size	ρ	T.	Age
Flora	2.15-2.35	0.03-0.13	1.5-8.0	139	6.5	S	1.0
Bapt.	2.26	0.10	6.3	12.4		X	
Vesta	2.26-2.48	0.03-0.16	5.0-8.3	519	3.6	V	1.5
Nysa	2.41-2.5	0.12-0.21	1.5-4.3	81*	2.0	S(F)	
Erig.	2.37	0.20	4.8	73	10.0	C	0.3
Juno	2.67	0.25	13.0	242	3.7		
Mass.	2.37-2.45	0.12-0.21	0.4-2.4	137	3.7		0.2
Rafita	2.55	0.16	7.0	12*		S	1.5
Maria	2.5-2.71		12.0-17.0			S	3.0
Eun.	2.53-2.72	0.08-0.22	11.1-15.8	257	3.5	S	2.5
Misa	2.66	0.18	1.2	73		C	0.5
Adeona	2.67	0.15	12.6	150	1.2	C	0.7
Nem.	2.75	0.12	6.2	184	1.8	C	0.2
Lydia	2.73	0.08	6.0	86		C,X	
Padua	2.75	0.07	5.9	97		XC	0.3
Chl.	2.73	0.24	11.0	116	7.7	C	0.7
Merxia	2.75	0.13	4.7	32			0.2
Gefion	2.74-2.82	0.08-0.18	7.4-10.5	13		S	1.2
Agnia	2.78	0.09	2.4	28		C	0.1
Dora	2.80	0.23	6.8	27		C	0.5
Bras.	2.86	0.11	15.6	55		CX	0.1
Kor.	2.83-2.91	0-0.11	0-3.5	35		S	2.5
Eos	2.99-3.03	0.01-0.13	8.0-12.0	104	10.1	K	1.3
Tirela	3.12	0.23	15.5	18			
Themis	3.08-3.24	0.09-0.22	0-3.0	184	1.8	C,B	2.5
Hygiea	3.06-3.24	0.09-0.19	3.5-6.8	422	2.2	C	2.0
Ver.	3.17	0.10	9.3	111	8.4	C,P,D	0
Theob.	3.19	0.25	13.7	64		F	
Naema	2.94	0.07	12.6	54			0.1
Ceres	2.76	0.79	10.6	945		G	
Astrid	2.79	0.05	1.01	35		C	0.2
Bower	2.57	0.15	8.4	36		C	
Hilda	3.7-4.2	> 0.07	< 20	171		P	
Karin	2.86	0.08	1.0	19*			0
Mel.	3.12	0.22	13.4	146	4.5	C	

B.2. SPECTRAL TYPE CLASSIFICATION OF ASTEROIDS

Table B.4:

Family	a	e	i	size	ρ	T.
Phoacaea	2.40	0.26	21.6	75		S
7784	2.27	0.24	23.3	6		
Pallas	2.77	0.23	34.84	545	3.7	B,C
Atalante	2.75	0.30	18.43	106	6.2	C
Gallia	2.77	0.18	25.31	98	16.1	GU
Hansa	2.66	0.06	22.0	56		S
Gersuind	2.59	0.27	15.7	41		S
Watsonia	2.76	0.10	18.0	49		L
Barcelona	2.63	0.16	32.9	25		S
Anacostia	2.74	0.20	15.9	86		SU
Tina	2.80	0.25	19.7	21		
Dennispalm	2.64	0.26	31.4	17		DSU
Brucato	2.61	0.13	28.6	13		
Myriostos	2.59	0.30	20.6	3.6		
1998 DN_2	2.64	0.12	28.5	5.1		
1999 PM_1	2.68	0.24	28.2	4.9		
Kunitaka	2.67	0.17	17.7	3.2		
2001 YB_{113}	2.58	0.11	22.5	4.3		
1998 LF_3	2.60	0.19	30.0	7.2		
2001 OF_{13}	2.64	0.30	31.2	5.7		
2004 EW_7	2.62	0.27	27.2	2.6		
Euphrosyne	3.15	0.22	26.3	255.9	1.2	C
Eucharis	3.13	0.20	18.9	106.7		S
Ornamenta	3.11	0.16	24.9	118.4		C
Alauda	3.19	0.02	20.6	194.7	1.6	C
Armenia	3.11	0.10	19.1	94.4		
Kartvelia	3.22	0.12	19.1	66.0		CPU
Vassar	3.09	0.22	21.9	36.3		
Pannonia	3.15	0.14	17.8	29.2		
Moravia	3.24	0.70	24.1	27.0		
Filipenko	3.17	0.21	17.0	56.1		
Higson	3.20	0.09	21.0	21.8		
Snelling	3.16	0.12	21.7	24.4		
Zhvanetskij	3.18	0.19	16.9	30.8		
1995 SR_1	3.15	0.08	25.8	30.8		
1994 VD_7	3.15	0.12	20.8	10.4		
1998 HV_{32}	3.10	0.18	25.9	7.1		
1997 UG_5	3.24	0.18	18.5	9.9		

Acknowledgements

I acknowledge all the people that share with me work and pleasure discussions on astronomy and science in general, from the whole ADG group (Astrodynamical Group at the Department of Astrophysics) of Vienna to my geologists colleagues (of the IK-group), who shared with me their nice knowledge on planetary science. And the funding from University of Vienna doctoral school IK-1045 and Austrian Science Foundation Grant P21821-N19. Then out of science I want to thank for discussions, helps and suggestions, sometimes cooperation: Dr. Yuri Cavecchi, Dr. Giovanni Carraro, Prof. Werner Zeilinger, Prof. Boris Ivanov, Prof. G. Valsecchi, Dr. Simone Recchi, Dr. Thomas Posch, Mag. Pavel Smutny, Dr. Michele Maris, Prof. Mirel Birlan, Dr. Akos Kerezsturi and Dr. Sara Magrin.

Bibliography

- Asphaug E. 1997, M&PS, 32, 965-980
- Artemieva N., Karp T. & Milkereit B. 2004 , GGG, 5, 11016
- Assandri M. C. & Gil-Hutton R. 2008, A&A, 488, 339-343
- Barucci M. A., Cruikshank D. P., Mottola S. & Lazzarin M. 2002, Asteroids III, 273-278
- Beatty J. K., Beatty, J. K. 2007, S&T, 114, 1
- Belton M. J. S., Chapman C. R., Thomas P. C. & 13 coauthors 1995, Nature, 374, 785-788
- Bendjoya P. & Zappalá V. 2002, Asteroids III, 613-618
- Bertotti B. & Farinella P. 1990, Geophysics and Astrophysics Monographs, 31
- Beutler G. 2005, Methods of celestial mechanics. Vol. Gerhard Beutler. In cooperation with Leos Mervart and Andreas Verdun. Astronomy and Astrophysics Library
- Binzel R. P., Bus S. J. & Burbine T. H. 1998, AAS/Division for Planetary Sciences Meeting Abstracts, 30, 1041
- Binzel R. P., Bus S. J., Burbine T. H. & Rivkin A. S. 2001, Lunar Planetary Science, 32, 1633
- Binzel R. P., Rivkin A. S., Bus S. J. & Tokunaga A. T. 2004, AAS/Division for Planetary Sciences Meeting Abstracts #36 (Bulletin of the American Astronomical Society), 36, 1131
- Bland P. A., Spurný P., Towner M. C. & 11 coauthors 2009, LPSC, 40, 1664
- Bogard D. D. 2011, Chemie der Erde / Geochemistry, 71, 207-226
- Bottke W. F., Morbidelli, A., Jedicke R., Petit J. M., Levison, H. F., Michel, P. & Metcalfe T. S. 2002, Icarus, 156, 399-433

- Bottke W. F., Vokrouhlický D., Minton D., Simonson B. & Levison H. F. 2012, *Nature*, 485, 78-81
- Brasser R., Morbidelli A. 2011, *A&A*, 535, A41
- Britt T. H., Yeomans D., Housen K. & Consolmagno G. 2002, *Asteroids III*, 485-500
- Brož M., Morbidelli A., Bottke W. F., Rozenhal J., Vokrouhlický D. & Nesvorný D. 2013, *A&A*, 551, A117
- Burbine T. H., McCoy T. J., Meibom A., Gladman B. & Keil K. 2002a, *Asteroids III*, 653-667
- Burbine T. H. & Binzel R. P. 2002b, *Icarus*, 159, 468-499
- Bus S. J. 1999, PhD thesis (Massachusetts Institute of Technology)
- Bus S. J. & Binzel R. P. 2002a, *Icarus*, 158, 106-145
- Bus S. J. & Binzel R. P. 2002b, *Icarus*, 158, 146-177
- Carruba V., Michtchenko T. A. & Lazzaro D. 2007, *A&A*, 473, 967-978
- Carruba V., Michtchenko T. A., Roig F., Ferraz-Mello S. & Nesvorný D. 2005, *A&A*, 441, 819-829
- Carvano J. M., Lazzaro D., Mothé-Diniz T., Angeli C., A. & Florczak M. 2001, *Icarus*, 149, 173-189
- Carusi A., Valsecchi G. B. & Greenberg R. 1990, *CeMDA*, 49, 111-131
- Carry B. 2012, *Planet. Space Sci.*, 73, 98-118
- Cellino A., Bus S. J., Doressoundiraim A. & Lazzaro D. 2002, *Asteroids III*, 633-643
- Chapman C. R. & Davis D. R. 1975, *Science*, 190, 553-556
- Clark B. E., Bus S. J., Rivkin A. S., Shepard M. K. & Shah S. 2004, *AJ*, 128, 3070-3081
- Collins G. S., Melosh H. J. & Marcus R. A. 2005, *M&PS*, 40, 817
- Culler T. S., Becker T. A., Muller R. A. & Renne P. R. 2000, *Science*, 287, 1785-1788
- de León J., Licandro J., Serra-Ricart M., Pinilla-Alonso N. & Campins H. 2010, *A&A*, 517, A23

- Delisle M. J. & Laskar J. 2012, *A&A*, 540, A118
- Delva M. 1984, *CeMDA*, 485, 78-81
- Duffard R., de León J., Licandro J., Lazzaro D. & Serra-Ricart M. 2006, *A&A*, 456, 775-781
- Duncan M. J., Levison H. F. & Budd S. M. 1995, *AJ*, 110, 3073
- Dvorak R. & Freistetter F. 2007, *Lecture Notes in Physics* - Springer
- Eggl S. & Dvorak R. 2010, *Lecture Notes in Physics*, Berlin Spring Verlag, 790, 431-480
- Érdi B., Rajnai R., Sándor Z. & Forgács-Dajka E. 2012, *CeMDA*, 113, 95-112
- Everhart E. 1974, *CeMDA*, 10, 35-55
- Ferraz-Mello S. & Klafke J. C. 1991, *Predictability, Stability, and Chaos in N-Body Dynamical Systems* (Roeser S. and Bastian U. eds.), 177-184
- Fitzpatrick R. 2012, *An Introduction to Celestial Mechanics*, by Richard Fitzpatrick, Cambridge, UK: Cambridge University Press, 2012
- Fowler J. W. & Chillemi J. R. 1992, *IRAS Minor Planet Survey*. Phillips Laboratory, Hanscom Air Force Base, MA, 17-43
- Froeschlé C. & Morbidelli A. 1994, *Asteroids, Comets, Meteors 1993* (Milani A. and Di Martino M. and Cellino A. eds.), 189
- Fulvio D., Brunetto R., Vernazza P. & Strazzula G. 2012, *EPSC*, 84
- Gaffey M. J. & Gilbert S. L. 1998, *M&PS*, 33, 1281-1295
- Gaffey M. J. & Kelley M. S. 2004, *LPSC*, 35, 1812
- Galiazzo M. A., Bazso A. & Dvorak R. 2013a, *Planet. Space Sci.*, 84, 5-13
- Galiazzo M. A., Bazso A., Huber M., Losjak A., Dvorak R. & Koeberl C. 2013, *AN*, 9
- Galiazzo M. A., Bazso A. & Dvorak R. 2014a, submitted to *Memorie della Società Astronomica Italiana (10th Italian National Congress of Planetary Science)*, (9pp)
- Galiazzo M. A. 2014b, in preparation
- Gallardo T., Venturini J., Roig F. & Gil-Hutton R. 2011, *Icarus*, 214, 632-644

- Garrison D. H., Rao M. N. & Bogard D. D. 1995, *Meteoritics*, 30, 738
- Gayon-Markt J., Delbo M., Morbidelli A. & Marchi S. 2012, *MNRAS*, 424, 508-518
- Gladman B. J., Migliorini F., Morbidelli A. and 7 coauthors 1997, *Science*, 277, 197-201
- Gladman B. J. 1997, *Icarus*, 130, 228-246
- Gomes R., Levison H. F., Tsiganis H. F. & Morbidelli A. 2005, *Nature*, 435, 466-469
- Grady M. M. & Wright I. 2006, *Meteorites and the Early Solar System II*, D. S. Laretta and H. Y. McSween Jr. (eds.), University of Arizona Press, Tucson, 943 pp., 3-18
- Greenberg R. 1981, *AJ*, 87, 184-195
- Greenstreet S., Ngo H. & Gladman B. 2012, *Icarus*, 217, 355-366
- Halliday I., Griffin A. A. & Blackwell A. T. 1996, *M&PS*, 31, 185-217
- Hanslmeier A. & Dvorak R. 1984, *A&A*, 132, 203
- Hartmann O., Werner S. C., Ivanov B. A. & Neukum G. 2012, *EGU General Assembly Conference Abstracts (Abbasi A. and Giesen N.)*, 14, 10294
- Horner J., Evans N. W. & Bailey M. E. 2004a, *MNRAS*, 354, 798-810
- Horner J., Evans N. W. & Bailey M. E. 2004b, *MNRAS*, 355, 321-329
- Ivanov B. A., Neukum G., Bottke Jr. W. F. & Hartmann W. K. 2002, *Asteroids III*, 89-101
- Klafke J. C., Ferraz-Mello S. & Michtchenko T. 1992, *Chaos, Resonances and Collective Dynamical Phenomena in the Solar System (IAU Symposium, Ferraz-Mello ed.)*, 152, 153
- Knežević Z., Novaković B. & Milani A. 2010, *Publications de l'Observatoire Astronomique de Beograd*, 90, 11-18
- Koeberl C., Bottomley R., Glass B. P. & Storzer D. 1997, *Geochim. Cosmochim. Acta*, 61, 1745-1772
- Koeberl C. 2006, *Elements*, 4, 211-216
- Koeberl C., Shukolyukov A. & Lugmair G. W. 2007, *E&PSL*, 256, 534-546
- Kresak 1979, *Asteroids ed. Gehrels T.*, 289-309

- Lazzarin M., Marchi S., Magrin S. & Danese S. 2005, AAS/Division for Planetary Sciences Meeting Abstracts #37 (Bulletin of the American Astronomical Society), 629
- Lazzaro D., Angeli C. A., Carvano J. M., Mothé-Diniz T., Duffard R. & Floreczak M. 2004, *Icarus*, 172, 179-220
- Levison H. F. 1996, *ASPL*, 107, 173-191
- Levison H. F. & Duncan M. J. 1997, *Icarus*, 127, 13-32
- Levison H. F., Shoemaker E. M. & Shoemaker C. S. 1997, *Nature*, 385, 42-44
- Marchi S., Lazzarin M., Paolicchi P. & Magrin S. 2004, 35th COSPAR Scientific Assembly (COSPAR Meeting, Pillé J. P. ed.), 35, 2736
- Marchi S., Lazzarin M., Paolicchi P. & Magrin S. 2005, *Icarus*, 175, 170-174
- Malavergne V., Brunet F., Richter K., Zanda B., Avril C., Borensztajn S. & Berthet S. 2012, *LPSC*, 43, 1860
- Martellato E., Cremonese G., Marzari F., Massironi M. & Capria M. & T. 2007, *Memorie della Società Astronomica Italiana Supplement*, 11, 124
- McEachern F. M., Čuk M. & Stewart S. T. 2010, *Icarus*, 210, 644-654
- McEwen A. S., Bierhaus E. B. 2006, *AREPS*, 34, 536-567
- McFadden L.-A. A., Weissmann P. R. & Johnson T. V. 2007, AAS/Division for Extreme Solar Systems Abstracts
- Michel P., Froeschlé C. & Farinella P. 1996, *EM&P*, 72, 151-164
- Michel P., Migliorini F., Morbidelli A. & Zappalá V. 2000, *Icarus*, 145, 332-347
- Migliorini F., Morbidelli A., Zappalá V., Gladman B. J., Bailey M. E. & Cellino A. 1997, *M&PS*, 32, 903-916
- Milani A. & Knežević Z. 1990, *CeMDA*, 49, 347-411
- Milani A. & Knežević Z. 1992, *Icarus*, 98, 211-232
- Milani A. & Knežević Z. 1994, *Icarus*, 107, 219-254
- Milani A., Knežević Z. & Cellino A. 2010, *Icarus*, 207, 769-794
- Minton D. A. & Malhotra R. 2011, *ApJ*, 732, 53
- Morbidelli A. & Henrard J. 1991a, *CeMDA*, 51, 131-167

- Morbidelli A. & Henrard J. 1991b, *CeMDA*, 51, 169-197
- Morbidelli A. & Gladman B. 1998, *M&PS*, 33, 999-1016
- Morbidelli A. & Nesvorný D. 1999, *Icarus*, 139, 295-308
- Morbidelli A., Bottke Jr. W. F., Froeschlé C. & Michel P. 2002, *Asteroids III*, 409-422
- Morbidelli A. 2006, *ArXiv Astrophysics e-prints* (arXiv:astro-ph/0512256)
- Morbidelli A., Lunine J. I., O'Brien D. P., Raymond S. N. & Walsh K. J. 2012, *AREPS*, 40, 251-275
- Morrison D., Harris A. W., Sommer G., Chapman C. R. & Carusi A. 2002, *Asteroids III*, 739-754
- Muller R. A. 2001, *Catastrophic Events and Mass Extinctions: Impact and Beyond*, 3089
- Murray C. D. & Dermott S. F. 1999, *Solar system dynamics* by Murray C. D., 1999
- Nemchin A. A., Zeigler R. A. & Grente M. L. 2013, *LPI*, 1719, 1834
- Nesvorný D., Jedicke R., Whiteley R. J. & Ivezić Ž. 2005, *Icarus*, 173, 132-152
- Nesvorný D. & Morbidelli A. 1998, *AJ*, 116, 3029-3037.
- Nittler L. R., Starr R. D., Lim L. and 12 coauthors 2001, *M&PS*, 36, 1637-1695
- Novaković B., Cellino A. & Knežević Z. 2011, *Icarus*, 216, 69-81
- Opeil C. P., Consolmagno G. J. & Britt D. T. 2010, *Icarus*, 208, 449-454
- Öpyk E. J. 1958, *Irish Astronomical Journal* 1958, 5, 37 – +
- Parker A., Ivezić Ž., Jurić M. and 3 coauthors 2008, *Icarus*, 198, 138-155
- Polishook D., Binzel R. P., Lockhart M. and 4 coauthors 2012, *Icarus*, 221, 1187-1189
- Rabe E. 1971, *NASA Special Publication*, 267, 407
- Rabinowitz D. L. 1996, *Completing the Inventory of the Solar System* (Rettig T. and Hahn J. M. eds.), 13-28
- Richardson D. C. & Scheeres D. J. 2002, *ESA Special Publication*, 737-739

- Rickman H. & Froeschlé C. 1980, *Moon and Planets*, 22, 125-128
- Rickman H. 1991, *Advances in Space Research*, 11, 7-18
- Rudawska R., Vaubaillon J. & Atreya P. 2012, *A&A*, 541, id.A2, 5 pp.
- Saha P. 1992, *Icarus*, 100, 434-439
- Shaw H. F. & Wasserburg G. J. 1982, *E&PSL*, 60, 155-177
- Sitarski G. 1999, *AcA*, 49, 421-431
- Spurný P., Bland P. A., Shrbený L. & 9 coauthors 2012, 47, 163.185
- Swindle T. D., Isachsen C. E., Weirich J. R. & Kring D. A. 2009, *M&PS*, 44, 747-762
- Tholen D. J. 1989, *Asteroids II*, 1139-1150
- Tholen D. J. & Barucci M. A. 1989, *Asteroids III*, 298-315
- Thomas P. & Veverka J. 1977, *Icarus*, 30, 595-597
- Tiscareno M. S. & Malhotra R. 2003, *AJ*, 126, 3122-3131
- Tiscareno M. S. & Malhotra R. 2009, *AJ*, 138, 827-837
- Veverka J., Farquhar B., Robinson M. & 41 coauthors 2001, *Nature*, 413, 390-393
- Warner B. D. & Harris A. W. 2007, *AAS/Division for Planetary Sciences Meeting Abstracts #39 (Bulletin of the American Astronomical Society)*, 39, 432
- Warner B. D., Harris A. W., Vokrouhlický D., Nesvorný D. & Bottke W. F. 2009, *Icarus*, 204, 172-182
- Weissman P. R. 1996, *Completing Inventory of the Solar System (series Astronomical Society of the Pacific Conference Series)*, 107, 265-288
- Werner S. C. & Neukum G. 2003, *EGS - AGU - EUG Joint Assembly*, 627
- Westman A., Wannberg G. & Pellinen-Wannberg A. 2004, *Annales Geophysicae*, 22, 1575-1584
- Wieczorek M. A., Neumann G. A., Nimmo F. and 13 coauthors 2013, *Science*, 339, 671-675
- Williams J. G. 1969, *PhD Thesis (University of California, Los Angeles)*
- Xu S., Binzel R. P., Burbine T. H. & Bus S. J. 1995, *Icarus*, 115, 1-35

BIBLIOGRAPHY

Yeomans D. K. 1998, AAS/Division for Planetary Sciences Meeting Abstracts #30
(Bulletin of American Astronomical Society), 30, 1038

Zappalá V., Cellino A., Farinella P. & Knežević Z. 1990, AJ, 100, 2030

Zappalá V. 1995, Icarus, 116, 291

Abstract

The Near-Earth Asteroids (*NEAs*) are relatively small celestial bodies with perihelion distances of less than 1.3 au. They can have impacts with the terrestrial planets and therefore they are a permanent danger for the Earth and some of them are also called Potential-Hazardous Asteroids, *PHAs*.

In this work some of the possible sources of *NEAs* are analysed in detail. In particular we analyse two asteroid groups, the Hungarias and the Vestians from the Main Belt region (asteroids from between the orbits of Mars and Jupiter), and the inner region of the Centaurs, bodies between the orbits of Jupiter and Saturn. In addition a photometrical study of an important approaching comet, *C/2012 S1 ISON*, plus some hints on its orbits, close encounters and some physical constraints, i.e. the encounter velocity, are presented. Furthermore, another work on the origin of a paleo-impact event, namely the Bosumtwi crater one, is studied.

One of the main parts of this thesis is devoted to the dynamical behaviour of the Hungaria Group, which consists of asteroids moving in an orbital region of the inner Main Belt, with semi-major axes between 1.78 au and 2.03 au and confined mainly by the ν_6 secular resonance, the mean motion resonances 4:1 with Jupiter and 3:4 with Mars. A dynamical study of a small group of 200 Hungarias has been performed. These asteroids have been integrated in a first step for 100 million years, using a simplified model of the planetary system (only the planets from Mars to Saturn are considered). Out of this sample, in a second step, 11 objects that suffered from large eccentricities and inclinations during the first integration have been chosen and then their orbits were followed with a dynamical model, including also Venus and the Earth. This is a statistical investigation, therefore 11 real asteroids, and 50 clones (with only slightly different initial conditions) for each asteroid, have been integrated. It turned out that 91% of these Hungaria clones become *PCAs* (Planet Crossing Asteroids) within the integration time (again 100 million years). A low rate of impacts with the terrestrial planets have been found. The number of close encounters with the terrestrial planets, their impact velocities and angles have been computed too (Galiazzo et al., 2013a). In addition, the diameter of the putative craters made by Hungaria collisions with the terrestrial planets were computed (Galiazzo et al., 2014a). The Moon seems not to be relevant for the statistics of close encounters and impacts (Bazso & Galiazzo 2013). Approximately 30 observed V-type asteroids (objects with a spectrum similar to

the basaltic achondrite which are mostly remnants of the parent body, the asteroid 4 Vesta) from the NEA-region have been chosen. Similarly to the Hungaria study, computations of the physical and statistical aspects of the impacts with the terrestrial planets were performed.

Concerning the (inner) Centaurs, it has been found that the asteroids and also comets between Jupiter and Saturn can become *PCAs* even in a short time scale of 1 Million years. Only a very small percentage of them escape, having close encounter with Saturn.

For the first time, the origin of a relatively young paleo-impact event, the Bosumtwi crater (in the Republic of Ghana, Africa) has been investigated. This crater has been chosen for this study because of its relatively young age (1.07 Myr; Koerberl et al., 1997) and unusually good constraints on the direction of the impactor (Artemieva et al., 2004 and Galiazzo et al., 2013b). This helps to reconstruct the impactor's orbit and learn about its origin (or its most probable origin), using a "statistical-dynamical" analysis. The most probable origin of the impactor is an high-inclined asteroid family in the middle Main Belt and the impactor should have been an asteroid with an original orbital inclination greater than 35° .

This thesis studies some of the most important sources of *NEAs*, especially in the Main Belt, the Hungaria and the Vesta Family, and it improves the study of the impacts with the planets in the Solar System and the origins of the impactors.

Zusammenfassung

Asteroiden, deren Abstand zur Sonne im Perihel einen Wert von 1.3 au unterschreiten werden “Near-Earth Asteroids” (NEAs) genannt. Diese Himmelskörper können also mit den terrestrischen Planeten kollidieren und sind daher eine permanente Bedrohung für die Erde. Aus diesem Grund werden sie auch oft als “Potential-Hazardous Asteroids” (PHAs) bezeichnet. In dieser Arbeit wurden nun mögliche Quellen für NEAs im Detail analysiert. Im speziellen wurden zwei Asteroiden Gruppen untersucht, die Hungarias und Vestians aus dem Hauptgürtel der Asteroiden zwischen Mars und Jupiter und der innere Bereich der Centauren, welche sich zwischen Jupiter und Saturn befinden. Zusätzlich wird eine photometrische Studie des nahe vorbei gehenden Kometen C/2012 S1 ISON, inklusive der Abschätzung seines Orbits, möglicher naher Begegnungen und physikalischer Einschränkungen (z.B. mögliche Aufschlaggeschwindigkeiten) präsentiert. Außerdem wurde die mögliche Herkunft des Paleo-Impakts, welcher den Bosumtwi Krater gebildet hat untersucht. Ein wichtiger Teil dieser Arbeit ist dem dynamischen Verhalten der Hungaria Gruppe gewidmet, welche aus Asteroiden besteht, die sich im inneren Bereich des Hauptgürtels zwischen 1.78 und 2.03 AE befinden und hauptsächlich durch die ν_6 säkulare Resonanz, die 4:1 Resonanz mit Jupiter und die 3:4 Resonanz mit Mars begrenzt wird. Dazu wurde eine dynamische Studie einer kleinen Gruppe von 200 Hungarias durchgeführt, wobei hier ein vereinfachtes Modell des Sonnensystems (es wurden nur die Planeten von Mars bis Saturn berücksichtigt) für 100 Mill. Jahre integriert wurde. In einem nächsten Schritt wurden die 11 Objekte, welche hohe Exzentrizitäten und Inklinationen bekommen hatten in einem dynamischen Modell weiterintegriert welches auch die Venus und die Erde enthält. Um eine statistische Auswertung zu ermöglichen; wurden zusätzlich zu diesen 11 Objekten noch 50 Klone pro Objekt mit gering abweichenden Anfangsbedingungen berechnet. Dabei stellte sich heraus, dass 91% der Hungaria Klone innerhalb der Integrationszeit (100 Mill. Jahre) zu Erdbahnkreuzern (PCAs) werden. Weiters konnte auch eine geringe Anzahl von Einschlägen auf die terrestrischen Planeten gefunden werden. Die Anzahl der nahen Begegnungen mit den terrestrischen Planeten, sowie die Geschwindigkeit und der Winkel des Einschlages wurden bestimmt und in Galiazzo et al. (2013a) veröffentlicht. In einer weiterführenden Arbeit (Galiazzo et al., 2014a) wurden die Durchmesser der von den Einschlägen der Hungarias verursachten Krater berechnet. Es kon-

nte auch gezeigt werden, dass der Mond für die Statistik von nahen Begegnungen und Einschlägen vermutlich keine Rolle spielt. In einer weiteren Studie wurden 30 bekannte V-Typ Asteroiden (Objekte mit einem zu basaltischem Achondrite ähnlichem Spektrum, welche hauptsächlich Überreste des Asteroiden 4 Vesta sind) aus der Region der NEAs gewählt. Ähnlich wie bei der Studie der Hungarias wurden auch hier physikalische und statistische Aspekte von Einschlägen auf terrestrische Planeten untersucht. Betreffend der Centauren konnte gezeigt werden, dass auch diese Asteroiden und Kometen zwischen Jupiter und Saturn in einer relativ kurzen Zeit von 1 Mill. Jahren zu PCAs werden können. Weiters zeigte sich, dass nur ein sehr geringer Prozentsatz der Centauren Bahnen außerhalb des Saturns erreichen, bzw. nahe Begegnungen mit ihm haben können. Zum ersten Mal wurde auch der Ursprung des relativ jungen Paleo-Impakt Kraters Bosumtwi (Ghana, Afrika) untersucht. Dieser Krater wurde wegen seines jungen Alters von 1.07 Mill. Jahren und der ungewöhnlich guten Einschränkungen für die Richtung des Impaktors gewählt (Artemieva et al., 2004, Galiazzo et al., 2013b). So konnte der Orbit des Impaktors rekonstruiert und mit Hilfe einer statistisch-dynamischen Analyse sein wahrscheinlichster Ursprung bestimmt werden. Dabei stellte sich als wahrscheinlichster Ursprung eine Asteroiden Familie mit hohen Inklinationen im Hauptgürtel heraus, wobei der Impaktor eine Inklination von mehr als 35° gehabt haben muss. Zusammenfassend untersucht diese Studie die wichtigsten Quellen der NEAs, besonders im Hauptgürtel der Asteroiden die Hungaria und Vesta Familie und verbessert so das Wissen über Einschläge auf die terrestrischen Planeten unseres Sonnensystems, sowie den Ursprung der Impaktoren.

Curriculum Vitae: Mattia Galiazzo

Personals:

Name: Mattia Galiazzo

Born: 04. January 1975, Bassano del Grappa (VI), Italy

Email: mattia.galiazzo@univie.ac.at

Education

1989-1996 High school based on mathematics and physics - “Istituti Filippin” (Liceo Scientifico), Paderno del Grappa (TV), Italy

1992 Diploma of Intermediate English at the Saint Peter’s School - York, U.K.

2006 Diploma of informatics: “Instruments and Systems of marketing-knowledge and privacy in informatics systems cod.”

2009 Master degree in Astronomy (Msc) at the Univesity of Padova

2010-2013 Doctoral School at the University of Vienna, Austria: Planetology: From Asteroids to Impact Craters (NEO asteroids and Impact Crater Studies)

Others

1995 Secretary at a private tributary office - Selvazzano Dentro (PD), Italy

1997 Military service - Casarsa della Delizia (PN), Italy

2003 Photometric observations (direct) at the 1.22m telescope of Asiago (Pennar), Italy

2007 Transports (magazines) - Padova, Italy

2008 Fac-totum of Hotel Toscanelli - Padova, Italy

1997-2009 Private Teaching of Math, Physics and Chemistry - Middle and High schools students, Padova and Venezia, Italy

1996-2009 Master Science in Astronomy (observational and theoretical astronomy) at the Department of astronomy at the University of Padova (Italy)

2009 Master thesis in Astronomy about: “Photometry of Minor Bodies of the External Solar System”

2010-2013 Doctoral School at the University of Vienna, Austria: “Planetology: From Asteroids to Impacts Craters” (NEO asteroids and Impact Crater Studies)

2011-now Photometric observations (remote control) at the 1.5m Schoepfl Telescope of Vienna, Austria

2011-12 Collaboration research, asteroids dynamical research at SYRTE and IMCEE at the Observatoire de Paris, Paris, France

2013 Member of the ALPO (The Association of Lunar & Planetary Observers), USA

2013 Collaboration research for the FWF Project P23810: “Dynamics and observational prospects of co-orbital planets in double stars”

2013 Member of CIOC/Ison group (Comet Ison Observing Campaign)

Talks

- 04 2010 5th Austrian Hungarian workshop on Trojans and related Topics (Vienna, Austria). Title of my presentation: “Light curves and colors of the Centaurus 2060 Chiron (1997 UB) and 10199 Chariklo (1997 CU26)”
- 05 2010 Ecole thematique du CNRS: Impact et recontres proches dans les systeme solaire - Cussac, France. Title of my presentation: “Light curves and colors of the Centaurus 2060 Chiron (1997 UB) and 10199 Chariklo (1997 CU26)”
- 03 2011 8th Alexander von Humboldt Colloquium for Celestial Mechanics (Bad Hofgastein, Austria). Title of my presentation: “The Hungaria asteroid family as source for Earth-colliding NEAs”
- 11 2011 Journees 2011 ”Systèmes de référence spatio-temporels” (Vienna, Austria). Title of our* presentation: “Lunar effects on close encounters of Hungarias with the Earth” (*with A.Bazso)
- 07 2012 Seminar of the Observatoire de Paris (Paris, Vienna). Title of my presentation: “A statistical dynamical study of meteorite impactors: case study from Bosumtwi”
- 09 2012 6th Workshop of Young Researchers in Astronomy and Astrophysics (Budapest, Hungary).
Title of my presentation: “A statistical dynamical study of meteorite impactors: case study from Bosumtwi”
- 11 2012 Panel Kolloquium, Nordlingen, Germany. Title of my presentation: “A statistical dynamical study of meteorite impactors: case study from Bosumtwi”
- 02 2013 XI Congresso Nazionale di Scienze Planetarie, Bormio, Italy. Title of my presentation: “Hungaria asteroids: Resonances, close encounters and impacts with Terrestrial Planets”
- 09 2013 CELMEC VI (The Sixth International meeting on Celestial Mechanics), San Martino al Cimino (Orvieto), Italy.
Title of my presentation: “V-types asteroids: impacts and close encounters with Terrestrial Planets”

Posters

- 10 2011 EPSC-DPS Joint Meeting 2011 (Nantes, France). Title of the poster: “The Vesta Asteroid Family: Study of the family and close encounters with terrestrial planets”

- 03 2012 43rd Lunar and Planetary Science Conference (The Woodlands, Texas, USA). Title of the poster: “The Vesta Asteroid Family: Study of the Family and Close Encounters with Terrestrial Planes and Dynamical Influences by (1) Ceres and (4) Vesta”

Invited talks

- 07 2012 Séminaires << Temps et Espace >> (IMCEE et SYRTE, Observatoire de Paris, France). Title of my presentaiton: “A statistical dynamical study of meteorite impactors: case study from Bosumtwi”
- 06 2013 Kuffner Sternwarte, Vienna, Austria. Title of my presentation: “Asteroids and planetary encounters”

Publication List

Publications

Galiazzo M. A., Bazso A., R. Dvorak, 2013, “The Hungaria Asteroids: resonances, close encounters and impacts with terrestrial planets”, Planetary and Space Science, <http://dx.doi.org/10.1016/j.pss.2013.03.017> (in print)

Galiazzo M. A., Bazso A., M. Huber, A. Losiak, R. Dvorak, C. Koeberl, 2013, “A statistical dynamical study of meteorite impactors: case study from Bosumtwi”, Astronomical Notes, issue #9, 2013

Dvorak R., Eggl S., Suli, A., Sándor Z., **Galiazzo M.**, Pilat-Lohinger E., “Water delivery in the early Solar System”, AIP Conference Proceedings, 1468

Galiazzo M. A., Bazso A., R. Dvorak, 2013, “The Hungaria Asteroids: Close encounters and impacts with terrestrial planets”, submitted to “MEMORIE della Società Astronomica Italiana”

Galiazzo M. A., Zeilinger W. W., “Photometry of Comet C/2012 S1 ISON”, Journal A.L.P.O. (Association of Lunar and Planetary Observers, “The Strolling Astronomer”), June 2013, USA

Non-Refereed articles and abstract-books

Galiazzo M., Carraro G., Maris M., De la Fuente Marcos, R., Montalto, M., 2010, “Lightcurves and colors of 2060 Chiron (1997 UB) and 10199 Chariklo (1997 CU₂₆)”, Proceedings of the 4th Austrian-Hungarian workshop on Celestial Mechanics 04/2010

Bazso A., **Galiazzo M.**, “Lunar effects on close encounters of Hungaria asteroids and near-Earth asteroids with the Earth”, Journées “Systèmes de référence spatio-temporels”, 2011

.....★.....★.....★.....★.....★.....★.....★.....★.....★.....★.....★.....★.....
*A thing of beauty is a joy forever:
Its loveliness increases; it will never
Pass into nothingness;*³

³John Keats